REGULATION OF DYNEIN LOCALIZATION AND CILIOGENESIS BY ASUNDER VIA ITS ROLE IN THE RNA PROCESSING COMPLEX, INTEGRATOR

By

Jeanne Nicole Jodoin

Dissertation

Submitted to the Faculty of the

Graduate School of Vanderbilt University

In fulfillment of the requirements

For the degree of

DOCTOR OF PHILOSOPHY

in

Cell and Developmental Biology

December 2013

Nashville, Tennessee

Approved:

Laura Lee, M.D./Ph.D.

Irina Kaverina, Ph.D.

Anne Kenworthy, Ph.D.

Donna Webb, Ph.D.

Ryoma Ohi, Ph.D.

For my supportive family

and my mentor for giving me this opportunity

ACKNOWLEDGMENTS

First and foremost, I need to thank my mentor, Laura Lee. Not only did Laurie offer me my first job out of college, she gave me my first look into the wonderful world of hardcore academic research. She has given me every opportunity to learn, develop my skills, and become a thoughtful, independent scientist. She has taught me everything I know about working in a research lab, and I will forever be indebted to her for her generosity, patience, and guidance. I have loved working in Laurie's lab, and I also want to thank Ethan Lee, who was also, at one point, my first employer out of college (only 25% though). Your enthusiasm for science- both the good and bad- is infectious, and it has been a pleasure working with you and your lab. The people to whom I credit the majority of my happiness in grad school are the members of the Lee Labs, both the first generation and the current. Poojitha Sitaram (my best friend forever) and Sarah Hainline have been fantastic labmates who are always there to lend a hand or offer some advice, and I will always appreciate Poojitha's fly work that she provided for my papers (plus the added entertainment of mimicking you when we talk). The members of Ethan's lab- (Tiny) Tony Chen, Brian (no nickname given) Hang, and Kenyi (Kenya) Saito- have made lab enjoyable and fun, and I appreciate all of your input to my projects!

I would like to thank my collaborators in the Wagner lab: Eric Wagner and Todd Albrecht. Eric has been great to work with- he is encouraging, enthusiastic, and hilarious. I want to thank Todd for his patience with my 20,000 western blots that I have sent him. I would also like to thank my collaborators in the Reversade lab: Bruno Reversade and

Mohammad Shboul. They have been fantastic reagent generators and a great help with my manuscripts.

I would like to thank my committee members, Irina Kaverina, Ryoma (Puck) Ohi, Anne Kenworthy, and Donna Webb for all the great advice, support, and encouragement they have given me during my graduate career.

I must thank my family. They have been a terrific source of encouragement and motivation. They have been so patient and understanding, and most importantly, very generous, with a daughter who has chosen a path of the long-term student. (Don't worry mom and dad- I am employed now!)

Throughout my years here, I have made many friends at Vanderbilt and within the department whom I would like to thank for being a source of entertainment, for being a support system when things go wrong, and for being a cheerleader when things go right. I am forever grateful for your friendship. I want to specifically thank Christopher Arnette, my Sunshine, for his friendship, support, and sassy attitude! I will miss our daily breaks from science to gossip (I mean discuss science)!

Finally, I want to thank my biggest cheerleader of all, my husband Matthew Broadus. If not for his love and support during my years here, I don't believe I would have made it through to the other side in one piece. Not only was he there to talk me off any ledges, but he took time to remind me to celebrate my accomplishments. I am so lucky to have such a caring, intelligent, and motivating person in my life, and I look forward to seeing what the future (science and not) holds for both of us.

Lastly, I am deeply appreciative of the support I have received from the Program in Developmental Biology (led by Chris Wright) and Microtubule and Motors club (led

by Irina Kaverina) as well as the financial support I received from the NIH Institutional Predoctoral Reproductive Biology training grant (2T32HD007043).

TABLE OF CONTENTS

LIST OF FIGURES

LIST OF TABLES

CHAPTER I

INTRODUCTION

The Cell Cycle

The cell cycle is made up of a series of coordinated events that will ultimately lead to the replication of DNA within the cell and the equal division of DNA and other cellular components into two identical daughter cells. This is a highly regulated process involving several checkpoints. Additionally, mechanisms are in place to ensure that the cell cycle progression occurs in a unilateral direction and prevents it from reversing. Much of what we know about the cell cycle has come from studies of simple model organisms. Initial experiments in *Saccharomyces cerevisiae and Schizoaccharomyces pombe, Xenopus laevis, Drosophila melanogaster, and Caenorhabditis elegans* were among the first to contribute an understanding of the cell cycle.

In eukaryotic cells, the cell cycle consists of four distinct stages: G1 (gap phase 1), S (synthesis), G2 (gap phase 2), and mitosis (Figure 1.1). The G1, S, and G2 phases are collectively known as interphase. The gap phases, G1 and G2, which occur at the end of mitosis and S phase, respectively, play an essential role in regulating the cell cycle. Each gap phase contains checkpoints, which can be thought of as a monitoring system for the cell cycle (Figure 1.1, red bars) (Lara-Gonzalez et al., 2012; Yasutis and Kozminski, 2013). These checkpoints serve to provide two functions: 1) detect when defects are present that may prevent the cell from properly executing the cell cycle, and 2) prompt a response that leads to a delay in the cell cycle, thereby, allowing the cell to correct the

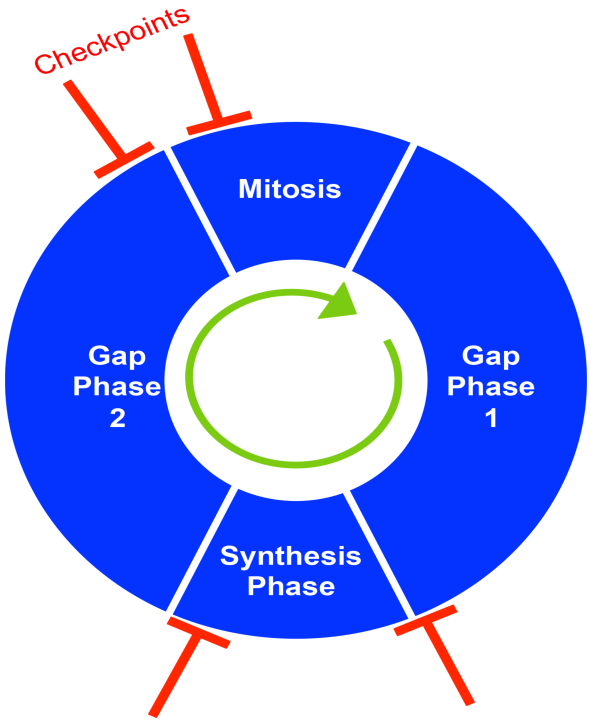

Figure 1.1 – Cell cycle stages. Cartoon depicting the stages of the cell cycle. Red bars indicate checkpoints within the cell cycle. Green arrow indicates direction of cell cycle. Adapted from Yasutis and Kozminski, 2013.

error (Lara-Gonzalez et al., 2012; Yasutis and Kozminski, 2013). In addition to this regulatory role, these gap phases also allow for cellular growth before and after mitosis (Schafer, 1998).

The synthesis phase of the cell cycle allows for the duplication of DNA content. It is essential to the cell that this phase is completed with little error. Multiple polymerases are employed by the cell to generate an identical copy of its DNA material. To ensure this proper execution of the genome duplication, the cell utilizes multiple mechanisms to repair or bypass sites of DNA damage (Branzei and Foiani, 2008). This copy of the genetic material produced in S-phase is packaged in the form of chromosomes that will later be divided in the final stage of the cell cycle, mitosis.

Mitosis

Though mitosis may differ from organism to organism, the purpose of mitosis remains the same, to generate two identical daughter cells from the mother cell. There are two distinct types of mitosis: closed mitosis, where the NE remains intact, and open mitosis, in which the NE is broken down (Boettcher and Barral, 2013). Mitosis is made up of four phases: prophase, metaphase, anaphase, and telophase (Figure 1.2).

Prophase is made up of a set of coordinated events that primes the cell to enter into division correctly. Errors in these events can lead to defects ranging from late entry into the next phase of mitosis, improper spindle positioning, incomplete nuclear envelope breakdown (NEBD), to apoptosis. At the onset of prophase, known as the G2/M transition, the cell will begin to condense its chromosomes, which are loosely bundled during interphase. Phosphorylation of histones precede the condensation of chromosomes

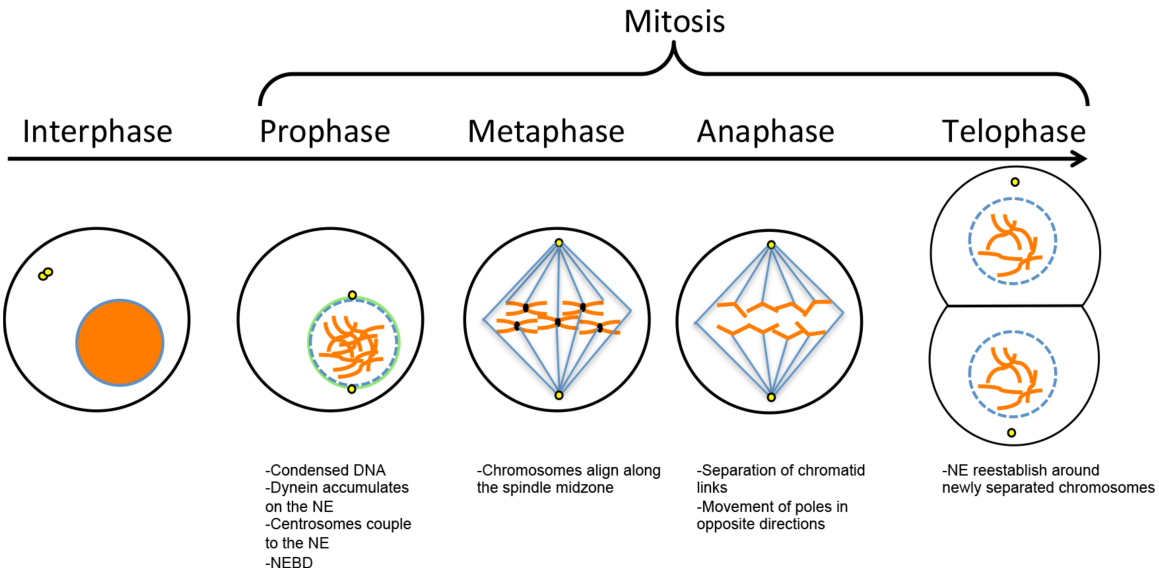

Figure 1.2 – Mitosis. Stages of mitosis are illustrated. Orange represents DNA content, green represent dynein, blue circle represents nuclear envelope, blue lines represent spindle microtubules. Adapted from Yasutis and Kozminski, 2013.

and can be used biochemically to detect this cell cycle stage. In prophase cells, a pool of dynein becomes anchored on the NE, where it is essential for multiple functions (Anderson et al., 2009; Gonczy et al., 1999; Payne et al., 2003; Robinson et al., 1999; Salina et al., 2002). This perinuclear pool of dynein facilitates the coupling of centrosomes to the nuclear surface (Anderson et al., 2009; Bolhy et al., 2011; Gonczy et al., 1999; Malone et al., 2003; Robinson et al., 1999; Splinter et al., 2010; Vaisberg et al., 1993). Centrosomes then separate and migrate along the NE to opposite sides, establishing the poles of the bipolar spindle (Vaisberg et al., 1993). At the end of prophase, the NE breaks down in cells that undergo open mitosis. Dynein motors accumulated on the NE, along with other factors, play a role in promoting NEBD by exerting a force on the NE, ultimately leading its shearing (Salina et al., 2002; Vaisberg et al., 1993). The completion of NEBD signifies the end of prophase.

In metaphase, the cell forms the bipolar spindle, the major machinery that executes cell division. During metaphase, the condensed chromosomes align along the spindle midzone. There are three types of microtubules present within the spindle: 1) kinetochore microtubules, which attach to a structure located in the central region of the chromosome known as the kinetochore, 2) spindle microtubules, which provide the structure to the spindle, and 3) astral microtubules, which anchor the spindle in the center of the cell (Kops and Shah, 2012). It is essential for the progression of mitosis that all chromosomes be anchored to a kinetochore microtubule. It is thought that the lack of kinetochore attachment serves as a “pause” signal, preventing unaligned chromosomes from entering anaphase (Kops and Shah, 2012; Lara-Gonzalez et al., 2012).

Anaphase marks the beginning of a physical separation of the chromosomes. This phase occurs in two distinct parts, anaphase A and anaphase B. In anaphase A, the links binding the sister chromatids are cleaved. This cleavage, along with the shortening of kinetochore microtubules, allows for the initial separation of chromosomes along the spindle midzone (Kops and Shah, 2012). In anaphase B, microtubules emanating from the spindle poles generate forces that physically pull the two centrosomes and their attached chromosomes in opposite directions (Kops and Shah, 2012; Lara-Gonzalez et al., 2012).

Telophase, the final stage of mitosis, produces two identical daughter cells. During this stage, nuclear membranes reform around the newly separated chromosomes, cellular components such as the Golgi and mitochondria are reassembled, and the DNA undergoes decondensation (Schafer, 1998; Yasutis and Kozminski, 2013). The completion of this stage is marked by cytokinesis, facilitated by the contractile ring, which is responsible for the complete separation of the newly formed cells (Boettcher and Barral, 2013).

The Dynein Motor Complex

The cell is constantly undergoing dynamic processes such as the trafficking of cargo, organelles, and mRNA along the microtubules or actin, positioning of organelles within the cytosol, and the separation of its DNA content into two daughter cells (Holzbaur and Vallee, 1994). The evolutionarily conserved molecular motors are essential for mediating these processes. Three families of motors have been identified: myosins, kinesins, and dynein. Myosin motors move along actin filaments (Mason and

Martin, 2011), while kinesin and dynein motors power cargo along microtubules, albeit in opposing directions with few exceptions (Hirokawa et al., 2009; Holzbaur and Vallee, 1994).

Dynein motors play a role in a large number of cellular functions, including transport of cargo along the microtubules towards their minus end, nuclear migration and positioning in polarized cells, ciliogenesis, establishment of the bipolar spindle, and executing the proper separation of chromosomes into two daughter cells during mitosis (Kardon and Vale, 2009). Due to its vast number of functions and their diverse nature, dynein is tightly regulated to properly perform these tasks. While the motor itself is directly regulated by phosphorylation and its subunit composition, adaptor proteins have the capacity to interact directly with the motor and modulate its function.

In contrast to the myosin and kinesin motors, which display a large diversity within each motor family, there are only two forms of dynein in the cell: axonemal and cytoplasmic (Allan, 2011; Kardon and Vale, 2009). Axonemal dynein is required for the sliding of microtubules, resulting in the beating of flagella and motile cilia. This form of dynein is only found in cells in which these structures are present (Vallee, 1993). Cytoplasmic dynein, which is found in all cells, is required for minus-end-directed transport (towards the microtubule organizing center) within the cell, including retrograde transport along cilia (Allan, 2011; Kardon and Vale, 2009; Kolomeisky and Fisher, 2007).

Cytoplasmic dynein has well-defined roles in all stages of the cell cycle. During interphase, dynein is required for ciliogenesis, cargo transport, organelle positioning and assembly, vesicle trafficking, and nuclear migration (Kardon and Vale, 2009). During

mitosis, dynein accumulated on the NE is required for nucleus-centrosome coupling, centrosome separation and migration to the poles of the imminent bipolar spindle, building and support of the bipolar spindle, and chromosome separation (Allan, 2011; Kardon and Vale, 2009). The regulation of cytoplasmic dynein will be the focus of this body of work.

Dynein is a large multimeric complex, with its total size nearing 2 MDa, making it the largest of the molecular motors. The dynein complex is composed of two catalytic heavy chains, two intermediate chains, two to four light intermediate chains, and two light chains (Figure 1.3). The chains range in size: the heavy chains are approximately 500 kDa, the intermediate chains are 74 kDa, the light intermediate chains are between 50 and 60 kDa, and the light chains are less then 20 kDa (Allan, 2011; Kardon and Vale, 2009). The two genes encoding the heavy chains are less divergent then genes encoding other motor proteins and share a large amount of sequence similarity along the length of the proteins (Holzbaur and Vallee, 1994).

The dynein motor can be broken down into two regions: the head regions and the stem region. Dynein contains two identical head regions that are made up of the heavy chains (Redwine et al., 2012). The heavy chains each consist of six ATPase domains that form a single polypeptide (Redwine et al., 2012). Dynein "walking" along the microtubules is facilitated by the force-generating ATPase activity of these six ATPase domains (Redwine et al., 2012). The motor attaches to microtubules through the stalk, a coiled-coil microtubule-binding domain that protrudes from the heavy chains. Additionally, components of the heavy chains form the carboxy-terminal head that acts as

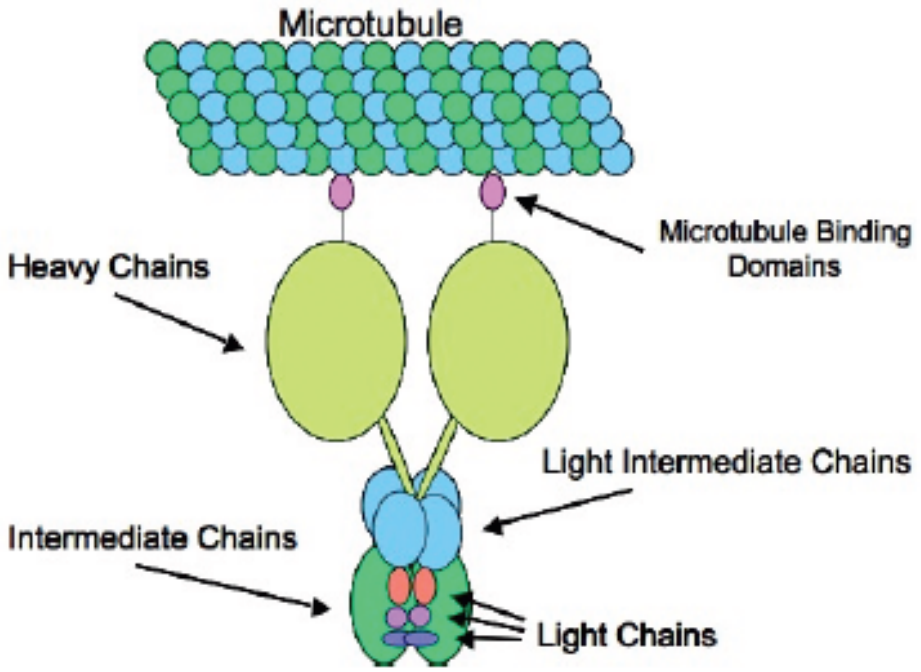

Figure 1.3 – The dynein complex. Cartoon depicting the components of the dynein motor complex as well as the microtubule binding domain. Adapted from Suslka and Pfisher, 2000.

a scaffold for the non-catalytic subunits to bind, thereby forming the entire dynein complex (Kardon and Vale, 2009).

The non-catalytic chains found in the stem region give the most variability to the motor. Variation in chain composition has been proposed to result in distinct dynein complexes that perform specific functions within the cell (Kardon and Vale, 2009). Additionally, these non-catalytic chains serve to facilitate the binding of dynein to its cargo and adaptor proteins (Li et al., 2004). Individual light chains have been reported to have additional dynein-independent roles within the cell. For example, dynein light chain 1, which is required for the stability of the motor in the cell, is also required to satisfy the spindle assembly checkpoint and for dynein-facilitated chromosome separation (Mische et al., 2008; Sivaram et al., 2009). Dynein light chain TcTex-1 acts as an effector of the G protein βγ subunits and is required to regulate neurite outgrowth (Sachdev et al., 2007), while dynein light chain LC8 is required for microtubule polymerization and bundling (Asthana et al., 2012). Additionally, dynein light intermediate chain 1 is required for the stability of photoreceptor development and survival (Kong et al., 2013).

Dynein moves along the microtubule with its attached cargo at a usual 8 nm-long step, but its step size can increase up to 32 nm. Optical trap experiments have shown that the size of each dynein step decreases with an increasing cargo load (Salina et al., 2002). The processivity of the motor is attributed to its two head regions: one will remain attached the microtubule while the other moves forward one step. These two motor regions also give dynein the capacity to sidestep to a neighboring protofilament while moving to the minus end of the microtubule in order to bypass obstacles along that microtubule (Allan, 2011; Redwine et al., 2012). Additionally, it has recently been shown

that dynein uses its two head regions to crosslink and slide anti-parallel microtubules (Tanenbaum et al., 2013).

The Dynactin Complex

Dynactin was initially identified *in vitro* as a complex required to activate dynein movement along microtubules (Schroer, 2004). For this reason, the complex was named the dynein-activating complex, or dynactin. Dynactin is commonly found in a complex with dynein throughout the cell and has been reported to be essential for many dynein-dependent functions. For example, dynactin has been shown to be required for the anchoring of dynein at the plasma membrane as well as the linkage of certain cargos to the dynein motor (Schroer, 2004).

Dynactin is a large multimeric complex, nearing 1.2 mDa in size (Figure 1.4). This complex is composed of 11 subunits that form two distinct structures: the rod and projecting arm (Schroer, 2004). The rod, which consists of the Arp1, Arp11, Actin, CapZ, p62, p27, and p25 subunits, assists in linking cargo to dynein. The projecting arm consists of the p150, Dynamitin, and p24/p22 subunits and is required for the coupling of dynein and dynactin. The largest subunit of the complex, p150, provides the essential link between dynein and dynactin complexes (Bader and Vaughan, 2010; Holzbaur and Vallee, 1994), while the Dynamitin subunit has been shown to be essential in connecting the dynactin rod and projecting arm (Schroer, 2004).

There is an abundance of literature describing the composition of dynein and dynactin complexes as well as defining the essential cellular events requiring the dynein-

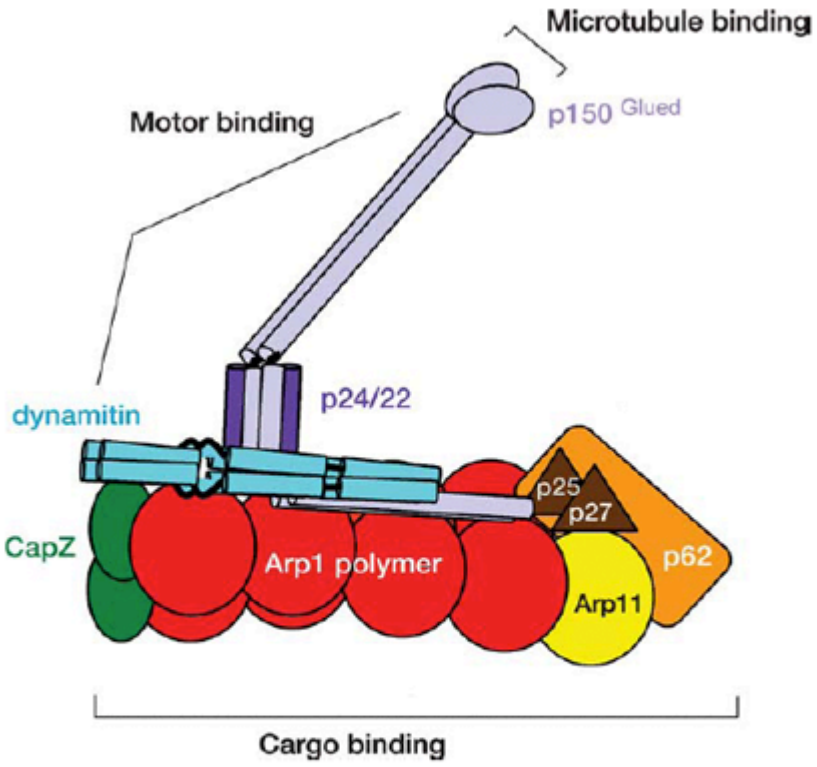

Figure 1.4 – The dynactin complex. Cartoon depicting the components of the dynactin complex as well as the microtubule, motor, and cargo binding domains. Adapted from Schroer, 2004.

dynactin complex. What is lacking, however, is a comprehensive understanding of the mechanisms by which these complexes are regulated to perform their functions within the cell.

Perinuclear Dynein

Due to its large number of roles in the cell, dynein motors exist under many layers of regulation. These forms of regulation include phosphorylation of dynein chains, subunit composition within the stem region, bound cargo or dynein-regulatory proteins, and subcellular localization (Kardon and Vale, 2009). A pool of dynein stably anchored to the nuclear surface has been observed in multiple species (Anderson et al., 2009; Bolhy et al., 2011; Gonczy et al., 1999; Hu et al., 2013; Payne et al., 2003; Robinson et al., 1999; Salina et al., 2002; Splinter et al., 2010). Though little is known about what regulates this localized pool of dynein, it has been shown to be required for numerous functions, including roles at the G2/M transition.

Perinuclear dynein has been shown to be essential for pulling the centrosomes towards the NE at the G2/M transition and facilitating centrosome coupling to the NE in *Drosophila* spermatocytes and cultured human cells (Anderson et al., 2009; Bolhy et al., 2011; Hu et al., 2013; Splinter et al., 2010). In a one-cell *C. elegans* embryo, perinuclear dynein is required for the migration of the male pronucleus towards the female pronucleus, which is positioned close to the centrosome (Malone et al., 2003). In rat radial glia progenitors, perinuclear dynein has recently been shown to be essential for apical migration of the nucleus, a prerequisite step for mitosis and proper neurogenesis (Hu et al., 2013). Perinuclear dynein is additionally required to facilitate separation of the

coupled centrosomes and their migration to opposite sides of the cell, thereby establishing the poles of the bipolar spindle (Robinson et al., 1999; Salina et al., 2002; Vaisberg et al., 1993). Finally, this pool of dynein residing on the NE has been implicated in assisting in the process of NEBD. It has been hypothesized that as the motor walks along the NE towards the centrosomes positioned at the prospective poles, it will begin to pull apart the NE (Beaudouin et al., 2002; Salina et al., 2002). Following NEBD, dynein accumulates on the kinetochores and along the spindle microtubules (Allan, 2011). It has not been established, however, whether the dynein residing on the bipolar spindle at the kinetochores is derived specifically from the pool of dynein anchored on the NE prior to NEBD. While a few proteins that promote dynein recruitment to the NE have been identified, a gap remains in our knowledge of the functions and regulation of this pool of dynein.

Regulators of Perinuclear Dynein

Though the presence of dynein motors anchored on the NE is evolutionarily conserved, the exact molecular mechanisms for its attachment appear to vary. In the one-cell *C. elegans* embryo, dynein is anchored to the nuclear surface by the KASH/SUN domain-containing proteins ZYG-12 and SUN-1, which span the outer and inner layers of the NE, respectively (Malone et al., 2003; Zhou et al., 2009). In *Drosophila* testes, *asun* has been shown to be essential for the recruitment of dynein to the NE in late G2 spermatocytes (Anderson et al., 2009). Within mammalian somatic cells and neuronal cells, at least two distinct protein scaffolds have evolved to ensure the proper execution of this critical event (Figure 1.5). These two proteins, Bicaudal D2 (BICD2) and

centromere protein-F (CENP-F), are key components of two non-redundant pathways that both employ nuclear pore complex (NPC) interactions to anchor dynein motors directly to the nuclear surface (Bolhy et al., 2011; Splinter et al., 2010).

BICD2 is a well-characterized dynein-adaptor protein that binds the stem region of the motor. Throughout the cell cycle, BICD2 is bound to both dynein and kinesin motors, though its function changes in a cell cycle-dependent manner. In G1, BICD2 interacts directly with Rab6 vesicles and functions in promoting their trafficking (Splinter et al., 2010). In G2, BICD2 migrates to the NE, where it interacts directly with a nucleoporin, RanBP2, found on the cytoplasmic face of the NPC. At the G2/M transition, BICD2 anchors the motor through its direct interactions with both the motor and RanBP2 (Splinter et al., 2010). BICD2-RanBP2 anchoring of dynein is conserved in both cultured human cells and rat radial glia progenitors (Hu et al., 2013; Splinter et al., 2010).

CENP-F is exclusively nuclear during the majority of the cell cycle, however, it becomes partially cytoplasmic in late G2. This cytoplasmic pool of CENP-F interacts directly with the centrosomal-bound dynein-adaptor proteins, NudE/L, as well as the Nup107-133 complex on the cytoplasmic face of the NPC (Bolhy et al., 2011). These two direct interactions are both essential for CENP-F to anchor dynein on the NE prior to mitotic entry (Bolhy et al., 2011).

asunder Regulates Dynein in *Drosophila* Spermatogenesis

Prior work in our lab identified *asun* as an essential regulator of perinuclear dynein during *Drosophila* spermatogenesis (Anderson et al., 2009). Spermatocytes of

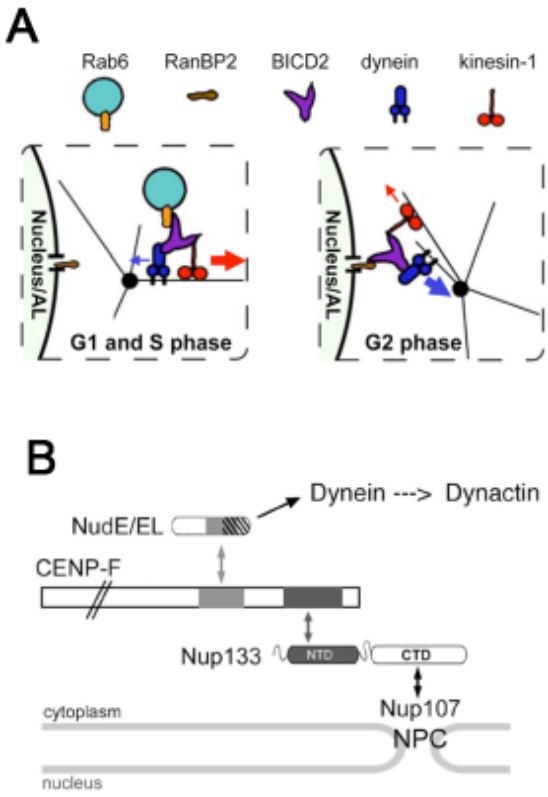

Figure 1.5 – Models for dynein anchoring to the nuclear surface via NPC. Two independent binding cassettes have been identified as essential for docking dynein on the nuclear envelope. A) BICD2 binds RanBP2 on the nuclear surface at G2/M (Splinter et al, 2010). B) CENP-F is bound to NudE/EL and Nup133, anchoring dynein to the nuclear surface (Bolhy et al., 2011).

asun mutant testes arrest at prophase of meiosis I, with severely decreased levels of perinuclear dynein. This absence of dynein on the NE results in a failure to properly couple centrosomes to the nuclear surface, and centrosomes remain free in the cytoplasm. The *asun* gene was named for this nucleus-centrosome coupling defect, with asunder meaning "set apart in space or time." *asun* spermatocytes that progress beyond the prophase arrest exhibit defects in spindle assembly, chromosome segregation, and cytokinesis during the meiotic divisions. The severe reduction in the perinuclear pool of dynein observed in *asun* spermatocytes is the likely basis for this constellation of defects.

ASUN displays a dynamic localization during male meiosis: ASUN is sequestered in the nucleus in early G2 spermatocytes and appears in the cytoplasm during late G2 (Anderson et al., 2009). This localization shift of ASUN from nuclear to cytoplasmic coincides with the recruitment of dynein to the nuclear surface (i.e. ASUN appears in the cytoplasm as dynein begins to accumulate on the NE). We previously hypothesized that cytoplasmic ASUN plays a direct role in recruiting dynein to the nuclear surface of male germline cells of *Drosophila*, thereby ensuring nucleus-centrosome coupling and fidelity of the meiotic divisions. The localizations of ASUN observed in *Drosophila* testes appear to be conserved in higher organisms: localizations ranging from nuclear to cytoplasmic were observed following over-expression of tagged versions of both *Drosophila* ASUN (dASUN) and human ASUN (hASUN) in cultured human cells.

Human Asunder

The human homologue of ASUN, identified by sequence homology, was originally termed *Germ Cell Tumor 1* (*GCT1*) for its presence in a genomic region that is

amplified and its up-regulation in human testicular seminomas (Bourdon et al., 2002). *GCT1* was identified in a screen aimed at elucidating factors of this particular cancer. We herein present data to justify changing the name of this human gene to "*asun*" based on its conserved role in promoting dynein recruitment to the NE and, consequently, nucleus-centrosome coupling.

Another group has identified hASUN as a subunit of the snRNA processing complex, Integrator (INT; described below), in a mass spectrometry study aimed at identifying novel components of this complex (Malovannaya et al., 2010). Further work has shown that hASUN is essential for the snRNA processing activity of the INT complex (Chen et al., 2012). In this study, INT activity was assessed using a novel cell-based assay in which cells were stably transfected with a GFP reporter that turns "on" when 3'-end processing of U7 RNA is disrupted (Chen et al., 2012). siRNA-mediated down-regulation of hASUN in cells carrying this reporter resulted in a robust GFP signal, indicating that hASUN is required for U7 RNA processing by the INT complex.

Small Nuclear RNA

Small nuclear ribonucleic acid (snRNA), also known as U-RNA, is a class of RNAs of roughly 150 nucleotides in length that are present in the nucleus (Matera et al., 2007). The pre-snRNAs are transcribed by RNA Polymerase II or III (RNApolII or RNApolIII) and receive a 5'-monomethylguanosine cap and 3'-end processing by INT in the nucleus. Following this processing, snRNAs are transported to the cytoplasm where they undergo additional 3'-end cleavage and hypermethylation of the 5'-end. These cytoplasmic modifications are required to assemble the snRNAs into stable small nuclear

ribonucloproteins (snRNPs), which consist of snRNAs associated with specific proteins (Matera et al., 2007). The 5'-end hypermethylation of snRNAs is used to import these snRNPs back into the nucleus (Matera and Shpargel, 2006). The most common snRNAs include U1, U2, U4, U5, U7, U11, and U12. These are the core components of the spliceosome, a nuclear complex required for splicing, or intron removal, of precursor messenger RNA (pre-mRNA) (Newby and Greenbaum, 2002).

The spliceosome is a large RNA-protein complex consisting of five U-RNAs and ~15 proteins that is essential for the proper maturation of mRNA. Defects in this complex can lead to catastrophic consequences for the cell (Nilsen, 2003). To promote intron splicing, snRNPs bind to specific sequences within the pre-mRNA and facilitate intron removal. In addition to splicing, the process of pre-mRNA maturation includes the addition of a 5'-end cap, 3'-end cleavage, and the addition of a poly-A tail to each pre-mRNA (Wahl et al., 2009). The resulting mature mRNAs are transported to the cytoplasm where they are translated to proteins by the ribosomes (Wahl et al., 2009).

The Integrator Complex

INT was originally identified as a protein complex coupled to the carboxy-terminal end of RNApolII. This complex consists of three subunits, each of which is designated as "IntS" followed by a unique identifying number based on size from largest to smallest (Baillat et al., 2005). INT is a highly conserved complex with readily identifiable orthologs in many species with at least one exception: *Saccharomyces cerevisiae* (Chen and Wagner, 2010). Initial investigations into the function of INT found that the depletion of its subunits lead to an accumulation of misprocessed snRNAs,

thereby establishing its role in snRNA processing (Baillat et al., 2005). Down-regulation of any of the individual INT subunits results in loss of function of the complex with only a couple of exceptions. IntS10 is not required for snRNA processing by the complex in cultured human cells, and IntS3 is not required in *Drosophila* S2 cells (Chen et al., 2012). Initial investigations into the function of INT found that the depletion of its subunits lead to an accumulation of misprocessed snRNA, thereby establishing its role in snRNA processing (Baillat et al., 2005).

During the processing of snRNAs, INT remains coupled to RNApolII as it transcribes the snRNA. Following identification of a conserved sequence in the 3'-end, termed the 3'-end box, of the nascent snRNA transcript, INT facilitates a cleavage at this site, releasing the newly cleaved transcript (Albrecht and Wagner, 2012) (Figure 1.6). It is important to note that the 3'-end box is unlikely to be the termination site for RNApolII, as it has been shown that the polymerase continues transcribing the RNA following the 3'-end processing of the snRNA by INT (Chen and Wagner, 2010). This finding indicates that the 3'-end box likely serves as a recognition site for INT to cleave specific snRNAs. Following their processing by INT, these snRNAs become incorporated into snRNPS that serve as essential components of the spliceosome as described above.

Underscoring the importance of INT in the cell is the identification of defects caused specifically by its loss. In cultured mammalian cells, siRNA-mediated loss of IntS4 leads to defective formation of nuclear structures known as Cajal bodies, which have been implicated in RNA metabolic processes such as biogenesis, maturation, and recycling (Takata et al., 2012). Down-regulation of either IntS6 or IntS11 disrupts proper differentiation of adipocytes (Otani et al., 2013a). *In vivo*, INT has been shown to be

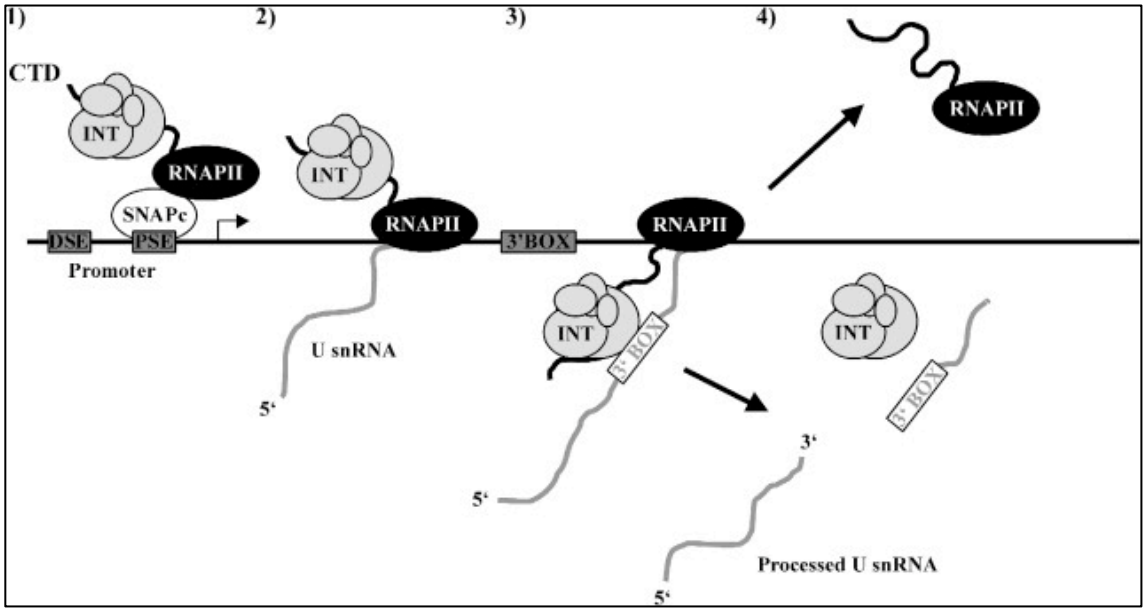

Figure 1.6 – Integrator complex. 1) INT is coupled to the C-terminal tail of RNAPII. 2 and 3) INT remains coupled during RNA transcription until it recognizes a 3'end-BOX sequence (a specific sequence that signifies the terminal end of a snRNA). 4) INT will cleave the 3'-end BOX, releasing the processed U snRNA. Adapted from Baillat at al., 2005.

required for multiple functions in *C. elegans,* zebrafish, and *Drosophila* (Kamath et al., 2003; Otani et al., 2013a; Rutkowski and Warren, 2009; Tao et al., 2009). Mutations in IntS7 result in abnormal craniofacial development in the worm as well as defects in both craniofacial and abdominal development in the fly (Golling et al., 2002; Kamath et al., 2003; Rutkowski and Warren, 2009). In zebrafish, loss of IntS5, IntS9, or IntS11 results in aberrant splicing of *smad1* and *smad5* transcripts, thereby leading to a disruption of erythrocyte differentiation (Tao et al., 2009). Due to the importance of proper mRNA maturation for viability of the cell, I hypothesize that additional phenotypes associated with loss of a functional INT complex will likely be identified in the future.

Ciliogenesis

Cilia are highly conserved, membrane-bound organelles that project outward from the cell membrane. They exist in two forms: 1) motile cilia, which utilize axonemal dynein to create a beating movement, and 2) PC, nonmotile sensory organelles (Ishikawa and Marshall, 2011). These microtubular projections are distinguished by the presence of a set of post-translational modifications, including acetylation, detyrosination, polyglutamylation, and glycylation, which ensure the stability and biochemical properties of the axoneme (Salisbury, 2004). The axoneme is a common structure shared by both motile and primary cilia. The axoneme of each primary cilium contains a ring of nine outer microtubule doublets without central microtubules (referred to as a 9+0 axoneme), while the axoneme of a motile cilium contains two central microtubule singlets in addition to the nine outer doublets (referred to as a 9+2 axoneme), allowing for its movement (Hagiwara et al., 2004; Ishikawa and Marshall, 2011). While several motile

cilia may be present in a given cell, only one primary cilium is allowed per cell (Ishikawa and Marshall, 2011).

PC formation occurs when the cell has entered quiescence or G1 in the cell cycle. At this time, the mother centriole migrates to the cell membrane where it matures into a basal body (BB); the cilium will emanate from this newly differentiated basal body (Kim and Dynlacht, 2013a; Salisbury, 2004). Characteristics of a mature BB include the presence of the basal feet, which assemble as the centriole is maturing, and transition fibers, which grow from the distal end of the BB and aide in membrane docking (Graser et al., 2007; Kim and Dynlacht, 2013a). For motile cilia, the process of ciliogenesis is quite different. Motile cilia are formed when the cell has reached terminal differentiation, and BB arise *de novo* using the mother centriole as a template to allow for multiple cilia per cell (Ishikawa and Marshall, 2011; Salisbury, 2004).

Once the PC are properly formed, their length must remain tightly regulated due to their critical roles in signaling (Basten and Giles, 2013; Ko, 2012). PC length appears to be maintained through the same mechanisms and regulations used to control PC formation (Ishikawa and Marshall, 2011). Additionally, interflagellar trafficking proteins, kinesins, and cytoplasmic dynein, which all function in moving cargo along the primary cilium, also play essential roles in regulating its length (Basten and Giles, 2013; Ko, 2012; Rajagopalan et al., 2009; Salisbury, 2004).

In order to progress through the cell cycle and into mitosis, PC must disassemble and be reabsorbed into the cell, as the presence of PC is not compatible with formation of the bipolar spindle (Ishikawa and Marshall, 2011; Kim et al., 2011; Salisbury, 2004; Wang et al., 2013). To facilitate disassembly, the post-translational modifications, which

provide stability to PC, must be reversed. Specifically, the removal of acetylation collapses the structure, resulting in a quick shortening of PC (Kim et al., 2011; Wang et al., 2013). Following the disassembly of a primary cilium, the BB becomes unanchored from the plasma membrane and loses its BB status (Salisbury, 2004).

Introduction to My Dissertation Research

My research is focused on the regulation of dynein at the G2/M transition, when the motor is directly anchored to the NE. In this dissertation, I present all my research aimed at elucidating an additional mechanism for regulating this accumulation of dynein on the NE. I start by presenting a novel regulator of this process, hASUN. I show that similar to its *Drosophila* homologue, hASUN has a conserved role in recruiting dynein to the NE prior to cell division; the loss of hASUN leads to defects in dynein recruitment to the NE resulting in additional downstream defects. Next, I present data pointing to a potential mechanism by which hASUN regulates perinuclear dynein. I report that hASUN promotes dynein recruitment in a manner dependent on its role within the RNA-processing complex, INT. I present an additional role for INT in regulating ciliogenesis in cultured human cells: loss of a functional INT complex results in a loss of PC formation in the cell. Finally, I present data that further support the model that INT regulates dynein recruitment to the NE and PC formation through two distinct mechanisms.

CHAPTER II

HUMAN ASUNDER PROMOTES DYNEIN RECRUITMENT AND CENTROSOMAL TETHERING TO THE NUCLEUS AT MITOTIC ENTRY

This chapter has been published (Jodoin et al., MBoC 2013).

Introduction

Cytoplasmic dynein plays critical roles in many cellular processes by carrying out minus-end-directed transport along microtubules (Holzbaur and Vallee, 1994). Dynein is a multimeric complex composed of heavy, intermediate, light intermediate, and light chains. Each heavy chain contains six ATPase domains that power the motor. Non-catalytic subunits regulate dynein by linking the complex to its cargo and adaptor proteins. Dynein complexes approach 2 MDa in size, making dynein the largest of all known motor complexes. The composition of dynein complexes and the cellular events requiring these complexes have been defined, although a comprehensive understanding of the mechanisms by which these complexes are regulated within cells is lacking.

Dynein complexes are subject to several modes of regulation, including phosphorylation, subunit composition, subcellular localization, and binding of accessory proteins. Dynactin, another large multimeric complex, was identified through *in vitro* studies as an activator of dynein; subsequent work suggested that dynein requires

dynactin to perform its cellular functions (Schroer, 2004). A dynein adaptor protein, Lissencephaly 1 (LIS1), binds directly to dynein heavy chains and is essential for multiple dynein functions, including coupling of centrosomes to the nucleus during neuronal migration (Kardon and Vale, 2009; Tanaka et al., 2004).

A dynein subpopulation stably anchored to the NE at the G2/M transition is essential for proper nucleus-centrosome coupling in multiple systems (Anderson et al., 2009; Bolhy et al., 2011; Malone et al., 2003; Splinter et al., 2010). Minus-end-directed movement of anchored dynein motors along astral microtubules has been hypothesized to draw centrosomes toward the nuclear surface to facilitate their attachment to the NE prior to NEBD (Burgess and Knight, 2004). This anchored pool of dynein has also been implicated in the process of NEBD (Beaudouin et al., 2002; Salina et al., 2002).

Although promotion of nucleus-centrosome coupling is a dynein-dependent function that is evolutionarily conserved, the exact molecular mechanisms appear to vary (Salina et al., 2002). Dynein is anchored to the nuclear surface via KASH and SUN domain-containing proteins in *C. elegans* embryogenesis and during neuronal migration in mice (Malone et al., 2003; Zhang et al., 2009). In a cultured mammalian cell line (HeLa), at least two distinct pathways are required to ensure proper execution of this critical event. These pathways both employ nuclear pore complex (NPC) interactions to anchor dynein motors to the nuclear surface. The first pathway uses RanBP2, a nucleoporin that associates with the cytoplasmic face of NPCs, as the docking site for BICD2 (Splinter et al., 2010). BICD2, directly bound to dynein, moves in a minus-end direction toward the nuclear surface just prior to the G2/M transition, thereby anchoring dynein at the NE. The second pathway uses another nucleoporin, Nup133, as a docking

site for CENP-F (Bolhy et al., 2011). Prior to G2/M, CENP-F directly binds dynein-bound NudE/EL; CENP-F then simultaneously binds Nup133 to anchor dynein, NudE/EL, and ultimately the centrosomes to the NE.

We previously identified *asun* as an essential regulator of dynein localization during *Drosophila* spermatogenesis (Anderson et al., 2009). Spermatocytes of *asun* mutant testes arrest at prophase of meiosis I with centrosomes unattached to the nucleus. *asun* spermatocytes that progress beyond this arrest exhibit defects in meiotic spindle assembly, chromosome segregation, and cytokinesis. The severe loss of perinuclear dynein in *asun* spermatocytes is the likely basis for this constellation of defects. Our studies revealed that dASUN plays a key role in recruiting dynein to the nuclear surface at G2/M, a critical step to establish nucleus-centrosome coupling and fidelity of meiotic divisions.

The human homologue of *asun* (also known as *GCT1* or *C12ORF11*) was originally identified in a screen for genes upregulated in testicular seminomas (Bourdon et al., 2002). While expression of *Drosophila asun* is limited to male and female germline cells, transcripts of the mouse homologue were detected in both germ lines and all somatic cells surveyed (Bourdon et al., 2002; Stebbings et al., 1998). These findings suggested that Asunder (ASUN) might play a broader role in mammals.

To further investigate the mechanism by which ASUN regulates dynein, we examined the function of the human homologue of ASUN (hASUN) in this study. We find that, like BICD2 and CENP-F, hASUN is required in cultured cells for enrichment of dynein on the nuclear surface at the onset of mitosis. hASUN depletion leads to mitotic defects, which are likely secondary to failure of dynein localization. We present a model

in which hASUN acts via a mechanism distinct from that of BICD2 and CENP-F to promote dynein recruitment to the nuclear surface at G2/M, a critical step to establish nucleus-centrosome coupling and fidelity of mitotic divisions.

Materials and Methods

Drosophila experiments

Flies were maintained at 25°C using standard techniques (Greenspan, 2004). *y w* was obtained from the Bloomington Drosophila Stock Center (Indiana University, Bloomington, IN) and used as the "wild-type" stock. The $asun^{f02815}$ allele (Exelixis Collection, Harvard Medical School, Boston, MA) and transgenic line with male germline-specific expression of CHY-dASUN were previously described (Anderson et al., 2009). cDNA encoding mASUN (clone details provided below) with an N-terminal CHY tag was subcloned into vector tv3 (gift from J. Brill, The Hospital for Sick Children, Toronto, Canada) for expression of CHY-tagged mASUN under control of the testes-specific *β2-Tubulin* promoter (Wong et al., 2005). Transgenic lines were generated by *P*-element-mediated transformation via embryo injection (Rubin and Spradling, 1982). A single transgene was mapped to the X chromosome and crossed into the $asun^{f02815}$ background using standard genetic crosses.

To test male fertility, individual adult males (2 d old) were placed in vials with five wild-type females (2 d old) and allowed to mate for 5 d. The percentage of males producing adult progeny and the average number of live adult progeny produced per fertile male were scored (≥10 males tested per genotype). Statistical analyses were

performed using Fisher's exact test (percentage of males producing progeny) and an unpaired Student's *t*-test (average number of progeny per fertile male).

Protein extracts were prepared by homogenizing dissected testes from newly eclosed males in SDS sample buffer. The equivalent of eight testes pairs was loaded per lane. Following SDS-PAGE, proteins were transferred to nitrocellulose for immunoblotting using standard techniques. Primary antibodies were used as follows: mCherry (1:500, Clontech) and mouse anti-beta-tubulin (E7, 1:5000, Developmental Studies Hybridoma Bank). HRP-conjugated secondary antibodies and chemiluminescence were used to detect primary antibodies.

Live testes cells were prepared for examination by fluorescence microscopy as described previously (Kemphues et al., 1980). Briefly, testes were dissected from newly eclosed adult males, placed in a drop of PBS on a microscopic slide, and gently squashed under a glass cover slip after making a small incision near the stem cell hub. Formaldehyde fixation was performed as described previously (Gunsalus et al., 1995). Briefly, slides of squashed testes were snap-frozen, immersed in 4% formaldehyde (in PBS with 0.1% Triton X-100) for 7 minutes at -20°C after cover slip removal, and washed three times in PBS. Primary antibodies were used as follows: mouse anti-DHC (P1H4, 1:120, gift from T. Hays [University of Minnesota, Minneapolis, MN]) (McGrail and Hays, 1997) and rat anti-alpha-tubulin (Mca77G, 1:300; Accurate Chemical & Scientific, Westbury, NY). Fixed samples were mounted in PBS with DAPI to visualize DNA. Wide-field fluorescent images were obtained using an Eclipse 80i microscope (Nikon) with Plan-Fluor 40X objective.

In experiments to determine the percentage of late G2 spermatocytes or immature

spermatids with perinuclear dynein or the percentage of prophase I spermatocytes with nucleus-centrosome coupling, at least 200 cells were scored per genotype; statistical analyses were performed using Fisher's exact test. To quantify the ratios of perinuclear to diffusely cytoplasmic dynein in late G2 spermatocytes (testes stained for DHC), following image acquisition, the average intensity of the DHC signal within a small rectangular region was sampled near the nuclear surface and in the surrounding cytoplasm using Adobe PhotoShop. The ratio of the intensities was determined. At least 30 cells from a minimum of three testes pairs were scored per genotype. Statistical analysis was performed using an unpaired Student's *t*-test.

Cell culture and treatments

Cell lines were maintained at 37˚C and 5% CO_2 in DMEM (Gibco) containing 10% FBS, 1% L-Glutamine, 100 μg/ml streptomycin, and 100 U/ml penicillin. U2OS and RPE cells were cultured in antibiotic-free media. Plasmid DNA was transfected into cells using Lipofectamine 2000 (Invitrogen) or Fugene HD (Promega). siRNA duplexes were purchased from Dharmacon. siGENOME NT siRNA#5 was used as negative control. siRNA sequences were designed to target human *ASUN* at its 5'-end (#1: 5'-GGAAAUAGAGGACGAAUAAUU-3') or its 3'-end (#2: 5'-CAGAAGAGGAAGAACGAAA-3'; *LIS1* (5'-GAGTTGTGCTGATGACAAG-3') (Shu et al., 2004); *CENP-F* (5'-CAGAATCTTAGTAGTCAAGTA-3') (Bolhy et al., 2011); or *BICD2* (5'-GGUGGACUAUGAGGCUAUC-3') (Splinter et al., 2010). hASUN siRNA#1 was used for all experiments in this study unless otherwise indicated. Cells were transfected with siRNA duplexes using DharmaFECT 1 transfection reagent

(Dharmacon) in two successive rounds and analyzed 3 d later. Lipofectamine 2000 (Invitrogen) transfection reagent was used for co-transfection of cells with siRNA and DNA constructs. Where indicated, cells were incubated in 5 μg/ml (16.6 μM) nocodazole (Sigma) for 3 h prior to fixation to enhance perinuclear localization of dynein. For metaphase arrest, cells were incubated for 16 h in 10 μM RO-3306 (Cdk1 inhibitor; Enzo Life Sciences) followed by incubation for 3 h in 10 μM MG-132 (proteasome inhibitor; Calbiochem). Approximately 80% of cells were arrested in metaphase under these conditions.

Fixation, immunostaining, and microscopy

Cells were either fixed in methanol (5 min at -20°C followed by washing with TBS plus 0.01% Triton X-100) or 4% formaldehyde (20 min at RT followed by 20 min permeabilization step with TBS plus 0.05% Triton X-100). Cells were blocked in TBS plus 0.01% Triton X-100 and 0.02% BSA prior to immunostaining. Primary antibodies were used as follows: C-hASUN (1:500), PH3 (Mitosis Marker; 1:1000, Millipore or 1:2000, Abcam), DIC (clone 74.1, 1:500, Abcam), Pericentrin centriolar marker (clone 28144, 1:2000, Abcam), c-Myc (9E10, 1:1000), beta-tubulin (clone E7, 1:1000, Developmental Studies Hybridoma Bank), CENP-F (clone 14C10 1D8, 1:200, Abcam), BICD2 (1:300; gift from A. Akhmanova [Erasmus Medical Center, Rotterdam, The Netherlands]), and NPC marker (Mab414, 1:1000, Abcam). Appropriate secondary antibodies conjugated to Alexa Fluor 488 or Cy3 were used (1:1000, Invitrogen). Cells were mounted in ProLong Gold Antifade Reagent with DAPI (Invitrogen).

Wide-field fluorescence images were obtained using an Eclipse 80i microscope

(Nikon) with Plano-Apo 100X objective. Confocal stacks were taken by a Yokogawa QLC-100/CSU-10 spinning disk head (Visitec assembled by Vashaw) attached to a Nikon TE2000E microscope using a CFI PLAN APO VC 100× oil lens, NA 1.4, with or without 1.5× intermediate magnification, and a back-illuminated EM-CCD camera Cascade 512B (Photometrics) driven by IPLab software (Scanalytics). A krypton-argon laser (75 mW 488/568; Melles Griot) with AOTF was used for two-color excitation. Custom double dichroic mirror and filters (Chroma) in a filter wheel (Ludl) were used in the emission light path. Z steps (0.2 μm) were driven by a Nikon built-in Z motor.

Line scan analyses were performed using ImageJ. Ten representative cells were measured per condition; for each cell, twelve line scans distributed equally around the nuclear circumference were obtained. Lines scans presented within figures are 100 pixels in length and are oriented with the cytoplasmic end of each line to the left and the intranuclear end of each line to the right. To quantify the ratios of perinuclear to diffusely cytoplasmic DIC in stained HeLa cells, the average intensity of the DIC signal within a small rectangular region was sampled near the nuclear surface and in the surrounding cytoplasm using ImageJ. The ratio of the intensities was determined. At least 30 cells were scored per condition.

Statistical analyses of experiments reported herein were performed using Student's unpaired *t*-test unless otherwise noted. Error bars indicate SEM for all bar graphs. All experiments were performed a minimum of three times with at least 100 cells scored per condition unless otherwise noted.

Fluorescence activated cell sorting

Cells (~10^7) treated with NT or ASUN siRNA were fixed with 70% EtOH for 24 h followed by propidium iodide staining for 24 h. DNA content was assessed by measuring propidium iodide intensity levels. Gating was used to exclude cell debris and doublets from the DNA analysis. Flow cytometry experiments were performed in the VUMC Flow Cytometry Shared Resource.

DNA constructs

cDNA clone LD33046 encoding ASUN was obtained from the *Drosophila* Gene Collection. IMAGE cDNA clones encoding mASUN (#4459471) and human LIS1 (#5786560) were obtained from ATCC. Constructs for expression of the following N-terminally tagged proteins were generated by subcloning into vector pCS2: HA- and CHY-dASUN; HA- and Myc-mASUN; HA-, Myc-, and CHY-LIS1. The HA-LIS1 expression construct was a gift from Deanna Smith (University of South Carolina Biological Sciences, Columbia SC). The GFP-BICD2 expression construct was a gift from A. Akhmanova (Erasmus Medical Center, Rotterdam, The Netherlands) (Hoogenraad et al., 2001). Mobyle@Pasteur v1.0.4 was used to determine the percent identities and similarities between ASUN proteins from different species.

Anti-ASUN antibody production

Two rabbit polyclonal antibodies (M-hASUN Ab and C-hASUN Ab) were raised using synthetic peptides corresponding to the following amino acid residues of hASUN: IIKDSPDSPEPPNKKPLVEC (619-637) and CSVNNRAELYQHLKEENG (678-694),

respectively. Exogenous cysteine residues were added for conjugation and affinity purification purposes. After exsanguination, ELISA-positive antisera were antigen-affinity purified to a final concentration of ~1 mg/mL.

Immunoblotting and co-immunoprecipitation

Lysates were prepared using non-denaturing lysis buffer (50 mM Tris-Cl pH 7.4, 300 mM NaCl, 5 mM EDTA, 1% Triton X-100). Following SDS-PAGE, proteins were transferred to nitrocellulose for immunoblotting using standard techniques. Immunoblotting was performed using the following primary antibodies: c-Myc (9E10, 1:1000), HA (CAS 12, 1:1000), beta-tubulin (clone E7, 1:1000, Developmental Studies Hybridoma Bank), mCherry (1:500, Clontech), CENP-F (clone 14C10 1D8, 1:500, Abcam), DIC (clone 74.1, 1:500, Abcam), DMN (clone 25, 1:250, BD Biosciences), M-hASUN (1:300), and C-hASUN (1:500). BICD2 antibody (1:2500) was a gift from A. Akhmanova (Erasmus Medical Center, Rotterdam, The Netherlands) (Hoogenraad et al., 2001). HRP-conjugated secondary antibodies (1:5000) and chemiluminescence were used to detect primary antibodies. For co-immunoprecipitation experiments, anti-c-Myc agarose beads (40 μl; Sigma) were incubated with lysates of transfected HEK293 cells (500 μg) for 1 h at 4°C with shaking and washed 3X in lysis buffer. Samples were boiled in 6X sample buffer, resolved by SDS-PAGE, and analyzed by immunoblotting.

Sucrose density gradients

HeLa cells were transfected with either NT or hASUN siRNA. At 3 d post-transfection, lysates were prepared using non-denaturing lysis buffer (described above).

Lysates were layered on top of sucrose gradients (5 mL) with equal volumes of 30%, 20%, 10%, and 5% sucrose in PBS (137 mM NaCl, 7 mM Na_2HPO_4, and 3 mM NaH_2PO_4, pH 7.2). Samples were centrifuged at 46,000 rpm for 16 h in a swinging-bucket rotor (SW55ti; Beckman Coulter). Following centrifugation, fractions (167 mL) were collected and analyzed by immunoblotting. Molecular weight standards were obtained from BioRad.

Results

Mammalian ASUN can functionally replace dASUN during spermatogenesis

The predicted hASUN and mouse ASUN (mASUN) proteins are 95% identical and 97% similar to each other; comparison of the predicted mammalian and *Drosophila* ASUN proteins revealed that they are 43% identical and 64% similar. We sought to determine if a mammalian form of ASUN could functionally replace dASUN *in vivo*. Using the *Drosophila* model system, we established transgenic lines expressing mCherry-tagged mASUN (CHY-mASUN) exclusively in the male germ line (Figure 2.1A). We found that the presence of a single copy of the CHY-mASUN transgene significantly increased the percentage of $asun^{f02815}$ males (hypomorphic allele) that produced adult progeny (Figure 2.1B) (Anderson et al., 2009). We also observed a significant increase in the number of adult progeny produced per fertile male, albeit not to the level of wild-type controls (Figure 2.1C). We previously reported that germline expression of CHY-tagged dASUN fully rescued the sterility of *asun* males; the partial rescue obtained by germline

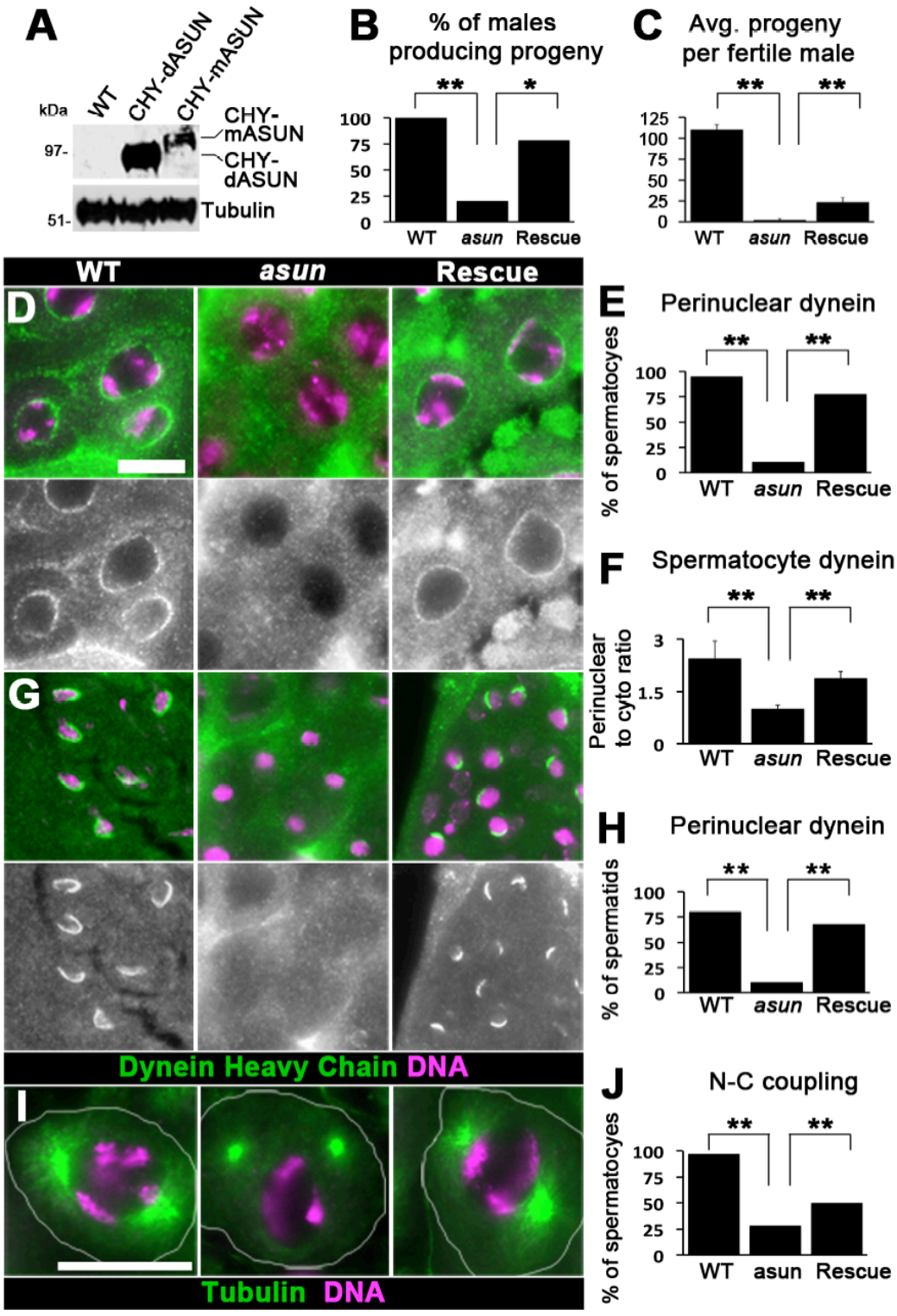
A
WT
CHY-dASUN
CHY-mASUN
kDa
97-
51-
CHY-mASUN
CHY-dASUN
Tubulin
B
% of males producing progeny
100
75
50
25
0
WT
asun
Rescue
C
Avg. progeny per fertile male
125
100
75
50
25
0
WT
asun
Rescue
WT
asun
Rescue
D
E
Perinuclear dynein
% of spermatocyes
F
Spermatocyte dynein
Perinuclear to cyto ratio
G
H
Perinuclear dynein
% of spermatids
Dynein Heavy Chain DNA
I
J
N-C coupling
% of spermatocyes
Tubulin DNA

Figure 2.1. mASUN partially rescues spermatogenesis defects of *Drosophila asun* mutants. (A) Anti-CHY immunoblot of testes extracts from *Drosophila* wild-type (WT) males with or without germline expression of CHY-dASUN or CHY-mASUN; a relatively low expression level of a fusion protein of the expected size was observed for the latter. Tubulin was used as loading control. (B, C) Male fertility assays. "Rescue" indicates *asun* males with germline expression of CHY-mASUN, which increased the percentage of *asun* males producing progeny (B) and the average number of progeny per fertile male (C). (D-H) Germline CHY-mASUN expression restored perinuclear dynein in *asun* primary spermatocytes and spermatids. (D-F) Representative G2 spermatocytes stained for DHC and DNA are shown (D) with bar graphs depicting percentages of spermatocytes exhibiting perinuclear DHC (E) and average ratios of perinuclear to diffusely cytoplasmic DHC signal intensities (F). (G, H) Representative immature spermatids stained for DHC and DNA are shown (G) with bar graph depicting percentages of spermatids exhibiting perinuclear DHC (H). (I, J) Germline CHY-mASUN expression restored nucleus-centrosome coupling in *asun* primary spermatocytes. (I) Prophase I spermatocytes stained for β-tubulin and DNA. (J) Quantification of nucleus-centrosome coupling in prophase spermatocytes. Asterisks, $p<0.0001$ (double) or $p<0.001$ (single). Scale bars, 50 μm.

expression of the mouse homologue might be due to the relatively low level of expression of this fusion protein in the fly testes (Figure 2.1A) (Anderson et al., 2009).

We previously identified a critical role for dASUN in recruitment of dynein motors to the nuclear surface and nucleus-centrosome coupling in *Drosophila* male germline cells (Anderson et al., 2009). We next asked whether a mammalian form of ASUN could similarly regulate these events. The severe reduction of perinuclear dynein heavy chain (DHC) that is a hallmark feature of *asun* G2 spermatocytes and immature spermatids was almost fully restored to wild-type levels by transgenic CHY-mASUN expression (Figure 2.1, D-H). We also observed a significant increase in the degree of nucleus-centrosome coupling at prophase in *asun* spermatocytes harboring the CHY-mASUN transgene (Figure 2.1, I and J). Together, these findings reveal that mASUN can functionally replace its *Drosophila* homologue *in vivo* to regulate dynein localization during spermatogenesis and suggest that the molecular function of ASUN is conserved across phyla.

hASUN is required for dynein anchoring to the NE at prophase

Based on the role of dASUN during male meiosis and the broader expression pattern of mASUN, we reasoned that vertebrate homologues of ASUN might promote dynein recruitment to the NE of somatic cells at the onset of mitosis. To test this hypothesis, we performed siRNA-mediated knockdown of hASUN in HeLa cells. We confirmed that ASUN was efficiently depleted from cells by immunoblotting with anti-peptide antibodies (M-hASUN Ab and C-hASUN Ab) directed against distinct epitopes in the C-terminal region of hASUN (Figure 2.2A). siRNA-treated cells were briefly

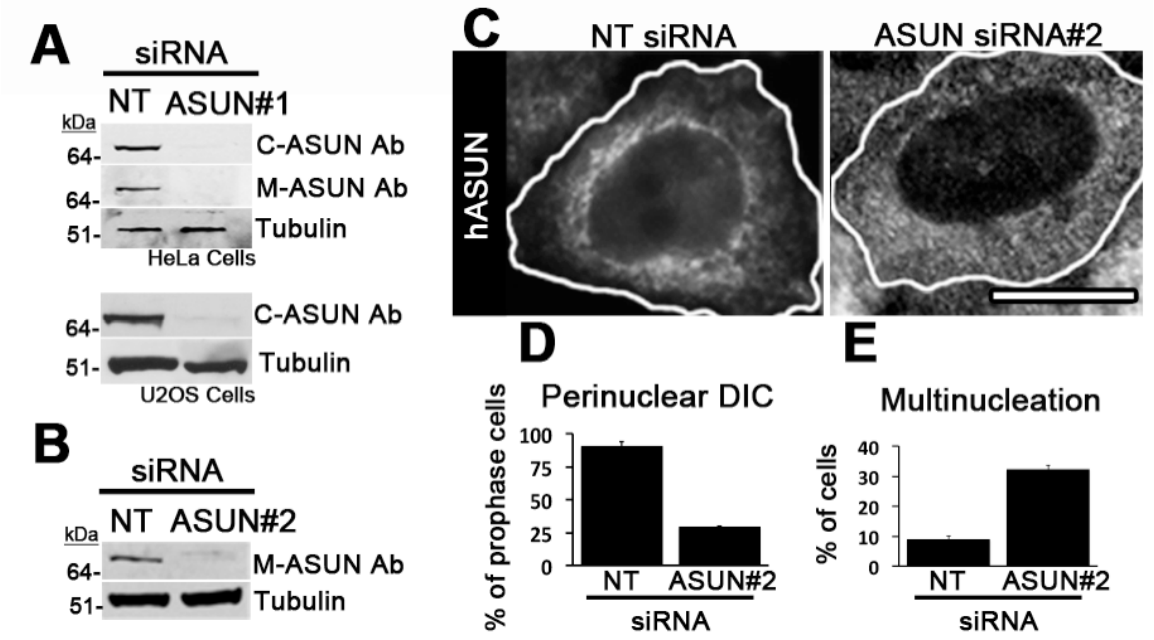

Figure 2.2. Knockdown of hASUN by two independent siRNA sequences. For all panels, HeLa or U2OS cells were treated for 3 d with NT siRNA (control), hASUN siRNA#1, or hASUN siRNA#2. (A, B) Immunoblotting of cell lysates revealed a similar degree of knockdown of hASUN protein using hASUN siRNA#1 (A) or hASUN siRNA#2 (B). Tubulin was used as loading control. (C) Cells were fixed and immunostained for hASUN. The cytoplasmic hASUN signal present in control cells was lost in hASUN-siRNA#2 cells. (D) Cells were nocodazole-treated, fixed, and stained for PH3, DIC, and DNA. The perinuclear pool of dynein was markedly reduced in hASUN-siRNA#2 cells compared to control cells. (E) Cells were fixed and stained for tubulin and DNA. Cells containing >2 nuclei were scored as multinucleated. An increased percentage of hASUN-siRNA#2 cells were multinucleated compared to control cells. Scale bar, 20 μm.

incubated with nocodazole to enhance perinuclear localization of dynein-dynactin complexes and accessory proteins prior to fixation and immunostaining for dynein intermediate chain (DIC) (Beswick et al., 2006; Bolhy et al., 2011; Hebbar et al., 2008; Splinter et al., 2010). We found that ~91% of NT-siRNA (non-targeting control) prophase cells showed strong perinuclear dynein staining (Figure 2.3, A and D-F). After hASUN knockdown, however, only ~30% of cells exhibited this pattern; instead, the majority of prophase cells displayed diffuse localization of dynein in the cytoplasm (Figure 2.3, B and D-F). Using a second independent hASUN-siRNA sequence that efficiently depleted ASUN from cells, we observed a similar reduction in the percentage of prophase cells with perinuclear dynein (Figure 2.2, B-D).

We considered the possibility that hASUN might function to destabilize microtubules; in that case, downregulation of hASUN could inhibit nocodazole-induced depolymerization of microtubules, thereby blocking access of dynein to the NE. We performed immunostaining experiments to assess whether microtubules undergo a normal degree of nocodazole-induced depolymerization following loss of hASUN. We observed essentially identical tubulin staining patterns for NT-siRNA versus hASUN-siRNA cells in response to nocodazole treatment, suggesting that the lack of perinuclear dynein observed in hASUN-siRNA cells is not secondary to gross alterations of the microtubule network (Figure 2.4).

To further confirm that loss of perinuclear dynein in hASUN-siRNA HeLa cells was due to depletion of endogenous hASUN, we performed a rescue experiment by transiently expressing CHY-tagged dASUN (refractory to hASUN siRNA). CHY-dASUN restored perinuclear dynein in hASUN-siRNA prophase cells to levels similar to

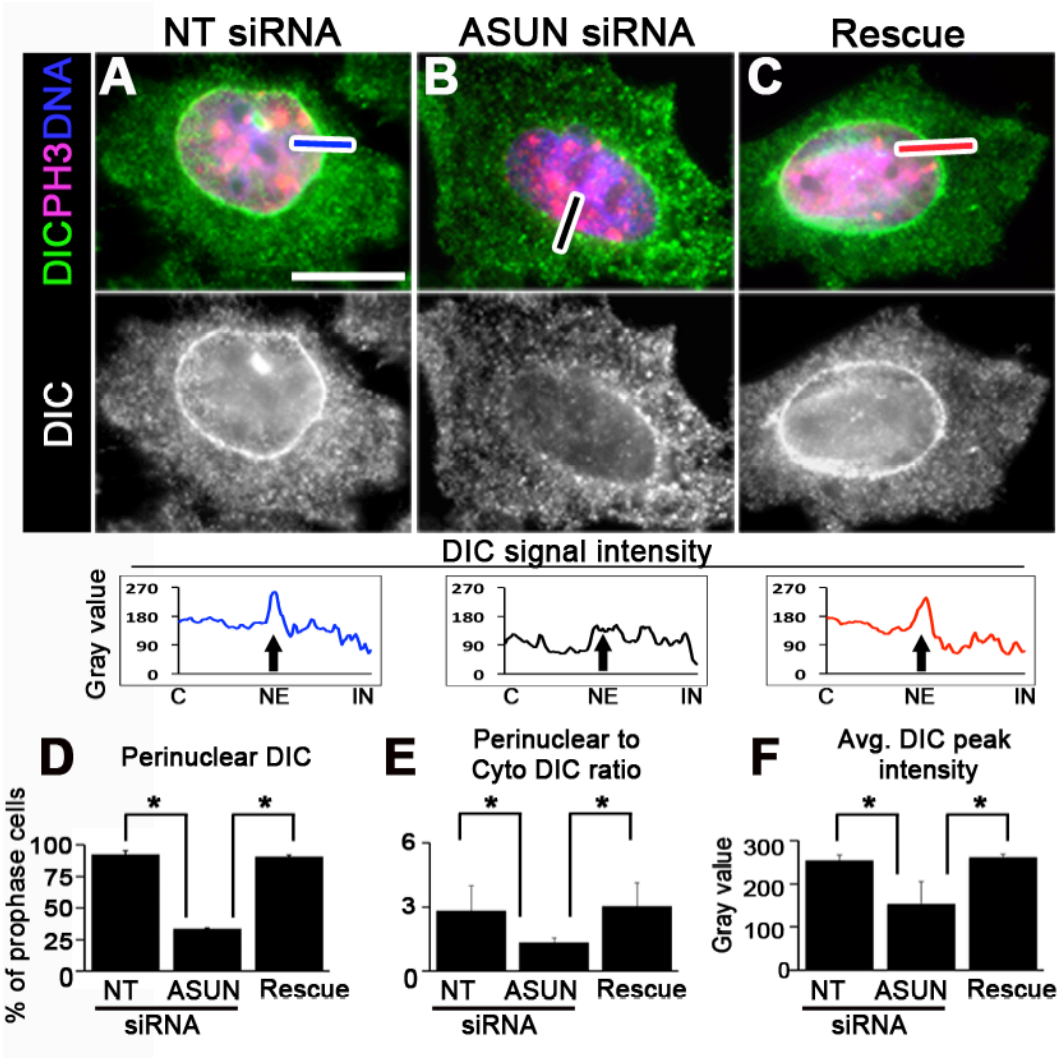

Figure 2.3. hASUN is required for localization of dynein to the NE at mitotic entry. (A-C) HeLa cells were transfected with NT siRNA, hASUN siRNA, or hASUN siRNA plus a CHY-dASUN expression construct ("Rescue"). After nocodazole treatment, cells were fixed and stained for DIC, PH3, and DNA. Both the percentage of prophase cells with perinuclear DIC and the ratio of perinuclear to cytoplasmic DIC signal intensity were reduced by hASUN knockdown (compare B to A); CHY-dASUN expression rescued these defects (C). Note that CHY-dASUN cannot be visualized in panel C because its signal intensity was much weaker than that of PH3 (visualized with Cy3-conjugated secondary antibodies). (D-F) Quantification of dynein localization defects in hASUN-siRNA cells. Representative line scans (corresponding to blue, black, and red lines in A, B, and C, respectively) of DIC intensity centered at the NE (marked by arrows) are shown below each micrograph with average peak intensities plotted in F. C, cytoplasmic. IN, intranuclear. Asterisks, $p<0.0001$. Scale bars, 20 μm.

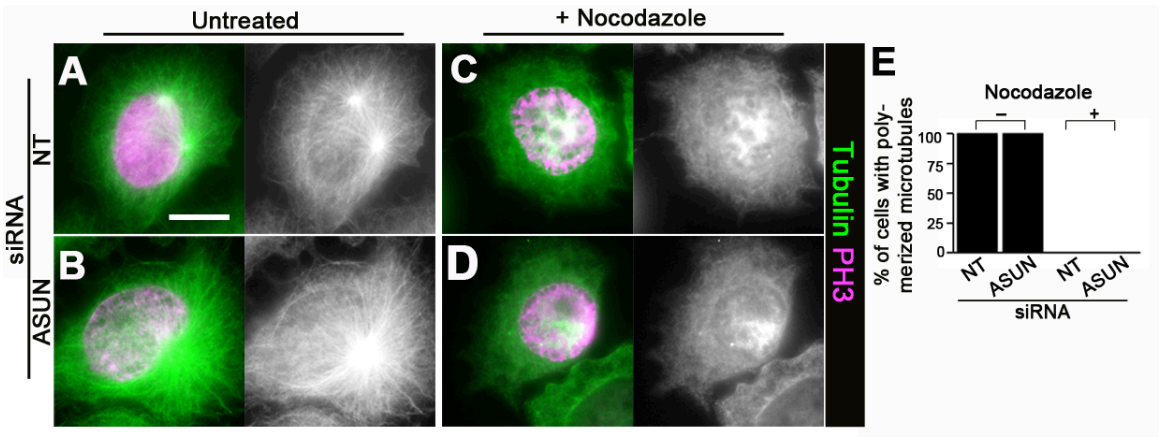

Figure 2.4. hASUN knockdown does not inhibit microtubule depolymerization by nocodazole. HeLa cells were transfected with NT or hASUN siRNA, treated with nocodazole for 3 h or left untreated, fixed, and stained for Tubulin and PH3. (A-B, E) Without nocodazole treatment, polymerized microtubules were present in 100% of NT-siRNA and hASUN-siRNA PH3+ cells. (C-E) Following nocodazole treatment, microtubules were depolymerized in 100% of both NT-siRNA and hASUN-siRNA PH3+ cells. Scale bar, 20 μm.

that of control cells (Figure 2.3, C-F). These results confirmed that loss of perinuclear dynein in hASUN-siRNA cells was specifically caused by hASUN depletion and demonstrated that dASUN can replace its human homologue to promote dynein recruitment to the NE at prophase.

We considered an alternative possibility that hASUN is required for stability of dynein-dynactin complexes rather than to promote their enrichment on the NE. Depletion of individual dynein-dynactin components can destabilize other subunits of these complexes (Mische et al., 2008; Schroer, 2004). We immunoblotted for DIC and Dynamitin (DMN; dynactin subunit) in extracts of HeLa cells following hASUN knockdown and found no changes in their cellular levels (Figure 2.5A). We also performed sucrose density gradient analysis to assess whether dynein complexes remained intact after hASUN knockdown and found no change in migration profiles (Figure 2.5B). Together, these data suggest that hASUN is not required to maintain integrity of dynein-dynactin complexes.

hASUN is required for proper coupling of centrosomes to the NE at prophase

Perinuclear dynein is essential for proper tethering of centrosomes to the NE at G2/M (Bolhy et al., 2011; Splinter et al., 2010; Tanenbaum et al., 2010). Based on the loss of perinuclear dynein we observed in hASUN-siRNA HeLa cells at prophase, we predicted that nucleus-centrosome coupling defects would ensue. We used the human osteosarcoma U2OS cell line for these studies. Due to the relatively decreased density of the microtubule network in these cells, centrosomes undergo a more dramatic migration

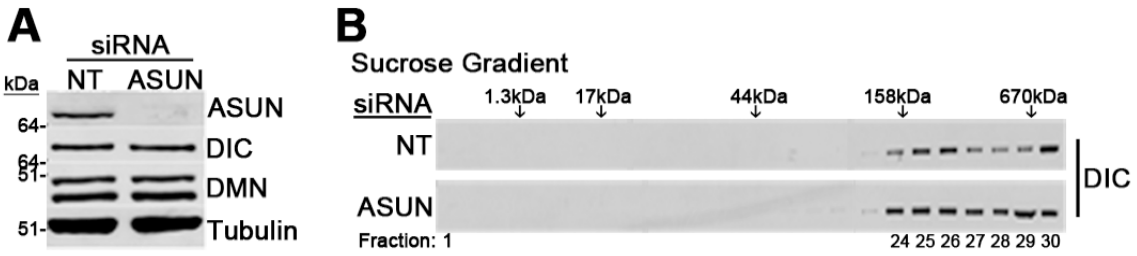

Figure 2.5. hASUN is not required for the stability of dynein-dynactin components or dynein complex integrity. HeLa cells were transfected with either NT or hASUN siRNA, and lysates were prepared 3 d later. (A) Immunoblotting confirmed normal levels of dynein-dynactin components (DIC and DMN) following hASUN siRNA. Tubulin was used as loading control. (B) DIC-containing dynein complexes exhibited a normal migration pattern on sucrose density gradients following hASUN knockdown. Arrows indicate elution peaks of molecular weight standards.

from the nucleus to the cortex at interphase and back to the nuclear surface at G2/M (Akhmanova and Hammer, 2010).

We found that ~19% of hASUN-siRNA U2OS cells exhibited loss of coupling of one or both centrosomes to the NE at prophase compared to a baseline rate of ~4% in control cells (Figure 2.6, A-E; Figure 2.2A). We measured an average distance of ~8 μm between the nucleus and centrosomes in hASUN-siRNA cells compared to a baseline distance of ~3 μm in control cells (Figure 2.6F). These data indicate that hASUN is required for normal linkage of centrosomes to the NE during prophase, and they further demonstrate evolutionary conservation of function of ASUN homologues.

hASUN is required for proper spindle formation and fidelity of mitotic divisions

Current evidence suggests that the perinuclear pool of dynein mediating nucleus-centrosome coupling at G2/M is also required for the fidelity of subsequent mitotic events (Splinter et al., 2010; Tanenbaum et al., 2010). If centrosomes are improperly coupled to the NE at prophase, their separation to prospective poles prior to NEBD may be random, leaving room for errors in mitotic spindle assembly and chromosome segregation (Tanenbaum et al., 2010). Given our identification of a role for hASUN in dynein recruitment and centrosomal tethering to the NE at mitotic prophase, we assessed whether loss of hASUN in HeLa cells would induce downstream mitotic defects.

We tested the capacity of HeLa cells to form normal bipolar spindles after hASUN knockdown. To enrich for cells with mitotic spindles, siRNA-transfected cells were treated with a Cdk1 inhibitor (RO-3306) and released into media containing a proteasome inhibitor (Vassilev, 2006). We found that ~35% of hASUN-siRNA cells

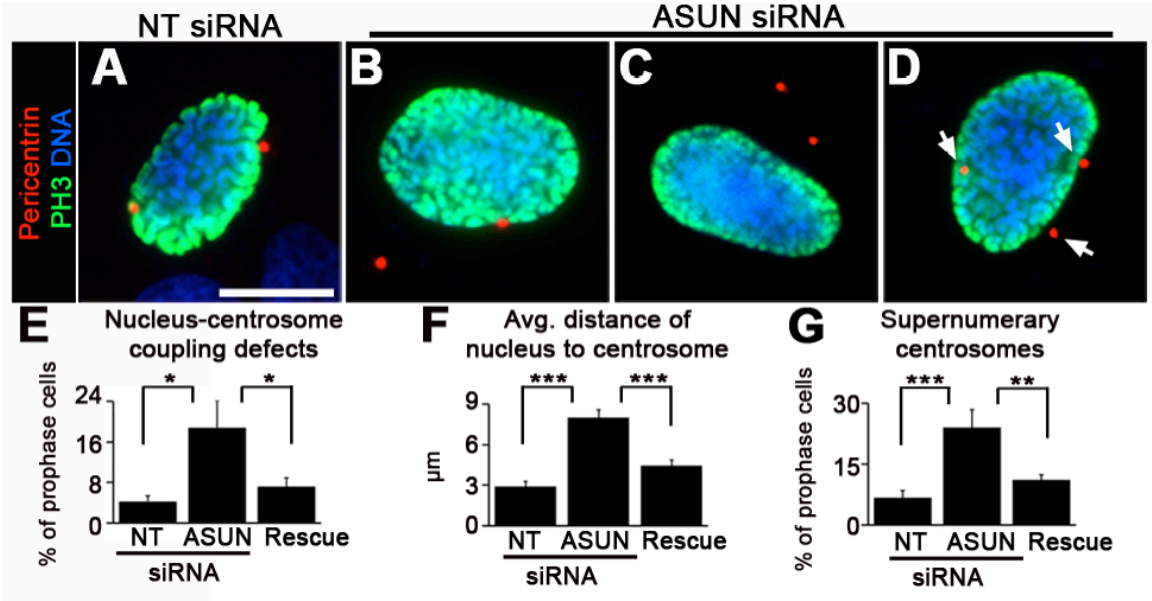

Figure 2.6. hASUN is required for recruitment of centrosomes to the NE at mitotic entry. (A-D) U2OS cells were transfected with NT or hASUN siRNA, fixed, and stained for Pericentrin (centrosomal marker), PH3, and DNA. hASUN knockdown yielded an increased percentage of prophase cells with loss of coupling of one (B) or both (C) centrosomes to the NE compared to control cells (A) as well as supernumerary centrosomes (arrows in D). (E-G) Quantification of centrosome defects in hASUN-siRNA cells. Expression of CHY-dASUN in hASUN-siRNA cells ("Rescue") corrected these defects. Asterisks, $p<0.0001$ (triple), $p<0.005$ (double), or $p<0.02$ (single). Scale bar, 20 μm.

exhibited mitotic spindle defects ranging from lack of chromosome congression to the metaphase plate, broadened spindles, and multipolar spindles; these defects, which were seen in ~11% of control cells, were fully rescued by CHY-dASUN expression (Figure 2.8, A-D and H). We found that these spindle defects of hASUN-siRNA cells were not associated with an increased mitotic index, suggesting that loss of hASUN does not cause any major delays in progression through mitosis (Figure 2.7).

We also assessed DNA content following loss of hASUN by microscopic examination of DNA-stained HeLa cells. We previously noted the presence of multinucleated HeLa cells after hASUN downregulation; this phenotype, however, was not quantified or further characterized (Lee et al., 2005). To quantify the multinucleation phenotype, we scored cells only if they contained greater than two nuclei due to the common occurrence of binucleation in control HeLa cells. We found that ~37% of hASUN-siRNA cells were multinucleated (typically containing three nuclei) compared to ~9% of control cells, and this defect was fully rescued by CHY-dASUN expression (Figure 2.8, E, F, and I). Furthermore, loss of hASUN caused an even more severe degree of multinucleation: ~6% of hASUN-siRNA cells contained >4 nuclei, which we never observed in control cells (12/177 and 0/165 cells, respectively; Figure 2.8G). Using a second independent siRNA sequence, we also observed multinucleation of HeLa cells following hASUN knockdown (Figure 2.2E).

A common cause of multinucleation involves successful completion of chromosome segregation during mitosis followed by a lack of cell division; increased centriole number is another indicator of cytokinesis failure (Godin and Humbert, 2011). In addition to multinucleation, we observed supernumerary centrosomes in ~24% of pro-

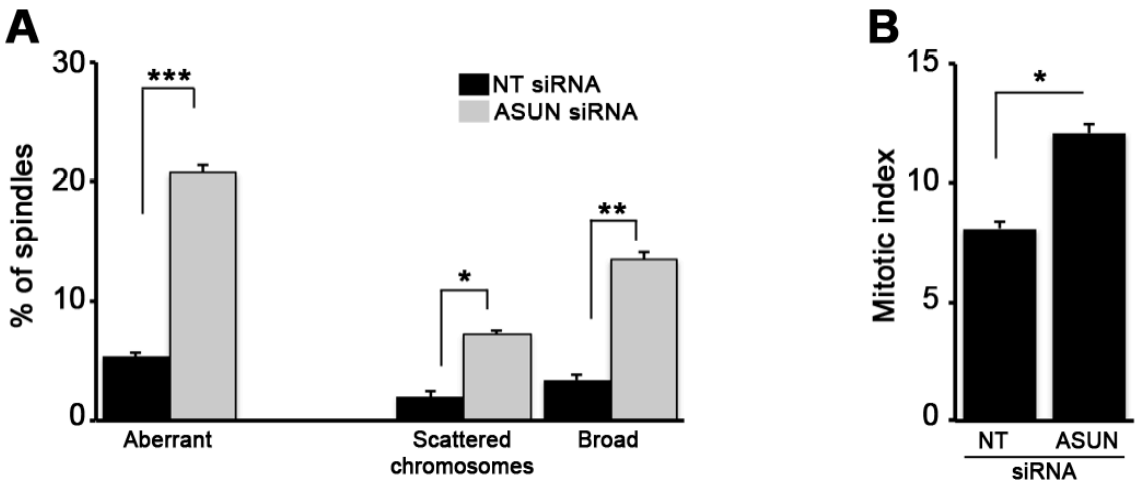

Figure 2.7. Quantification of mitotic spindle defects and mitotic index after hASUN knockdown. (A) HeLa cells were transfected with NT or hASUN siRNA, fixed, and stained for Tubulin and DNA. Bar graph displays quantification of mitotic spindle defects (total on left, subdivided into classes on right) in hASUN-siRNA versus NT-siRNA metaphase cells without drug treatment. For each siRNA condition, at least 300 metaphase spindles were scored. (B) HeLa cells were transfected with NT or hASUN siRNA, fixed, and stained for PH3 and DNA. Bar graph displays mitotic index (number of PH3-positive cells/total number of cells scored, expressed as percentage). For each siRNA condition, at least 800 cells were scored per experiment. n = 3. Statistical analyses were performed using an unpaired Student's *t*-test (A) or Fisher's exact test (B). Asterisks, $p<0.00002$ (triple), $p<0.0002$ (double), or $p<0.001$ (single).

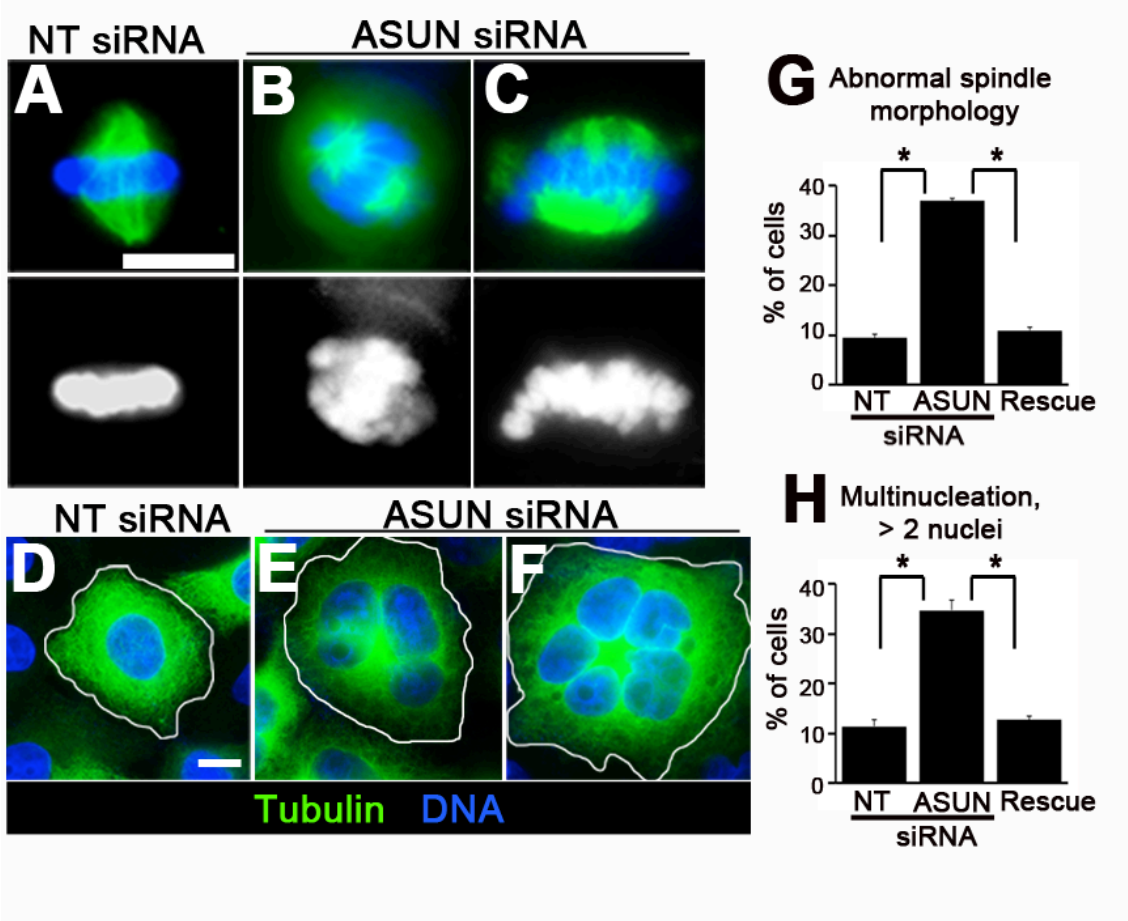

Figure 2.8. Loss of hASUN causes mitotic spindle defects and multinucleation. (A-F) HeLa cells were transfected with NT or hASUN siRNA, fixed, and stained for tubulin and DNA. (A-C) Mitotic spindles. To enrich for mitotic spindles, cells were arrested in metaphase before fixation. NT-siRNA cells had bipolar spindles with tight alignment of chromosomes at metaphase (A). hASUN-siRNA cells had an increased percentage of abnormal spindles with defects such as scattering of chromosomes along spindles (B) and broadened spindles (C). (D-F) Interphase cells. An increased percentage of hASUN-siRNA cells (E, F) were multinucleated (>2 nuclei) compared to NT-siRNA cells (D). We occasionally observed a more severe degree of multinucleation (>4 nuclei) in hASUN-siRNA cells (F). (G, H) Quantification of spindle morphology defects (G) and multinucleation (H) in hASUN-siRNA cells. Expression of CHY-dASUN in hASUN-siRNA cells ("Rescue") corrected these defects. Asterisks, $p<0.0001$. Scale bars, 20 μm.

phase cells following hASUN knockdown compared to ~5% of control cells; this defect was corrected by expression of CHY-dASUN (Figure 2.6, D and G). Our data are consistent with a possible role for hAUN in mitotic events downstream of nucleus-centrosome coupling: proper spindle formation and execution of cytokinesis.

hASUN is required for dynein anchoring to the NE at prophase in non-transformed cells

To confirm that the observed loss of NE-bound dynein following knockdown of hASUN is independent of the transformed nature of HeLa cells, we performed a similar analysis using human retinal pigment epithelial (RPE) cells, which are non-transformed. We detected strong perinuclear localization of dynein after nocodazole treatment in 59% of control RPE cells; in contrast, we observed this staining pattern in only 12% of cells following knockdown of ASUN (Figure 2.9, A-D). We observed an increased frequency of multinucleation in RPE cells following ASUN knockdown, possibly due to downstream mitotic defects caused by loss of perinuclear dynein: ~35% of ASUN-siRNA cells had greater than one nucleus compared to ~10% of control cells (Figure 2.9, E-G). These data suggest that the role of ASUN in regulating recruitment of dynein to the nuclear surface is not limited to transformed cells.

hASUN is cytoplasmic at G2/M

We previously reported that a tagged form of dASUN exhibited a meiotic stage-specific localization pattern in *Drosophila* spermatocytes: intranuclear in early G2 and appearing in the cytoplasm in late G2, coincident with dynein recruitment to the nuclear

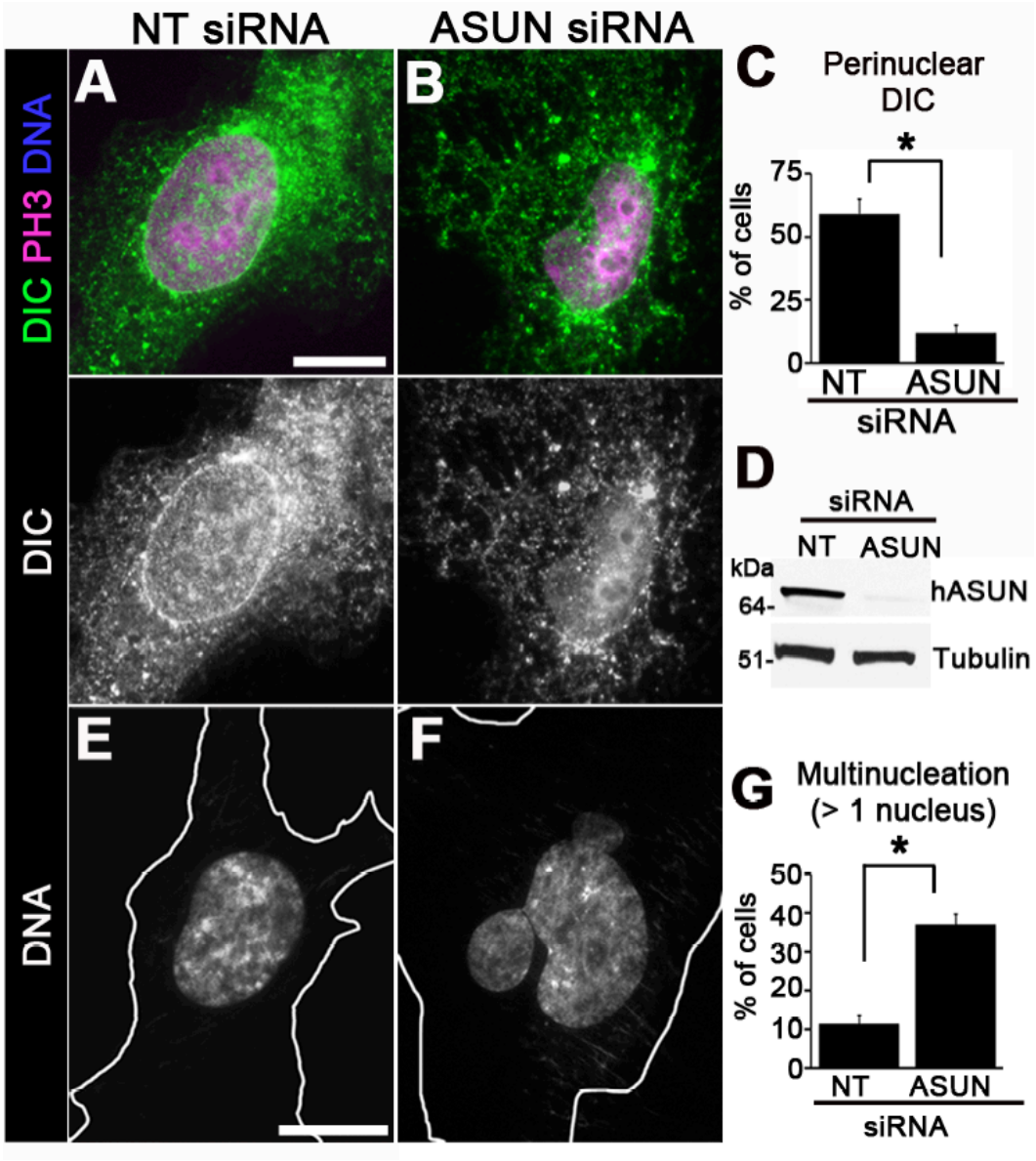

Figure 2.9. Loss of hASUN causes reduction of perinuclear dynein and multinucleation in non-transformed cells. (A-C) Dynein localization defects in hASUN-siRNA RPE cells. RPE cells were transfected with NT or hASUN siRNA. After nocodazole treatment, cells were fixed and stained for DIC, PH3, and DNA. The percentage of prophase cells with perinuclear DIC was reduced following hASUN knockdown (B) compared to control cells (A) (quantified in C). (D) Immunoblotting of lysates confirmed downregulation of hASUN. Tubulin was used as loading control. (E-G) A higher percentage of hASUN-siRNA RPE cells (F) were multinucleated (>1 nucleus per cell) compared to control cells (E) (quantifed in G). Asterisks, $p<0.0005$. Scale bars, 20 μm.

surface (Anderson et al., 2009). Tagged versions of dASUN and hASUN co-expressed in HeLa cells exhibited similar localization patterns during mitosis (Anderson et al., 2009).

To further understand the mechanism by which ASUN controls dynein localization at G2/M, we sought to determine the localization pattern of the endogenous protein in cultured human cells during prophase. Using C-hASUN Ab for immunostaining of HeLa cells, we found endogenous hASUN to be localized to the cytoplasm in ~98% of prophase cells (85/87 cells; Figure 2.10A). We used the following criteria to identify prophase cells: phosphorylated histone (PH3)-positive DNA and intact NE.

To further confirm that this localization pattern reflects that of endogenous hASUN, HeLa cells were transfected with either control or hASUN siRNA followed by immunostaining with C-hASUN Ab. The hASUN signal present in control cells was lost in hASUN-siRNA cells, demonstrating specificity (Figure 2.10, B and C). We confirmed these results with a second hASUN-siRNA sequence (Figure 2.2C). We found that Myc-tagged mASUN transiently expressed in HeLa cells tightly co-localized with endogenous hASUN, indicating a conserved localization pattern of the human and mouse homologues, which are ~95% identical at the amino acid level (Figure 2.10D).

Two dynein-recruiting proteins, BICD2 and CENP-F, have recently been reported to bind NPCs at prophase via direct interactions with the NPC components RanBP2 and Nup133, respectively (Bolhy et al., 2011; Splinter et al., 2010). Due to their similar functions in recruiting dynein complexes to the NE, we considered the possibility that hASUN might also bind to NPCs at prophase. We observed minimal co-localization,

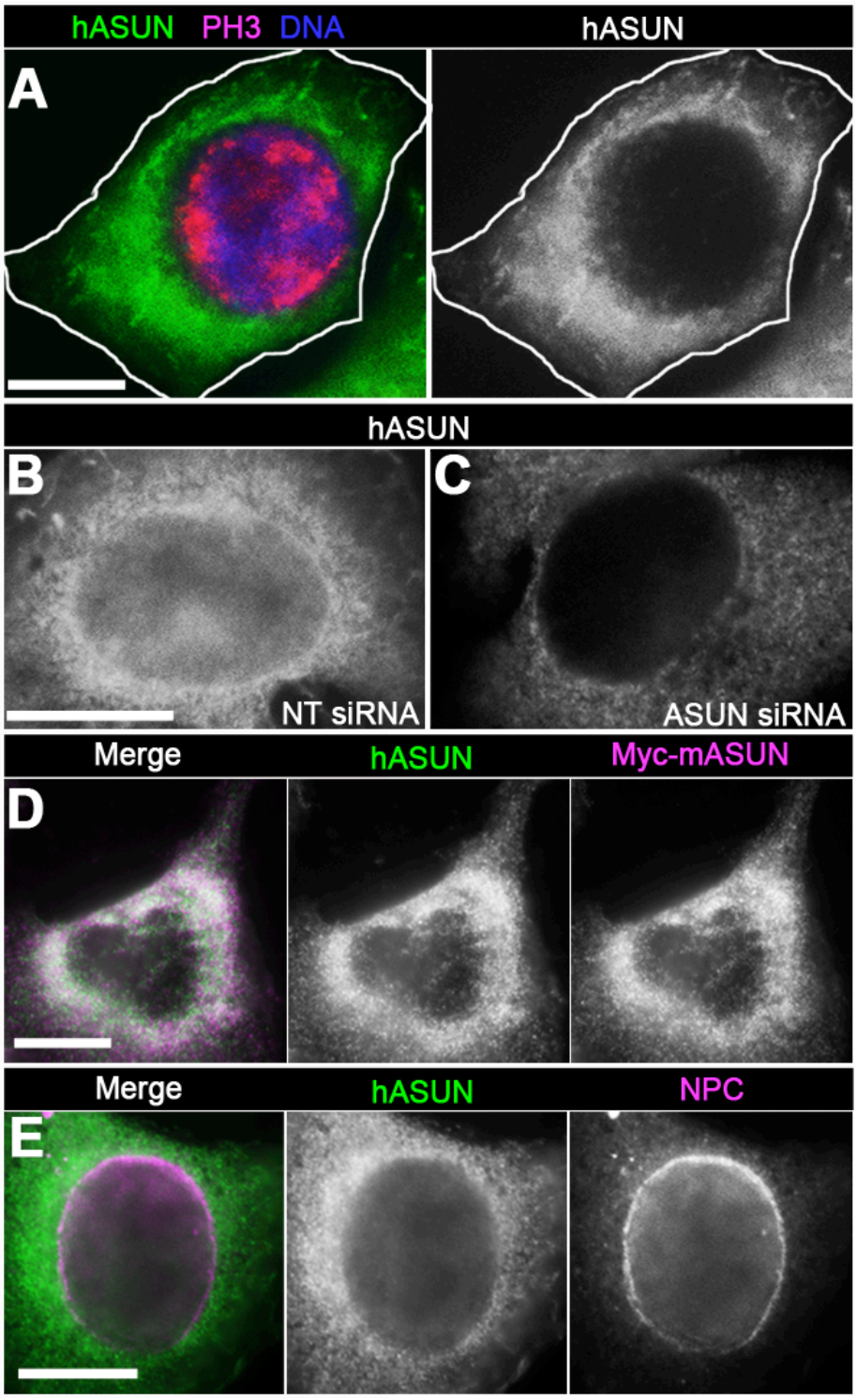
hASUN PH3 DNA
hASUN
A
hASUN
B
NT siRNA
C
ASUN siRNA
Merge
hASUN
Myc-mASUN
D
Merge
hASUN
NPC
E

Figure 2.10. Subcellular localization of ASUN. In all panels, HeLa cells were immunostained for endogenous hASUN using anti-peptide antibodies (C-hASUN Ab). (A) PH3 co-staining revealed endogenous hASUN localizes to the cytoplasm of prophase cells. (B, C) The hASUN signal of NT-siRNA cells (B) was lost in hASUN-siRNA cells (C), thereby demonstrating specificity. (D) Co-localization of endogenous hASUN and transiently expressed Myc-tagged mASUN. (E) Co-staining of endogenous hASUN revealed no significant overlap with the NPC marker Mab414. Scale bars, 20 μm.

however, of endogenous hASUN and a marker for NPCs in co-stained cells (Figure 2.10E).

hASUN interacts with the dynein adaptor, LIS1

We recently demonstrated a strong genetic interaction between *Drosophila asun* and *Lis-1*, co-immunoprecipitation and co-localization of dASUN and *Drosophila* LIS-1 proteins in cultured cells, and dependency of LIS-1 localization on dASUN during spermatogenesis (Sitaram et al.). Based on these findings, we considered the possibility that this interaction might be conserved between the mammalian homologues.

We showed co-immunoprecipitation of Myc-tagged mASUN and hemagglutinin (HA)-tagged human LIS1 following their co-expression in HEK293 cells, suggesting that these proteins exist within a complex; the capacity of these two proteins to co-immunoprecipitate was maintained when the affinity tags were switched (Figure 2.11, A and B; Figure 2.12). We also demonstrated co-immunoprecipitation of human LIS1 and *Drosophila* ASUN proteins, further indicating evolutionary conservation of this interaction (Figure 2.13). In further support of these data, we found that CHY-LIS1 co-localizes with endogenous hASUN in the perinuclear region of ~70% of nocodazole-treated HeLa cells (Figure 2.11, C and E). Line scans confirmed that hASUN and CHY-LIS1 have overlapping staining patterns, although tight co-localization was not consistently observed (Figure 2.11D). Despite the interaction observed between ASUN and LIS1, we did not detect co-immunoprecipitation of ASUN and dynein-dynactin subunits (Figure 2.14A).

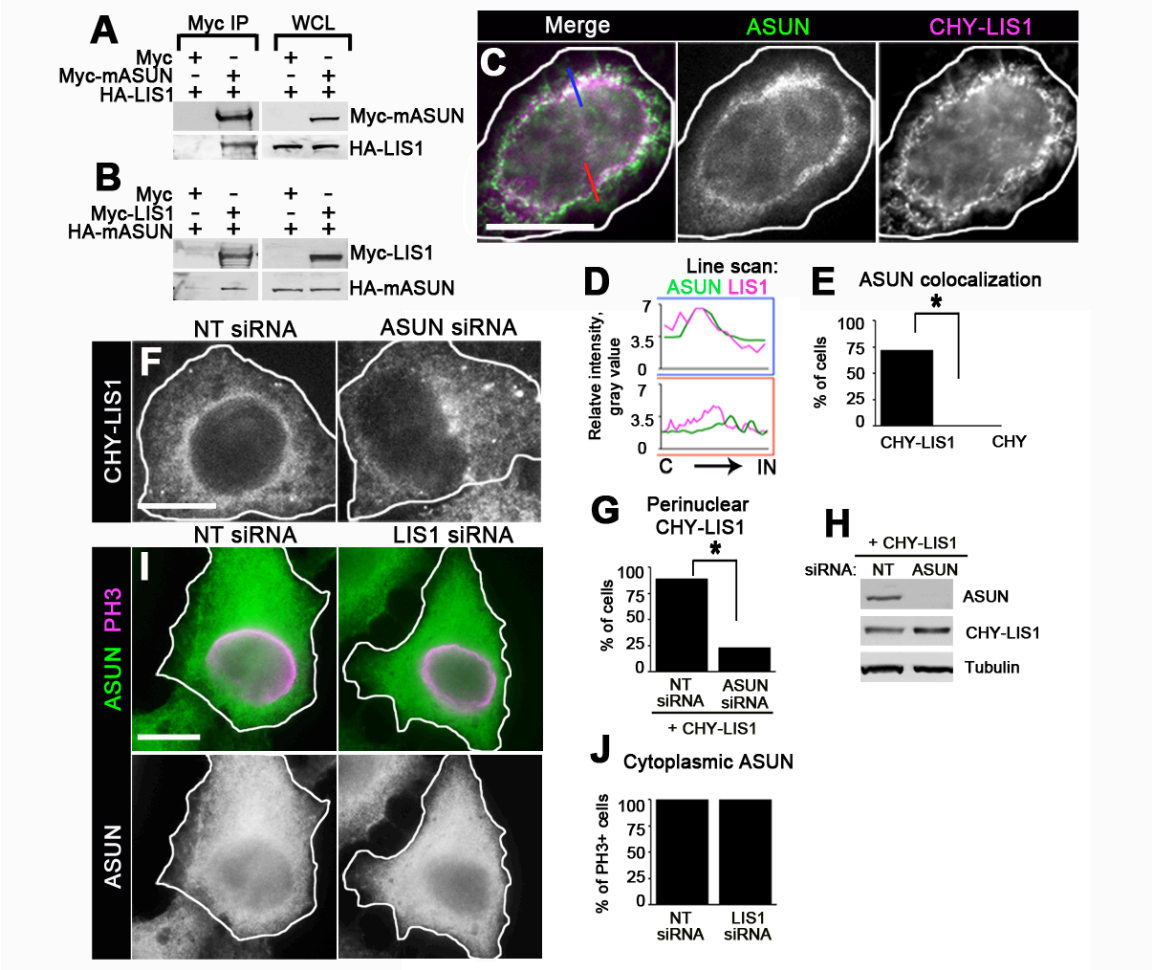

Figure 2.11. Interactions between ASUN and LIS1. (A, B) Co-immunoprecipitation experiments. (A, B) Lysates of HEK293 cells co-expressing the indicated tagged versions of mASUN and human LIS1 were used for Myc immunoprecipitation. Immunoblots of whole cell lysates (WCL) and Myc immunoprecipitates (IP) were probed with HA and Myc antibodies. Representative blots are shown. (C-E) Overlapping localizations of hASUN and CHY-LIS1. Transfected HeLa cells expressing CHY-LIS1 were treated with nocodazole, fixed, and stained for hASUN. (C) Representative cell with partial overlap of hASUN and CHY-LIS1 in the perinuclear region is shown. (D) Line scans centered at the NE (corresponding to blue and red lines in D) confirmed co-localization of hASUN and CHY-LIS1 in some but not all areas. C, cytoplasmic. IN, intranuclear. (E) Quantification of overlap of perinuclear CHY-LIS1 (but not CHY) and hASUN in a majority of transfected cells. (F-H) Perinuclear localization of CHY-LIS1 is hASUN-dependent. HeLa cells co-transfected with NT or hASUN siRNA plus CHY-LIS1 expression construct were treated with nocodazole and fixed. (F) Representative hASUN-siRNA cell with loss of perinuclear CHY-LIS1 compared to control is shown. (G) Quantification of the loss of perinuclear CHY-LIS1 following hASUN knockdown. (H) Immunoblotting revealed no change in steady-state levels of CHY-LIS1 protein after hASUN knockdown.

Figure 2.11 continued: Tubulin was used as loading control. (I, J) ASUN localization at G2/M is independent of LIS1. HeLa cells transfected with NT or LIS1 siRNA were stained for PH3 and ASUN. (I) NT-siRNA and LIS1-siRNA cells showed comparable ASUN staining patterns. (J) Quantification of cytoplasmic ASUN localization in PH3+ cells after LIS1 knockdown. Asterisks, $p<0.0001$. Scale bars, 20 μm.

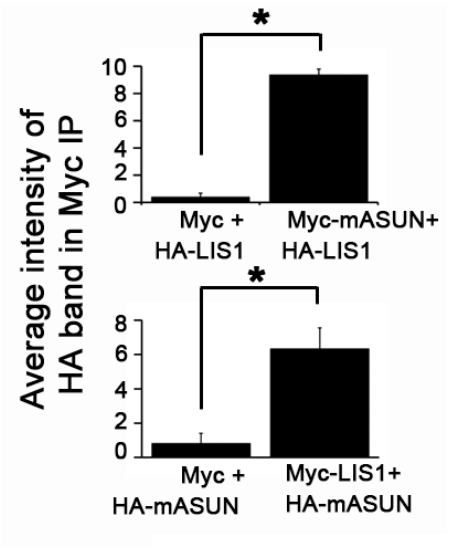

Figure 2.12. Co-immunoprecipitation of mASUN and human LIS1. Quantification of immunoblots presented in Figure 7, A and B. The average intensities of the HA band signals on immunoblots of Myc immunoprecipitates are shown.

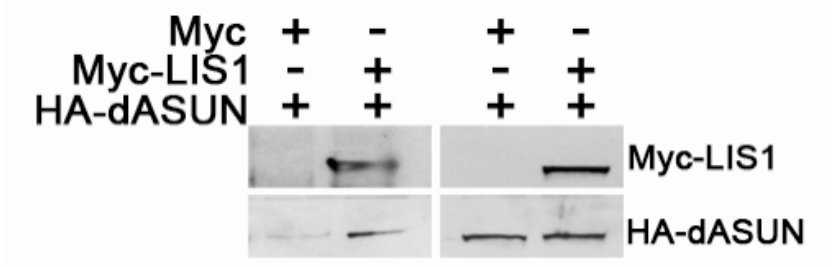

Figure 2.13. Co-immunoprecipitation of dASUN and human LIS1. Lysates of HEK293 cells co-expressing HA-tagged dASUN and either Myc (control) or Myc-tagged human LIS1 were used for Myc immunoprecipitation. Immunoblots of whole cell lysates (WCL) and Myc immunoprecipitates were probed with Myc and HA antibodies.

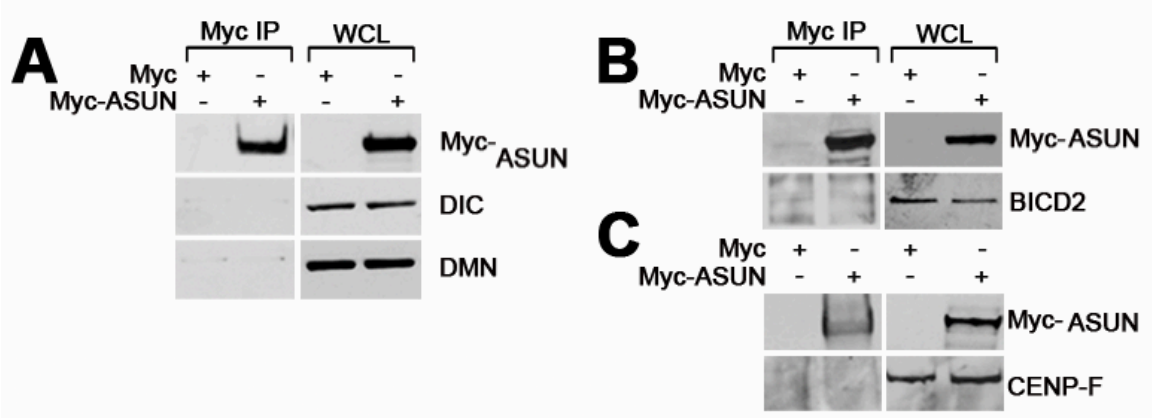

Figure 2.14. mASUN does not co-immunoprecipitate with BICD2, CENP-F, or dynein-dynactin components. Myc-tagged mASUN was transiently expressed in HEK293 cells, and lysates were prepared for Myc immunoprecipitation. Neither DIC (A), DMN (A), BICD2 (B), or CENP-F (C) proteins were detected by immunoblotting of the Myc immunoprecipitates.

To further explore the nature of the relationship between ASUN and LIS1, we tested whether hASUN is required for perinuclear enrichment of LIS1 at G2/M. Following nocodazole treatment, perinuclear CHY-LIS1 was detected in less than 25% of cells with loss of hASUN compared to ~80% of control cells (Figure 2.11, F and G). Immunoblot analysis revealed no change in CHY-LIS1 levels after hASUN knockdown, suggesting that ASUN is not required to maintain steady-state levels of LIS1 within cells (Figure 2.11H). These data are consistent with a model in which hASUN acts via LIS1 to recruit dynein complexes to the NE at prophase. The localization of ASUN at G2/M, however, was not dependent on LIS1 (Figure 2.11, I and J; Figure 2.15).

hASUN, BICD2, and CENP-F localize independently of each other at prophase

Two pathways, BICD2–RanBP2 and NudE/EL–CENP-F–Nup133, have been described that appear to operate independently to anchor dynein to the NE and facilitate proper positioning of centrosomes at the G2/M transition (Bolhy et al., 2011; Splinter et al., 2010). We confirmed that BICD2 and CENP-F co-localize to the NE of prophase HeLa cells as we would predict based on independent reports of their localization patterns (Figure 2.16A) (Bolhy et al., 2011; Splinter et al., 2010). As expected from our demonstration that the hASUN immunostaining pattern excludes the NE, we observed essentially no overlap of endogenous hASUN and GFP-BICD2 signals (Figure 2.16B). Furthermore, we observed no co-immunoprecipitation from cell lysates of ASUN with either BICD2 or CENP-F (Figure 2.14, B and C).

We asked whether knockdown of hASUN, BICD2, or CENP-F in HeLa cells would globally disrupt the structure of NPCs in such a way that docking of dynein motors

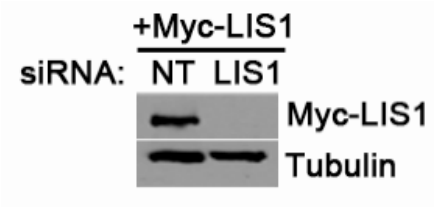

Figure 2.15. LIS1 siRNA effectively depletes its target protein. HeLa cells were co-transfected with a Myc-LIS1 expression construct and either NT or LIS1 siRNA. Lysates were analyzed by immunoblotting with Myc antibodies. Tubulin was used as loading control.

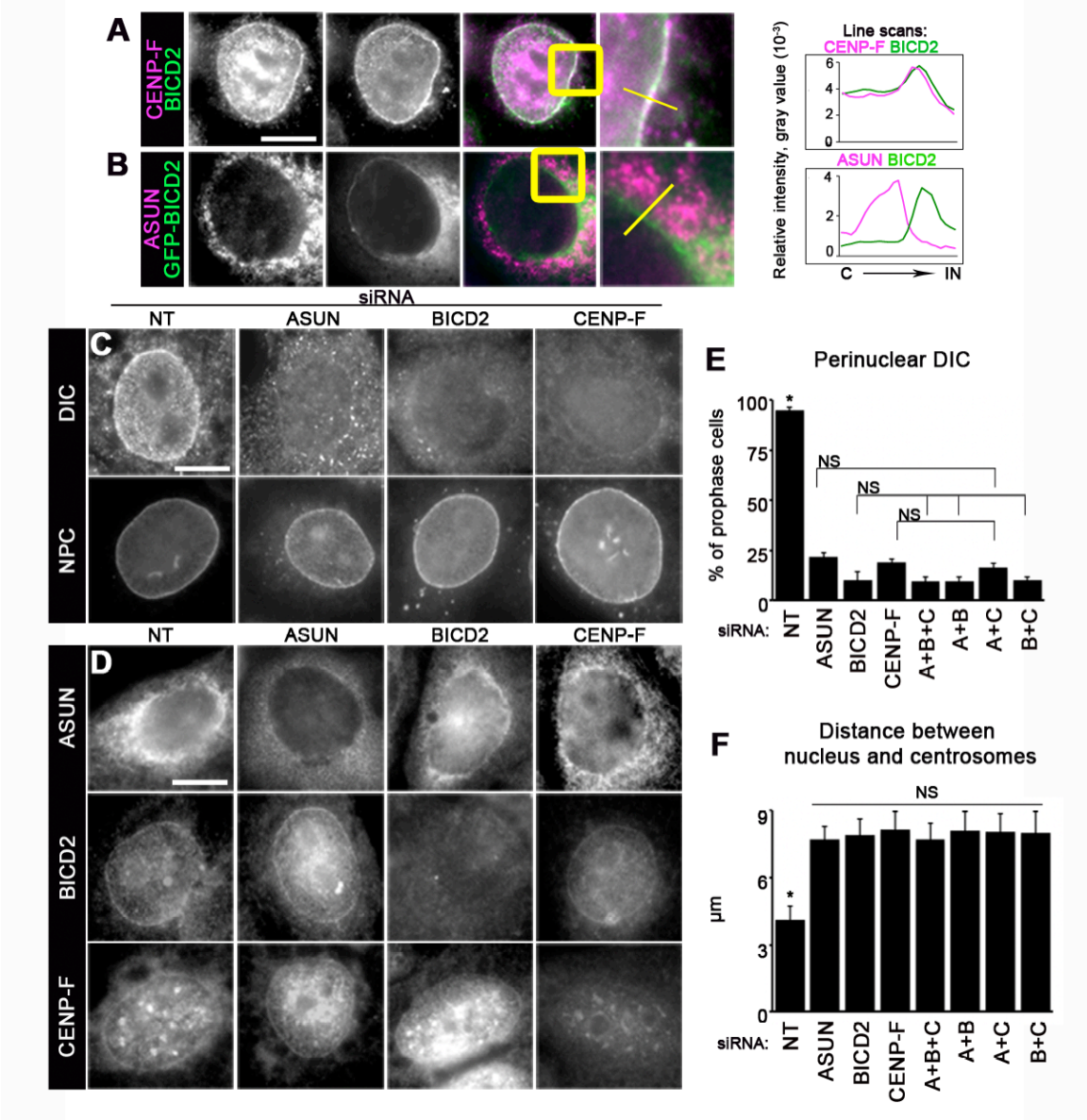

Figure 2.16. Relationship between hASUN, CENP-F, and BICD2 in recruiting dynein and centrosomes to the NE at mitotic entry. (A, B) HeLa cells were nocodazole-treated, fixed, and immunostained as indicated. Endogenous CENP-F and BICD2 co-localized on the NE (A), but no co-localization was observed for GFP-BICD2 and endogenous hASUN (B). Higher-magnification views (micrographs on far right) of co-stained cells in the vicinity of the NE correspond to regions enclosed by yellow boxes. Line scans centered at the NE (corresponding to yellow lines in higher-magnification views) confirmed significant overlap of CENP-F and BICD2 signals, but not hASUN and

Figure 2.16 continued: GFP- BICD2 signals. C, cytoplasmic. IN, intranuclear. (C-F) HeLa (C-E) or U2OS (F) cells were transfected with siRNA as indicated to downregulate hASUN ("A"), BICD2 ("B"), and/or CENP-F ("C"). Transfected cells were nocodazole-treated, fixed, and immunostained. (C) Perinuclear DIC was lost after hASUN, BICD2, or CENP-F knockdown without changes in the gross morphology of NPCs. (D) No change in hASUN, BICD2, or CENP-F localization was observed following knockdown of either of the other proteins. (E) Cells were immunostained for PH3, DIC, and DNA. Bar graph displays the percentage of prophase cells with perinuclear DIC for each knockdown condition. (F) Cells were immunostained for PH3, Pericentrin, and DNA. Bar graph displays the mean nucleus-to-centrosome distance for each knockdown condition. Asterisks, $p<0.0001$. Scale bars, 20 μm

to the nuclear surface might be blocked. In hASUN-siRNA cells exhibiting loss of dynein at the NE, nuclear pore morphology as assessed by immunostaining for an NPC marker resembled that of control cells; similarly, depletion of BICD2 or CENP-F caused loss of dynein at the NE without grossly disrupting NPCs (Figures 2.16C and 2.17).

We next assessed whether hASUN, BICD2, or CENP-F are localized within HeLa cells in an interdependent manner (Figure 2.16D). We observed no change in the cytoplasmic localization pattern of hASUN following depletion of BICD2 or CENP-F. Conversely, BICD2 and CENP-F localized normally to the NE in hASUN-siRNA cells. We confirmed the previous observations of Bolhy et al. (2011) that BICD2 and CENP-F are not reciprocally required for their anchoring to the NE. Together these data suggest that hASUN, BICD2, and CENP-F localize independently of each other at G2/M.

It was previously reported that inhibition of dynein function (via dynein antibody injection or dynaction subunit overexpression) does not disrupt the recruitment of BICD2 or CENP-F to the NE at G2/M (Bolhy et al., 2011; Splinter et al., 2010). We used siRNA-mediated knockdown to test whether the dynein adaptor, LIS1, is required to properly localize BICD2 or CENP-F. We observed no alteration in the localization patterns of BICD2 or CENP-F in prophase HeLa cells, providing further confirmation that functional dynein motors are not reciprocally required to recruit these proteins to the NE (Figure 2.18).

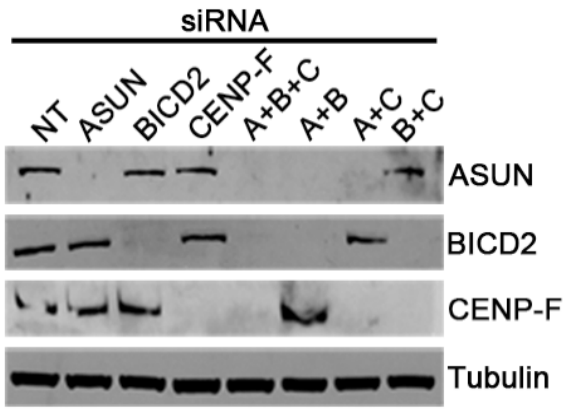

Figure 2.17. hASUN, BICD2, and CENP-F siRNAs effectively deplete their target proteins. HeLa cells were transfected with siRNAs as indicated to downregulate hASUN ("A"), BICD2 ("B"), and/or CENP-F ("C"). Lysates were analyzed by immunoblotting for hASUN, BICD2, and CENP-F. Tubulin was used as loading control.

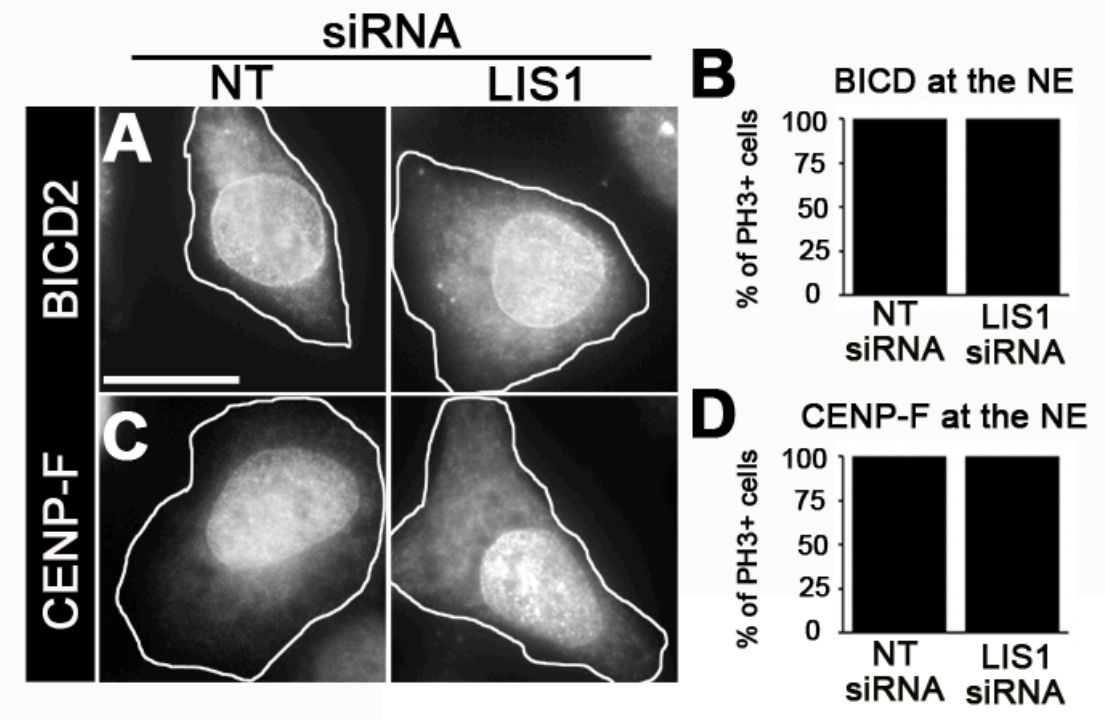

Figure 2.18. LIS1 knockdown has no effect on BICD2 or CENP-F localization at G2/M. HeLa cells were transfected with NT or LIS1 siRNA, nocodazole-treated, fixed, and immunostained for PH3 and either BICD2 or CENP-F. (A, C) BICD2 (A) and CENP-F (C) localize normally to the NE of PH3+ cells following LIS1 knockdown. (B, D) Quantification of BICD2 (B) and CENP-F (D) localization to the NE in PH3+ cells in control and LIS1-siRNA cells. Scale bar, 20 μm.

hASUN, BICD2, and CENP-F cooperatively regulate dynein recruitment to the NE at prophase

We investigated possible crosstalk between hASUN, BICD2, CENP-F in their regulation of dynein recruitment to the NE and nucleus-centrosome coupling at prophase. Following knockdown of these three proteins, either individually or in combination, we assessed perinuclear dynein localization in nocodazole-treated HeLa cells and average nucleus-centrosome distances in U2OS cells (Figure 2.16, E and F). We did not observe additive or synergistic effects on these phenotypes in the double- or triple-knockdown cells. Bolhy et al. (2011) reported similar findings for the average nucleus-centrosome distances in U2OS cells with double knockdown of BICD2 and CENP-F. These observations suggest that hASUN, BICD2, and CENP-F operate via distinct molecular mechanisms but converge to regulate dynein localization and centrosomal tethering to the NE in prophase.

Discussion

Proposed mechanism for hASUN-mediated recruitment of dynein to the NE during mitotic prophase

Two recent studies advanced our understanding of the mechanisms underlying the recruitment of dynein motors to the NE of cultured human cells at the onset of mitosis (Bolhy et al., 2011; Splinter et al., 2010). BICD2–RanBP2 and NudE/EL–CENP-F–Nup133 were identified as separate cassettes of proteins that provide sites to anchor dynein to the NE. We report herein our findings that hASUN is a third protein required

for this critical event in cultured cells. In contrast to the BICD2 and CENP-F cassettes, however, which can bind directly to components of dynein complexes, our data suggest that hASUN regulates the localization of dynein in an indirect manner via LIS1, an accessory protein of the motor. Another distinction is that BICD2 and CENP-F localize to NPCs within the NE, whereas hASUN localizes to the cytoplasm with exclusion of the NE.

We propose a model in which hASUN works in a manner distinct from that of BICD2 and CENP-F to mediate dynein recruitment to the NE at G2/M, a critical event required for nucleus-centrosome coupling prior to NEBD and faithful execution of mitotic divisions. Our data lead us to hypothesize that cytoplasmic hASUN transiently interacts with LIS1, which is bound to dynein heavy chains, to promote the enrichment and/or proper orientation of dynein complexes in the vicinity of the nuclear surface at G2/M. The BICD2–RanBP2 and NudE/EL–CENP-F–Nup133 cassettes then capture and stably anchor dynein complexes to NPCs. In the absence of hASUN, BICD2 and CENP-F are not sufficient to carry out the early steps in the process of dynein recruitment to the NE at G2/M; similarly, when either BICD2 or CENP-F are depleted from cells, hASUN can promote the enrichment/orientation of dynein complexes near the nuclear surface, but the complexes do not become stably anchored to the NE.

Why are so many factors required to carry out this important cellular process? A network of proteins might be required to move and properly orient dynein complexes at G2/M given their large size and multi-subunit composition. NudE, in addition to directly interacting with dynein motors, facilitates the interaction between LIS1 and dynein, suggesting that both ASUN and the NudE/EL–CENP-F–Nup133 cassette might converge

on dynein through LIS1 at the onset of mitosis (McKenney et al., 2010). It will be interesting to test in future experiments whether ASUN plays a role in promoting the interaction between CENP-F tethered to the NE and cytoplasmic NudE/EL–LIS1–dynein complexes at G2/M, a possible mechanism of action that would be consistent with our model.

Mitotic versus meiotic roles of ASUN

While ASUN remained largely uncharacterized in human cells prior to this study, we previously showed that it has cell cycle and developmental roles in other organisms. In *Drosophila*, dASUN regulates dynein localization and centrosomal tethering to the nucleus during spermatogenesis, and it is required for male fertility (Anderson et al., 2009). *Drosophila asun* mutants and HeLa cells depleted of ASUN exhibit strikingly similar disruptions of male meiosis and mitosis, respectively; these shared phenotypes underscore the likelihood that the transformed nature of the HeLa cell line is not responsible for the defects we have observed. Loss of dynein in prophase cells observed in ASUN-siRNA RPE cells further confirms this conclusion.

In *Xenopus*, we previously reported that the ASUN homologue plays a role during embryonic development (Lee et al., 2005). Downregulation of ASUN in *Xenopus* embryos via morpholino oligonucleotide injection resulted in disruption of gastrulation and polyploidy; the latter phenotype suggested that ASUN might regulate the mitotic cell cycles of early blastomeres during vertebrate embryogenesis. We also showed conservation of function between *Xenopus* and human ASUN homologues by restoring proper developmental progression in *Xenopus* ASUN morphants via co-injection of

mRNA encoding hASUN.

In contrast to *Drosophila asun*, which is expressed exclusively in germline tissues, mouse *ASUN* transcripts have been detected in all tissues, both somatic and germline, surveyed in a study by another group (Bourdon et al., 2002; Stebbings et al., 1998). The data we present herein indicate that hASUN plays an important role in human somatic cells during mitosis. The human *ASUN* gene is located within a genomic region that is amplified in testicular seminomas, raising the possibility that ASUN may also regulate division of male germline cells in vertebrates as it does in *Drosophila* (Bourdon et al., 2002).

Why might ASUN expression be limited to germline cells in flies? The absence of dASUN expression within somatic cells may be related to the lack of an absolute requirement for centrosomes during most life cycle stages of *Drosophila*. Centrioles, while important for the formation of centrosomes (as well as cilia and flagella), play non-essential roles in development from an embryo to an adult fly with the exception of early embryogenesis (Basto et al., 2006; Stevens et al., 2007). The process of spermatogenesis in adult male flies is also exceptional in that centrioles are required to form the cilium of spermatocytes and the axoneme of spermatids (Bettencourt-Dias et al., 2005). Centrioles within G2 spermatocytes undergo major changes in their positioning, moving to the cortex during the extensive growth phase to elaborate a cilium and then back toward the nucleus at G2/M; the necessity to re-establish nucleus-centrosome coupling at the time of meiotic entry may impose a stringent requirement for dynein-localizing proteins such as ASUN in these cells (Fuller, 1993). Bicaudal, the *Drosophila* homologue of BICD2, is a potential candidate to cooperate with dASUN in dynein recruitment to the nuclear surface

of G2 spermatocytes; our database searches, however, have revealed no CENP-F homologues in flies.

Evolved mechanisms for dynein regulation in multicellular organisms

Cytoplasmic dynein, most commonly studied for its roles in trafficking of organelles and directed cell movement, is also required in multicellular organisms for coordination of mitotic entry and exit (Dujardin et al., 2003). Specifically, dynein promotes the coupling of centrosomes to the NE, has been hypothesized to assist in NEBD, and functions along the mitotic spindle to facilitate chromosome segregation at anaphase (Dujardin et al., 2003; Lippincott-Schwartz, 2002; Tanenbaum et al., 2010). In contrast, only one role for dynein has been identified in budding yeast: proper positioning of the spindle during mitosis (Stuchell-Brereton et al., 2011).

It is interesting to note that none of the three proteins needed for localization of dynein to the NE of prophase HeLa cells (BICD2 and CENP-F as previously reported; hASUN as reported herein) have predicted homologues in either budding or fission yeasts. The centrosome-like structure in yeast, known as the spindle pole body, is embedded into the nuclear surface throughout interphase and mitosis in budding yeast (Jaspersen and Winey, 2004). Similarly, in fission yeast, the spindle pole body is tethered to the nuclear surface throughout interphase and will embed at mitosis (Lim et al., 2009). In both cases, dynein is not required for the process of spindle pole body-nucleus embedding (Jaspersen and Winey, 2004; Lim et al., 2009). Thus, metazoans appear to have evolved a finely tuned mechanism for regulating the localization of dynein

complexes at the onset of mitosis, with at least three proteins required to execute the recruitment and docking of these motors to the NE.

CHAPTER III

NUCLEAR-LOCALIZED ASUNDER REGULATES CYTOPLASMIC DYNEIN LOCALIZATION VIA ITS ROLE IN THE INTEGRATOR COMPLEX

This chapter has been published (Jodoin et al., MBoC 2013).

Introduction

Dynein, a minus-end-directed molecular motor, is a large multimeric complex that can be divided into distinct regions (Holzbaur and Vallee, 1994; Kardon and Vale, 2009). Protruding from the head region are two microtubule-binding domains that allow the motor to walk processively along the microtubule towards its minus end. This movement is driven by the force-generating ATPase activity of the catalytic domains found within the head region of the motor. The stem region, consisting of multiple light, light intermediate, and intermediate chains, is the most variable and is widely considered to serve as the binding site for dynein adaptors.

Within the cell, dynein exists in association with its activating complex, dynactin (Schroer, 2004). Together, the dynein-dynactin complex performs diverse functions within the cell, ranging from cargo transport, centrosome assembly, and organelle positioning to roles in chromosome alignment and spindle positioning during mitosis (Holzbaur and Vallee, 1994; Kardon and Vale, 2009). Dynein-dynactin complexes are subject to multiple layers of regulation, including binding of accessory proteins,

phosphorylation, subunit composition, and subcellular localization (Kardon and Vale, 2009). Localized pools of dynein have been identified and shown to be required for critical processes in the cell, although the mechanisms underlying the control of dynein localization are poorly understood (Kardon and Vale, 2009).

Across phyla, a stably anchored subpopulation of dynein has been reported to exist on the NE of cells (Anderson et al., 2009; Gonczy et al., 1999; Payne et al., 2003; Robinson et al., 1999; Salina et al., 2002). This pool of dynein is required for both stable attachment of centrosomes to the NE prior to NEBD and migration of centrosomes to opposite sides of the nucleus, thereby ensuring proper positioning of the bipolar spindle (Anderson et al., 2009; Bolhy et al., 2011; Gonczy et al., 1999; Jodoin et al., 2012; Malone et al., 2003; Robinson et al., 1999; Sitaram et al., 2012; Splinter et al., 2010; Vaisberg et al., 1993). Additionally, this pool of dynein appears to facilitate NEBD by forcibly tearing the NE, although the precise mechanism remains unknown (Beaudouin et al., 2002; Salina et al., 2002).

Two proteins, BICD2 and CENP-F, have been shown to directly anchor dynein to the nuclear surface at the G2/M transition in HeLa cells (Bolhy et al., 2011; Splinter et al., 2010). BICD2, a dynein adaptor protein, directly binds dynein and nucleoporin RanBP2, thereby anchoring the motors to the NE (Splinter et al., 2010). CENP-F directly interacts with dynein adaptor proteins NudE/EL and nucleoporin Nup133 to effectively anchor dynein to the NE (Bolhy et al., 2011). In both *Drosophila* spermatocytes and cultured human cells, we previously identified ASUN as an additional regulator of dynein recruitment to the NE at G2/M of meiosis and mitosis, respectively, although physical

interaction between ASUN and dynein has not been demonstrated (Anderson et al., 2009; Jodoin et al., 2012).

Spermatocytes within the testes of *Drosophila asun* males arrest at prophase of meiosis I with a severely reduced pool of perinuclear dynein and centrosomes that are not attached to the nuclear surface (hence the name "*asunder*") (Anderson et al., 2009). Spermatocytes that progress beyond this arrest exhibit defects in spindle assembly, chromosome segregation, and cytokinesis during the meiotic divisions. Using cultured human cells, we found that siRNA-mediated down-regulation of the human homologue of ASUN similarly resulted in reduction of perinuclear dynein during prophase of mitosis (Jodoin et al., 2012). Additional defects observed following loss of hASUN included nucleus-centrosome uncoupling, abnormal mitotic spindles, and impaired progression through mitosis.

In either *Drosophila* or cultured human cells, a direct mechanism for promotion of perinuclear dynein by ASUN has not been elucidated, although localization changes in ASUN coincide with the accumulation of dynein on the NE. *Drosophila* ASUN is largely restricted within the nucleus of early G2 spermatocytes and first appears in the cytoplasm during late G2, roughly coincident with the initiation of dynein recruitment to the nuclear surface (Anderson et al., 2009). Similarly, in prophase HeLa cells, when a perinuclear pool of dynein forms transiently at G2/M, hASUN is diffusely present in the cytoplasm (Jodoin et al., 2012). Based on these temporal associations of the localizations of ASUN and perinuclear dynein, we previously proposed that the cytoplasmic pool of ASUN likely mediates recruitment of dynein motors to the NE (Anderson et al., 2009; Jodoin et al., 2012).

INT is an evolutionarily conserved complex consisting of 14 subunits, although its biology is poorly understood (reviewed in (Chen and Wagner, 2010). INT was originally identified due to its association with the C-terminal tail of RNA polymerase II and was subsequently shown to be required for 3'-end processing of snRNAs (Baillat et al., 2005). These processed snRNAs play roles in gene expression via intron removal and further processing of pre-mRNAs (Matera et al., 2007). To discover novel components of INT that are required for its snRNA-processing function, a cell-based assay was developed in which generation of a GFP signal due to incomplete processing of a reporter U7 snRNA served as a read-out of INT activity (Chen et al., 2012). Using this approach, dASUN was identified as a functional component of INT: down-regulation of dASUN led to increase misprocessing of U7 and spliceosomal snRNA, thereby indicating its requirement for activity of the complex (Chen et al., 2012). Furthermore, dASUN was shown to biochemically interact with INT in a stoichiometric manner, an association that it is conserved in humans (Chen et al., 2012; Malovannaya et al., 2010). Collectively, these data provide compelling evidence that ASUN is a core Integrator subunit.

Given the divergent nature of the known activities of ASUN – critical regulator of cytoplasmic dynein localization and essential component of a nuclear snRNA-processing complex – we sought herein to determine whether these roles are independent of each other or derived from a common function. We find that depletion of individual INT components from HeLa cells results in loss of perinuclear dynein, recapitulating the phenotype observed in hASUN-siRNA cells (Jodoin et al., 2012). Additionally, we find that forced localization of either hASUN or dASUN to the cytoplasm inhibits their capacity to recruit dynein to the NE in the absence of endogenous ASUN. We present a

model in which ASUN acts within the nucleus in concert with other subunits of the Integrator complex, likely via processing of a critical RNA target(s), to promote recruitment of cytoplasmic dynein motors to the NE at G2/M.

Materials and methods

Drosophila spermatocyte experiments

Flies were maintained at 25°C using standard techniques (Greenspan, 2004). *y w* flies obtained from Bloomington *Drosophila Stock* Center (Indiana University, Bloomington, IN) were used as the "wild-type" stock. The $asun^{f02815}$ allele (Exelixis Collection, Harvard Medical School, Boston, MA) and a transgenic line with male germline-specific expression of CHY-tagged wild-type dASUN were previously described (Anderson et al., 2009). Transgenic lines for male germline-specific expression of CHY-tagged dASUN fusion proteins (constructs described below) were generated by *P*-element-mediated transformation via embryo injection (Rubin and Spradling, 1982). For each transgene, a single insertion mapping to the X chromosome was crossed into the $asun^{f02815}$ background using standard genetic crosses.

To test male fertility, individual adult males (2 d old) were placed in vials with five wild-type females (2 d old) and allowed to mate for 5 d. The average number of live adult progeny produced per fertile male was scored (≥10 males tested per genotype). Statistical analysis was performed using an unpaired Student's *t*-test.

Protein extracts were prepared by homogenizing dissected testes from newly eclosed males in SDS sample buffer. The equivalent of eight testes pairs was loaded per

lane. After SDS-PAGE, immunoblotting was performed as described below.

Live testes cells were prepared for examination by fluorescence microscopy as described previously (Kemphues et al., 1980). Briefly, testes were dissected from newly eclosed adult males, placed in a drop of phosphate-buffered saline (PBS) on a microscopic slide, and gently squashed under a glass cover slip after making a small incision near the stem cell hub. Formaldehyde fixation was performed as described previously (Gunsalus et al., 1995). Briefly, slides of squashed testes were snap-frozen, immersed in 4% formaldehyde (in PBS with 0.1% Triton X-100) for 7 minutes at -20°C after cover slip removal, and washed three times in PBS. Mouse anti-DHC primary antibody (P1H4, 1:120, gift from T. Hays [University of Minnesota, Minneapolis, MN]) and Cy3-conjugated secondary antibody (Invitrogen, Carlsbad, CA) were used (McGrail and Hays, 1997). Fixed samples were mounted in PBS with DAPI to visualize DNA. Wide-field fluorescent images were obtained using an Eclipse 80i microscope (Nikon, Melville, NY) with Plan-Fluor 40X objective. In experiments to determine the percentage of late G2 spermatocytes with perinuclear dynein, at least 200 cells were scored per genotype. Statistical analysis was performed using Fisher's exact test.

Cell culture and treatments

HeLa cells were maintained at 37˚C and 5% CO_2 in DMEM containing 10% FBS, 1% L-glutamine, 100 μg/ml streptomycin, and 100 U/ml penicillin (Life Technologies, Carlsbad, CA). Plasmid DNA was transfected into cells using Fugene HD (Promega, Madison, WI). siGENOME NT siRNA#5 (Dharmacon, Lafayette, CO) was used as negative control. siRNA used to silence hASUN (3'-UTR region; 5'-CAG CAA GAU

GGU AUA GUU A-3') was obtained from Dharmacon. siRNAs used to silence IntS1 (5'-CAU UUC UCC GUC GAU UAA A-3'), IntS2 (5'-CUC GUU UAG CUG UCA AUG U-3'), IntS3 (5'-GAA GUA CUG AGU UCA GAU A-3'), IntS4 (5'-CAG CAU UGU UCU CAG AUC A-3'), IntS5 (5'-CAA GUU UGU CCA GUC ACG A-3'), IntS6 (5'-CAC UAA UGA UUC GAU AAU A-3'), IntS7 (5'-GGC UAA AUA GUU UGA AGG A-3'), IntS9 (5'-GAA AUG CUU UCU UGG ACA A-3'), IntS10 (5'-GGA UAC UUG GCU UUG GUU A-3'), IntS11 (Albrecht and Wagner, 2012), IntS12 (5'-GUC AAG ACA UCC ACA GUU A-3'), and CPSF30 (5'-GUG CCU AUA UCU GUG AUU U-3') were obtained from Sigma-Aldrich (St. Louis, MO).

Cells were transfected with siRNA duplexes using DharmaFECT 1 transfection reagent (Dharmacon) and analyzed 3 d post-transfection. Fugene HD (Promega) transfection reagent was used for co-transfection of cells with siRNA and DNA constructs. Where indicated, cells were incubated in 5 μg/ml (16.6 μM) nocodazole (Sigma-Aldrich) for 3 h prior to fixation to enhance perinuclear localization of dynein. For G2/M arrest, cells were incubated for 16 h in 10 μM RO-3306 (Cdk1 inhibitor; Enzo Life Sciences, Plymouth, PA).

Cell fixation, immunostaining, and microscopy

Cells were fixed in methanol (5 min at -20°C followed by washing with Tris-buffered saline [TBS] plus 0.01% Triton X-100) and blocked in TBS plus 0.01% Triton X-100 and 0.02% BSA prior to immunostaining. Primary antibodies were used as follows: DIC (clone 74.1, 1:500, Abcam, Cambridge, MA) and c-Myc (9E10, 1:1000). Alexa Fluor 546-conjugated phalloidin (1:1000, Invitrogen) was used to stain F-actin.

Appropriate secondary antibodies conjugated to Alexa Fluor 488 or Cy3 were used (1:1000, Invitrogen). Cells were mounted in ProLong Gold Antifade Reagent with DAPI (Invitrogen). Wide-field fluorescence images were obtained using an Eclipse 80i microscope (Nikon) with Plano-Apo 100X objective.

Line scan analyses to quantify perinuclear dynein accumulation in HeLa cells were performed using ImageJ (National Institutes of Health, Bethesda, MD). Ten representative cells were measured per condition; for each cell, 12 line scans distributed equally around the nuclear circumference were obtained. To quantify the ratios of perinuclear to diffusely cytoplasmic DIC in stained HeLa cells, the average intensity of the DIC signal within a small rectangular region was sampled near the nuclear surface and in the surrounding cytoplasm using ImageJ. The ratio of the intensities was determined. At least 20 cells were scored per condition.

Statistical analyses of data from cultured cell experiments reported herein were performed using Student's unpaired *t*-test. Error bars indicate SEM for all bar graphs. All experiments were performed a minimum of three times with at least 200 cells scored per condition.

FACS analysis

siRNA-treated HeLa cells (~10^7) were fixed with 70% ethanol at 4˚C for 24 h and incubated in PBS containing propidium iodide (20 μg/ml) and RNAse A (0.2 mg/ml) (Sigma-Aldrich) at 4˚C for 24 h. FACS analysis was performed to determine propidium iodide intensity levels (a measure of DNA content). Gating was used to exclude cell debris and doublets from the DNA analysis. FACS experiments were performed in the

Flow Cytometry Shared Resource of Vanderbilt University Medical Center.

DNA constructs

cDNA clones encoding mASUN and dASUN have been previously described (Jodoin et al., 2012). The full-length *hASUN* open reading frame (ASUN; NCBI Reference Sequence: NM_018164 (gene); NP_060634.2 (protein)) was amplified from a human primary skin fibroblast cDNA library. The following forward and reverse primers were used to incorporate EcoRI and StuI restriction sites into the 5' and 3' ends, respectively, of the *hASUN* coding region followed by subcloning of the digested, purified fragment into expression vector pCS2: 5'-CCG GAA TTC CCA GGC ACG AAA GTT AAA AC-3' (ASUN-EcoRI-5') and 5'-AAA AGG CCT TTC TTC AAG TCA CTC TTC ACT GC-3' (ASUN-StuI-3').

Constructs for expression in HeLa cells of the following N-terminally tagged proteins were generated by subcloning into vector pCS2-Myc: Myc-dASUN, Myc-mASUN (previously described in Jodoin et al. 2012), and Myc-hASUN. To generate pCS2-Myc-NLS vector, the following nucleotide sequence was engineered into the pCS2-Myc vector to add a strong exogenous NLS (PKKKRKV; derived from SV40 large T antigen) C-terminal to the Myc tag: CCC AAG AAG AAG CGC AAG GTC (Kalderon et al., 1984). hASUN and dASUN were subcloned into pCS2-Myc-NLS for production of Myc-NLS-hASUN and Myc-NLS-dASUN, respectively, in transfected cells. We used a PCR-based approach to generate mASUN fragments for subcloning into pCS2-GFP expression vector (N-terminal tag; illustrated in Figure S4).

Vector tv3 (gift from J. Brill, The Hospital for Sick Children, Toronto, Canada) containing the testes-specific *β2-Tubulin* promoter was used to make constructs for *Drosophila* transgenesis (Wong et al., 2005). Sequence encoding a strong exogenous NLS (described above) was engineered into a previously described tv3-CHY vector to generate tv3-NLS-CHY. dASUN was subcloned into modified tv3 vector to produce NLS-CHY-dASUN in transgenic fly testes.

We used NLStradamus software to identify putative NLS motifs in hASUN, mASUN, and dASUN (Nguyen Ba et al., 2009). We used QuikChange II XL Site-Directed Mutagenesis Kit (Agilent Technologies, Santa Clara, CA) to mutate charged residues to alanines within these motifs of hASUN (Figure 4A), mASUN (Figure S4A), and dASUN (Figures 5A and S5).

GFP-Integrator subunits were subcloned into pcDNA4/myc-His A (Invitrogen) using purchased cDNA templates (Open Biosystems/Thermo Scientific, Huntsville, AL). The GFP-BICD2 expression construct was a gift from A. Akhmanova (Erasmus Medical Center, Rotterdam, The Netherlands) (Hoogenraad et al., 2001).

Immunoblotting

HeLa cell lysates were prepared using non-denaturing lysis buffer (50 mM Tris-Cl pH 7.4, 300 mM NaCl, 5 mM EDTA, 1% Triton X-100). Following SDS-PAGE, proteins were transferred to nitrocellulose for immunoblotting using standard techniques. Immunoblotting was performed using the following primary antibodies: c-Myc (9E10, 1:1000), beta-tubulin (clone E7, 1:1000, Developmental Studies Hybridoma Bank, University of Iowa, Iowa City, IA), mCherry (1:500, Clontech, Mountain View, CA),

CENP-F (clone 14C10 1D8, 1:500, Abcam), C-hASUN (1:300) (Jodoin et al., 2012), GFP B-2 (1:1000, Santa Cruz Biotechnology, Dallas, TX), IntS1, IntS4, IntS7, IntS9, IntS10, IntS11, IntS12, and CPSF30 (1:1000, Bethyl Labs, Montgomery, TX). HRP-conjugated secondary antibodies (1:5000) and chemiluminescence were used to detect primary antibodies.

Results

Multiple INT subunits are required for dynein recruitment to the NE

Two ASUN-dependent cellular functions have been reported: dynein recruitment to the NE at G2/M, and proper processing of snRNA by INT (Chen et al., 2012; Jodoin et al., 2012). We hypothesized that other components of the INT complex, like hASUN, may be required to promote dynein recruitment to the NE. To test this hypothesis, we performed siRNA-mediated knockdown of individual INT subunits in HeLa cells and assessed dynein localization. Prior to fixation and immunostaining for dynein intermediate chain (DIC), siRNA-treated cells were incubated briefly with 5μM nocodazole to stimulate recruitment of dynein-dynactin complexes to the NE. This treatment has been documented to recapitulate, in non-G1 cells, the enrichment of functional dynein-dynactin complexes on the NE that normally occurs at G2/M, making this an ideal assay for identifying factors involved in dynein localization (Beswick et al., 2006; Bolhy et al., 2011; Hebbar et al., 2008; Jodoin et al., 2012; Splinter et al., 2010).

Consistent with our previous report, we found that 78% of NT control siRNA cells had a striking enrichment of dynein on the NE after brief nocodazole treatment

(Figure 3.1, A and O); in contrast, the percentage of cells with perinuclear dynein was reduced to 20% following hASUN depletion (Figure 3.1, C and O) (Jodoin et al., 2012). In most cases, we found that treatment of cells with siRNA targeting individual INT subunits (each designated "IntS" followed by a unique identifying number) resulted in a similar reduction of cells with perinuclear dynein (Figure 3.1, D-I, K, M, and N). Importantly, we did not observe any overt effect on cellular health or growth after treatment with INT-targeting siRNAs, arguing against any potential reduction in cellular fitness as the cause of reduced perinuclear dynein. To further quantify the dynein phenotype, we compared the DIC immunofluorescence signals on the NE to that of the cytoplasm and also determined the average peak DIC intensity on the NE for each knockdown as previously described (Figure 3.2) (Jodoin et al., 2012). Depletion of IntS1-6, 9, 11, or 12 resulted in a marked decrease in both the ratio of NE-to-cytoplasmic dynein and the peak intensity of DIC on the NE, comparable to that observed for hASUN. IntS7 and IntS10 were the two exceptions: depletion of either of these INT subunits had no effect on perinuclear dynein accumulation compared to control cells (Figure 3.1, J, L, and O; Figure 3.2). We confirmed that all targeted proteins were efficiently depleted by immunoblotting of cell lysates after siRNA treatment or by a second, non-overlapping, siRNA (Figure 3.3). Taken together, these data show that the majority of the individual INT subunits are required for dynein recruitment to the NE.

We considered the possibility that loss of dynein accumulation on the NE upon INT depletion could be secondary to cell-cycle arrest. We performed fluorescence-activated cell sorting (FACS) analysis of DNA-stained HeLa cells following knockdown of individual INT subunits (Figure 3.4). We observed no differences between the cell-

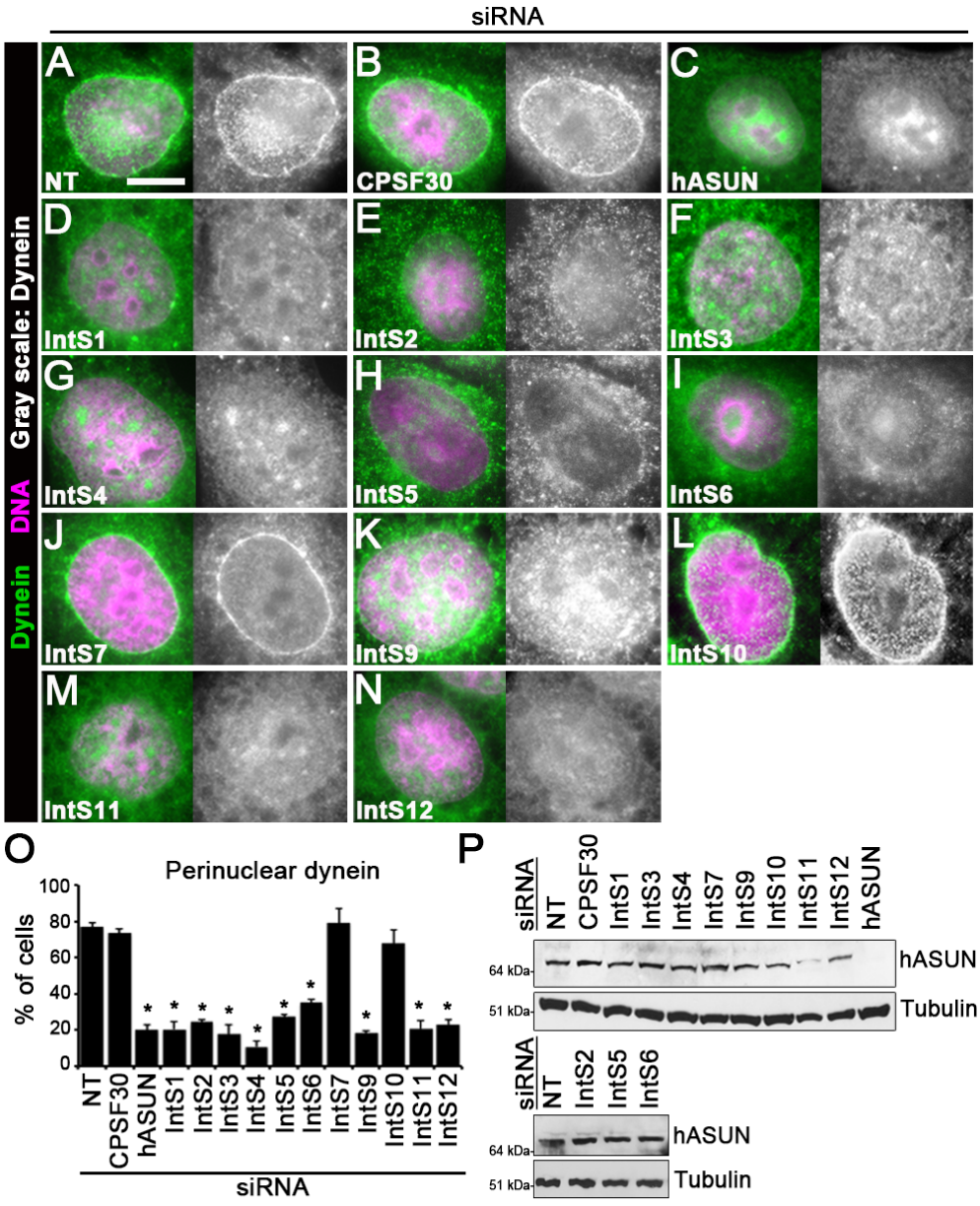

Figure 3.1. INT subunits are individually required for dynein recruitment to the NE. HeLa cells were transfected with siRNA as indicated. (A-L) Following siRNA treatment, cells were incubated in nocodazole, fixed, and stained for DIC and DNA. Loss of perinuclear dynein was observed upon individual knockdown of the majority of INT subunits. Scale bar, 20 μm. (M) Quantification of perinuclear dynein in cells following knockdown of INT subunits. Asterisks, $p<0.0001$. (N) hASUN immunoblot analysis of cell lysates after knockdown of INT subunits. Tubulin was used as loading control.

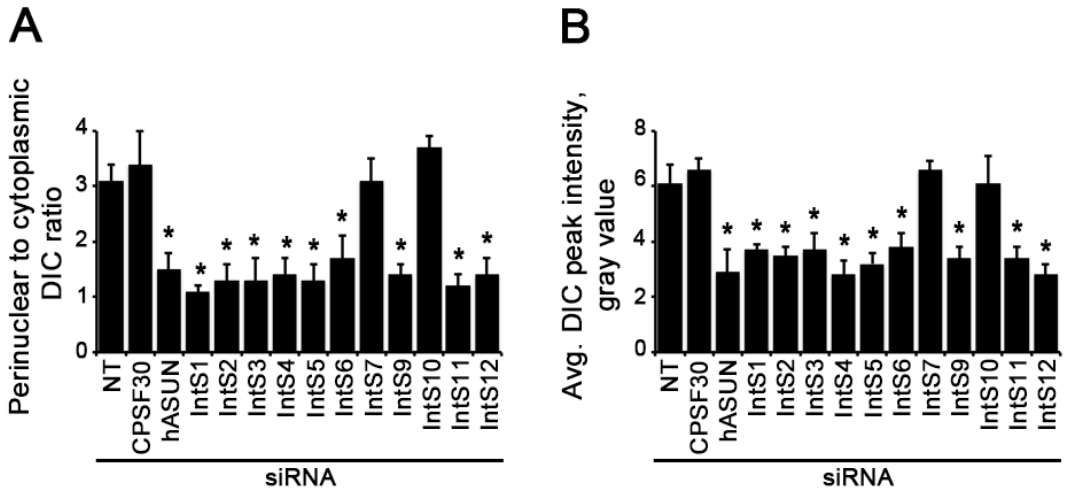

Figure 3.2. Quantification of perinuclear dynein in cells lacking INT subunits. HeLa cells were transfected with the indicated siRNAs. After nocodazole treatment, cells were fixed and stained for DIC and DNA. Line scans were drawn from the cytoplasm to the inside of the nucleus, traversing the NE. (A) Ratios of the intensity of the dynein signals on the NE to the cytoplasm. (B) Average peak intensities of dynein on the NE. Asterisks, $p<0.0001$ (relative to NT control).

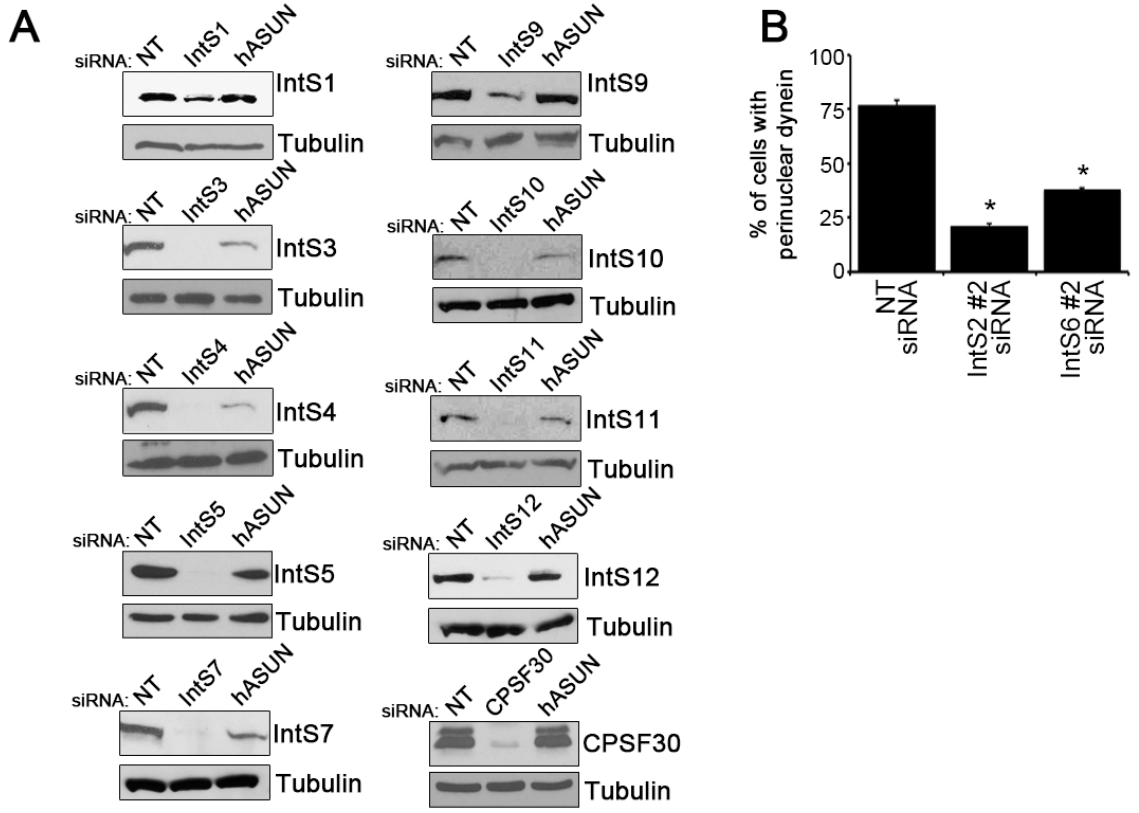

Figure 3.3. Immunoblot analysis of INT subunit levels in siRNA cells. HeLa cells were transfected with siRNA as indicated. (A) cell lysates were probed with INT subunit antibodies. Depletion of each individual subunit targeted by siRNA was confirmed (compare first and second lanes for each blot). Reduced levels of several subunits were observed in hASUN-siRNA cells (compare first and last lanes for each blot). (B) Following siRNA treatment, cells were incubated in nocodazole, fixed, and stained for DIC and DNA. Quantification of perinuclear dynein in cells following knockdown of individual INT subunits. Asterisks, $p<0.0001$ (compared to NT control).

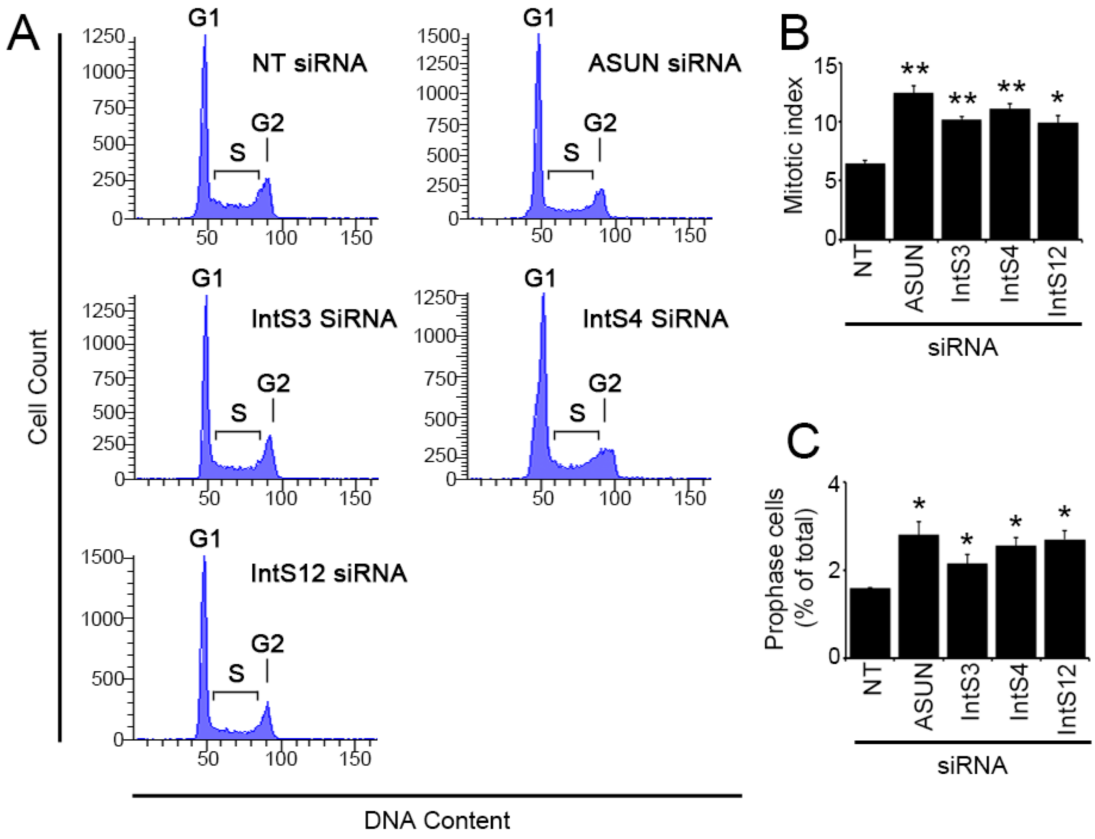

Figure 3.4. Knockdown of INT subunits does not cause cell-cycle arrest. (A) HeLa cells were transfected with siRNA as indicated, fixed, and stained with propidium iodide. DNA content was analyzed by FACS. NT-siRNA and INT subunit-siRNA cells had nearly identical cell-cycle profiles. (B, C) HeLa cells were transfected with siRNA as indicated, fixed, and stained for PH3 and DNA. Depletion of ASUN or other INT subunits resulted in a slight increase in the mitotic index (PH3+ cells/total cells) (B) as well as a slight increase in the fraction of prophase cells (PH3-positive cells with intact NE/total cells) (C). Single asterisks, $p<0.0005$; double asterisks, $p<0.0001$. For each siRNA condition, at least 800 cells were scored per experiment (n = 3).

cycle profile of hASUN- or other INT subunit-siRNA cells and that of control NT-siRNA cells (Figure 3.4A). We previously reported that hASUN depletion from HeLa cells results in a slightly increased mitotic index (Jodoin et al., 2012); we show herein that depletion of other INT subunits has a similar effect (Figure 3.4B). We also found that the percentage of prophase cells, the stage at which dynein normally accumulates on the NE, is slightly increased upon knockdown of ASUN or other INT subunits from HeLa cells (Figure 3.4C). These results indicate that loss of dynein recruitment to the NE in cells depleted of INT is not due to any substantial cell-cycle perturbation.

Table 3.1 summarizes our observations of the requirements for INT subunits in dynein localization and the previously reported requirements for INT subunits in snRNA processing (Chen et al., 2012; Ezzeddine et al., 2011). The two data sets compare favorably in that, for both processes, most INT subunits are required, whereas IntS10 is expendable. IntS7, however, was the sole exception in that it was shown to be required for snRNA processing, yet we found no effect of its down-regulation on dynein recruitment to the NE (Chen et al., 2012). Overall, these data are consistent with a model in which hASUN regulates dynein localization in an INT complex-dependent manner.

To show that loss of dynein localization is specific to disruption of an INT-mediated RNA processing event, and not secondary to a general disruption of RNA processing, we depleted cells of Cleavage Polyadenylation Specificity Factor 30 (CPSF30) and assessed perinuclear dynein. CPSF30 is involved in the recruitment of machinery that mediates 3'-mRNA cleavage and poly(A) tail synthesis (Barabino et al., 1997). We found that siRNA-mediated down-regulation of CPSF30 had no effect on

Table 3.1. Comparison of INT subunit requirements in snRNA processing versus dynein localization.

siRNA	snRNA Processing[a]	Dynein Localization[b]
hASUN	+	+
IntS1	+	+
IntS2	+	+
IntS3	+	+
IntS4	+	+
IntS5	+	+
IntS6	+	+
IntS7	+	-
IntS8	+	N.D.
IntS9	+	+
IntS10	-	-
IntS11	+	+
IntS12	+	+

[a]Analysis of requirements for INT subunits in U7 snRNA processing was previously reported (Chen et al. 2012).
[b]Analysis of requirements for INT subunits in dynein recruitment to the NE is presented herein (Figure 3.1).
"+" = Required.
"-" = Not required.
"N.D." = Not determined.

perinuclear dynein accumulation, suggesting a specific role for INT in this process (Figures 3.1, B and O; Figure 3.2).

hASUN levels are normal following depletion of INT

Given the established role of INT in snRNA processing, we considered the possibility that hASUN could be a downstream target (i.e. formation/splicing of mature *hASUN* transcripts might require a functional INT complex). In this case, lack of perinuclear dynein in cells with INT down-regulation would be secondary to a reduction in hASUN levels. To test this idea, we used previously generated anti-hASUN antibodies to probe immunoblots of lysates of HeLa cells after depletion of individual INT subunits (Jodoin et al., 2012). We found that hASUN protein levels remained largely unchanged in all lysates tested with the exception of a slight reduction after IntS11 depletion (Figure 3.1P). We next assessed the reciprocal possibility that hASUN might be required for stability of the INT complex. By immunoblotting, we observed decreased levels of IntS3, 4, 7, 10, and 11 in lysates of hASUN-siRNA HeLa cells relative to control cells (Figure 3.3). This observation is consistent with a recent report showing that levels of *Drosophila* IntS1 and 12 are interdependent, which may be due to their direct association within the complex (Chen et al., 2013). Taken together, these data indicate that failure of dynein localization in INT-depleted cells is not due to decreased hASUN production, and hASUN is required for the stability of several other subunits of the INT complex.

INT subunits exhibit a range of subcellular localizations

We previously showed that *Drosophila* ASUN exhibits a dynamic localization pattern: in the *Drosophila* testes, mCherry-tagged dASUN (CHY-dASUN) expressed via a transgene shifts from exclusively nuclear in early G2 to diffusely present throughout the spermatocyte by late G2 (Anderson et al., 2009). Similar localizations (ranging from nuclear to cytoplasmic to diffuse throughout the cell) were observed when GFP-tagged dASUN was expressed in HeLa cells (Anderson et al., 2009). Likewise, we found in the current study that Myc-tagged hASUN expressed in HeLa cells localized to the nucleus and/or cytoplasm, albeit with a predominantly nuclear pattern in most cells (Figure 3.5, A1-3; quantified in Table 3.2 and Figure 3.8D).

In both fly testes and HeLa cells, we previously observed a temporal correlation in which a pool of cytoplasmic ASUN is present at the onset of dynein accumulation on the NE at G2/M (Anderson et al., 2009; Jodoin et al., 2012). In fly spermatocytes, dASUN undergoes a shift from nuclear to first appearing in the cytoplasm during late G2, roughly coinciding with dynein recruitment to the NE (Anderson et al., 2009). In HeLa cells, hASUN localizes to the cytoplasm at prophase, a cell-cycle stage at which dynein is enriched on the NE (Jodoin et al., 2012). Due to this correlation, we previously hypothesized that a cytoplasmic pool of ASUN is required for recruitment of dynein motors to the NE at G2/M (Jodoin et al., 2012).

We considered the possibility that the INT complex might function within the cytoplasm to promote dynein recruitment to the NE in a manner independent of its role in snRNA processing within the nucleus. A broad survey of subcellular localization patterns

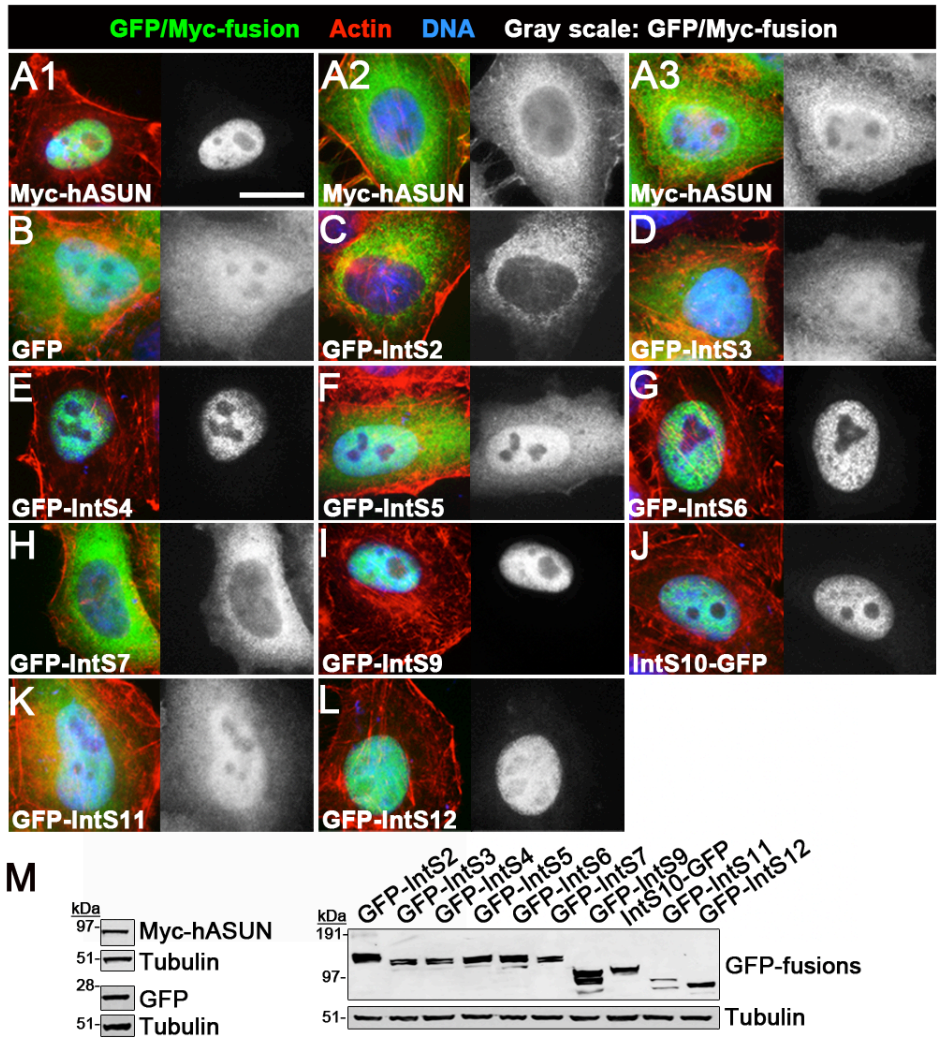

Figure 3.5. INT subunits localize to the nucleus, cytoplasm, or both. HeLa cells were transfected with the indicated expression constructs encoding tagged versions of INT subunits. (A-L) Following fixation, cells were stained with phalloidin and DAPI; cells expressing Myc-hASUN were also immunostained for Myc. (A) Myc-hASUN was either exclusively nuclear (A1) or distributed throughout the cell (A2). (B) GFP (control) was diffusely present throughout the cell. (C-L) GFP-tagged versions of other INT subunits localized to the nucleus (E, G, I, J, L), cytoplasm (C, H), or both (D, F). Scale bar, 20 μm. (M) Immunoblot analysis of lysates of transfected cells using antibodies against Myc or GFP tags revealed fusion proteins of the predicted sizes. Tubulin was used as loading control.

Table 3.2. Quantification of localizations of tagged INT subunits in transfected HeLa cells.

Subunit	Nuclear	Cytoplasmic	Diffuse
Myc-ASUN	87 ± 2.2	4 ± 1.9	9 ± 2.4
GFP-IntS2	---	100 ± 0	---
GFP-IntS3	---	---	100 ± 0
GFP-IntS4	97 ± 2.1	---	3 ± 2.1
GFP-IntS5	---	---	100 ± 0
GFP-IntS6	93 ± 1.4	---	7 ± 1
GFP-IntS7	---	93 ± 1	7 ± 1
GFP-IntS9	85 ± 2.5	---	15 ± 2.5
IntS10-GFP	81 ± 6.5	---	19 ± 6
GFP-IntS11	---	4 ± .5	96 ± 0
GFP-IntS12	100 ± 0	---	---

HeLa cells were transfected with the indicated expression constructs encoding GFP- or Myc-tagged versions of human INT subunits, fixed, and stained with phalloidin and DAPI. Cells expressing Myc-hASUN were also immunostained for Myc. Immunofluorescence microscopy was performed to assess localization patterns of INT fusion proteins (representative images presented in Figure 3.5A-L with quantification shown here). Localizations were scored as the percentage of cells with nuclear, cytoplasmic, or diffuse localization.

of INT subunits has not been previously reported. To address whether the INT complex exists in the cytoplasm, we expressed green fusion protein (GFP)-fusions of the majority of individual INT subunits in HeLa cells to visualize their localizations. We confirmed by immunoblotting for GFP that fusion proteins of the predicted sizes were stably expressed in transfected cells (Figure 3.5M).

We divided the INT subunits into three categories based on their localizations: predominantly nuclear (hASUN; IntS4, 6, 9, 10, and 12), predominantly cytoplasmic (IntS2 and 7), or evenly distributed between the nucleus and cytoplasm (IntS3, 5, and 11) (Figure 3.5, C-L; quantified in Table 3.2). Given these complex patterns, we could not exclude the possibility that the INT complex (or perhaps INT sub-complexes) could have potential roles in the cytoplasm in addition to its established role in snRNA processing in the nucleus. It is interesting to note, however, that knockdown of any of several INT subunits that localized predominantly to the nucleus (hASUN; IntS4, 6, 9, or 12; excluding the non-essential IntS10) resulted in loss of perinuclear dynein in HeLa cells; these observations suggest that a nuclear pool of INT might be required to promote recruitment of cytoplasmic dynein to the NE (Figures 3.1 and 3.5: Table 3.2).

Reduced levels of several INT subunits at G2/M

We further considered the possibility that a cytoplasmic pool of the INT complex might be required for dynein localization. In this case, the simplest model would be that INT acts in the cytoplasm at G2/M to mediate dynein recruitment to the NE. As a test of this model, we asked whether INT subunits are present at G2/M. HeLa cells expressing tagged INT subunits were either left untreated (asynchronous population) or treated with

an inhibitor of Cyclin-dependent kinase 1 (CDK1; to obtain a G2/M-arrested population) followed by immunoblotting of cell lysates to assess fusion protein levels (Vassilev, 2006). Treated cells acquired a rounded morphology consistent with a G2/M arrest, confirming efficacy of CDK1 inhibition. We found that the levels of 60% (6/10) of the INT subunits tested were markedly decreased in G2/M-arrested cells compared to asynchronously dividing cells (Figure 3.6A). In contrast, levels of four INT subunits, including hASUN (both endogenous and tagged), were unchanged at G2/M (Figure 3.6B). Other known regulators of dynein recruitment, BICD2 (tagged) and CENP-F (endogenous), as well as a GFP control showed no change in levels at G2/M (Figure 3.6C). Notably, four subunits required for dynein localization (IntS2, IntS5, IntS6, and IntS9) were found to be present at relatively low levels at G2/M (Figures 3.1 and 3.6A). These data have led us to conclude that INT is unlikely to directly mediate dynein recruitment to the NE at this stage. Instead, we propose that INT functions earlier in the cell cycle, possibly at the level of RNA processing during interphase, to subsequently affect dynein localization at G2/M.

Mammalian ASUN homologues contain a functional NLS

To determine if dynein recruitment to the NE is promoted by cytoplasmic ASUN, as we originally hypothesized, or by nuclear ASUN, as suggested by data presented herein, we needed a method to direct the localization of ASUN within cells to either of these two compartments (Jodoin et al., 2012). To identify critical regions of ASUN required for its nuclear localization, we began by performing a structure-function analysis of the mouse ASUN homologue. Full-length Myc-tagged mASUN expressed in transfet-

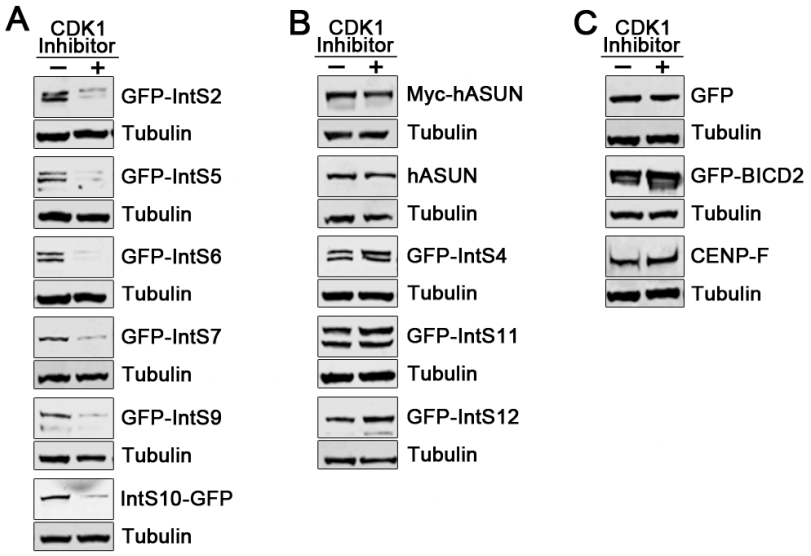

Figure 3.6. Levels of a subset of INT subunits are reduced at G2/M. HeLa cells were transfected with the indicated GFP- or Myc-fusion constructs and either left untreated (asynchronous population) or treated with a CDK1 inhibitor for 16 h (G2/M-arrested population). Immunoblot analysis of lysates of transfected cells using antibodies against GFP or Myc tags revealed decreased levels of several INT subunits at G2/M (A), whereas no changes were observed for other subunits (B). hASUN antibodies were used to assess endogenous hASUN levels. (C) No changes were observed in the levels of GFP (control), GFP-BICD2, or endogenous CENP-F at G2/M. Tubulin was used as loading control.

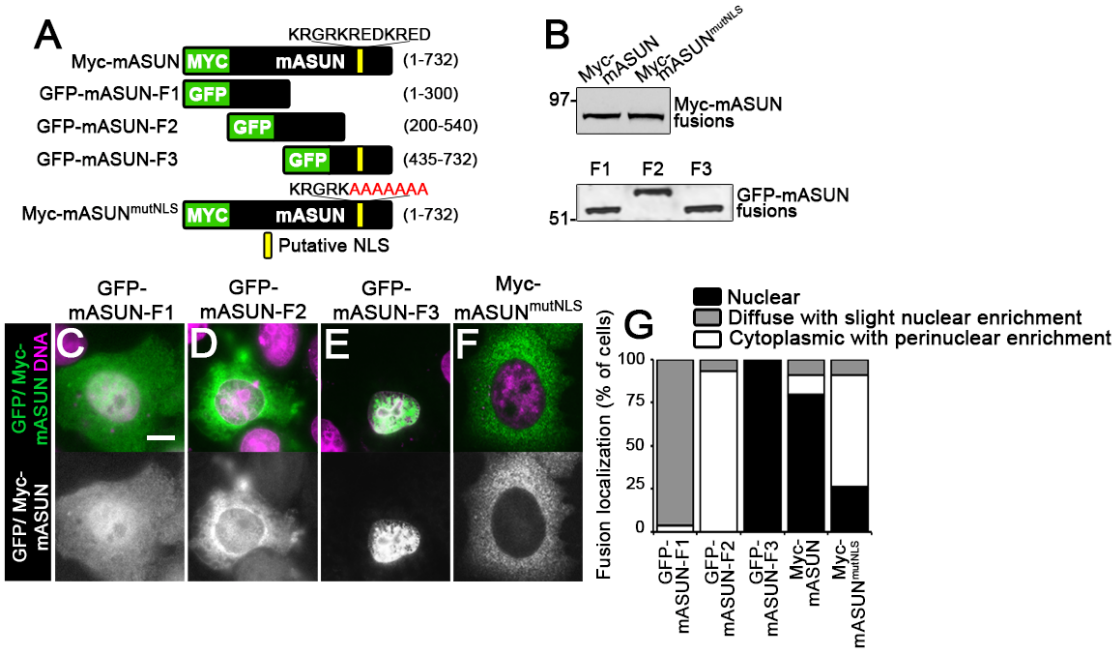

Figure 3.7. Functional NLS is conserved in mouse ASUN homolog. (A) Schematic of Myc- and GFP-tagged mASUN constructs. Myc-tagged full-length mASUN is shown at the top. The predicted NLS (yellow box) is in the C-terminal region of the protein. Three overlapping fragments of mASUN were fused to an N-terminal GFP tag: N-terminal (F1), middle (F2), and C-terminal (F3) mASUN. Myc-tagged full-length mASUN with mutation of the predicted NLS is shown at the bottom; "A" (red text) indicates each charged residue of the predicted NLS mutated to alanine in Myc-hASUNmutNLS. (B) Anti-Myc and anti-GFP immunoblots of transfected HeLa cells revealed fusion proteins of the predicted sizes. (C-F) Transfected HeLa cells were fixed and stained for DNA. Representative images of fusion protein localizations are shown. (C-E) GFP-mASUN-F1 localized diffusely (C), GFP-mASUN-F2 was in the cytoplasm, and GFP-mASUN-F3 (containing predicted NLS) was exclusively nuclear. (F) Cells expressing Myc-mASUNmutNLS were also stained for Myc. Mutation of the predicted NLS largely restricted localization of mASUN to the cytoplasm. Scale bar, 20 μm. (G) Quantification of mASUN fusion protein localizations in transfected HeLa cells.

ed HeLa cells was concentrated in the nucleus, with some cells showing diffuse or cytoplasmic localization (Figure 3.7, A and G). We divided full-length mASUN into three overlapping fragments (F1-3) and generated constructs for expression of each fragment fused to GFP at its N-terminal end (Figure 3.7A). Upon expression in transfected HeLa cells, we found that the three GFP-tagged mASUN fragments had distinct localization patterns. GFP-mASUN-F1 (N-terminal fragment) was present throughout the cell with slight enrichment in the nucleus (Figure 3.7, C and G), whereas GFP-mASUN-F2 (middle fragment) was predominantly cytoplasmic with slight perinuclear enrichment (Figure 3.7, D and G). GFP-mASUN-F3 (C-terminal fragment) appeared to be exclusively nuclear, suggesting that it likely contains critical sequences that mediate nuclear localization of full-length mASUN (Figure 3.7, E and G). For all mASUN constructs used herein, fusion proteins of the predicted sizes were observed by immunoblotting of transfected HeLa cell lysates (Figure 3.7B).

We used NLS prediction software to identify a putative NLS in the C-terminal region of mASUN (Figure 3.7A). We generated Myc-mASUN^{mutNLS} by performing site-directed mutagenesis to alter several charged residues to alanines within this region (Figure 3.7A). When expressed in transfected HeLa cells, Myc-mASUN was predominantly nuclear, whereas Myc-mASUN^{mutNLS} was predominantly cytoplasmic, thereby confirming functionality of the candidate NLS (Figure 3.7, F and G).

We also used NLS prediction software to identify a putative NLS in the C-terminal region of the human ASUN homologue that was 100% identical to the verified NLS of mASUN (Figures 3.8A and 3.7A). We performed site-directed mutagenesis to change several charged residues in this sequence to alanines, thereby generating Myc-

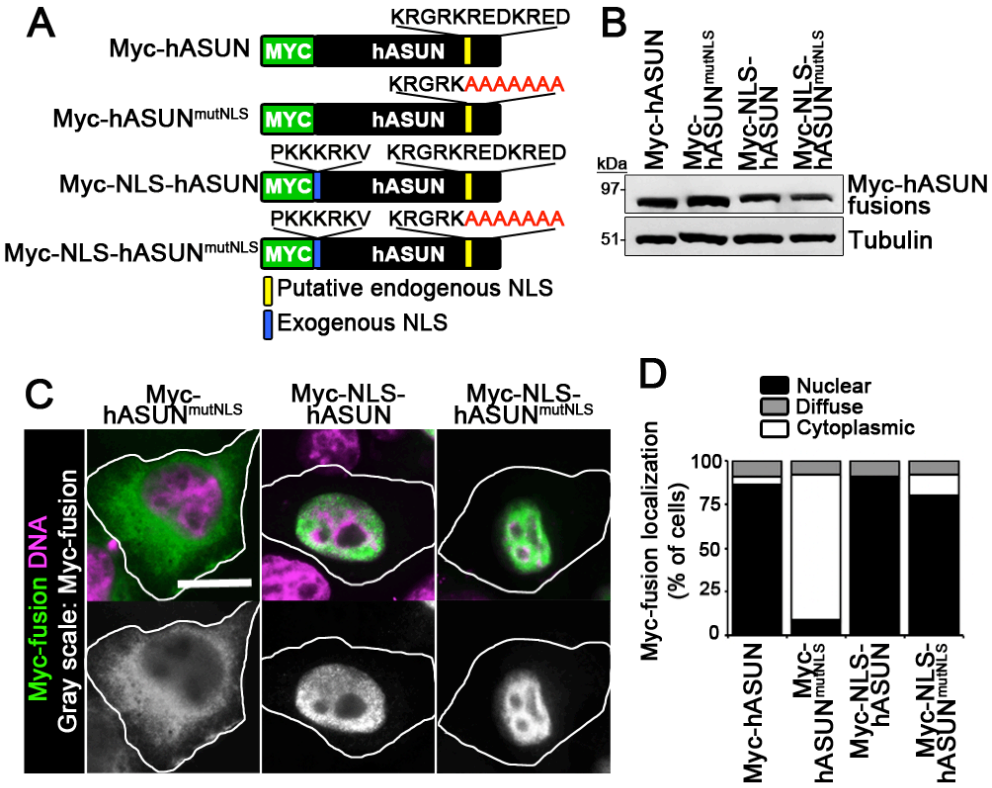

Figure 3.8. Identification of functional NLS in human ASUN. (A) Schematic of Myc-tagged hASUN with predicted NLS (yellow box) in the C-terminal region of the protein. "A" (red text) indicates each charged residue of the endogenous NLS mutated to alanine in Myc-hASUN^{mutNLS} and Myc-NLS-hASUN^{mutNLS}. An exogenous NLS (blue box) was added between the Myc tag and either hASUN or hASUN^{mutNLS} to generate Myc-NLS-hASUN and Myc-NLS-hASUN^{mutNLS}, respectively. (B) Myc immunoblot analysis of lysates of transfected HeLa cells revealed Myc-hASUN fusion proteins of the predicted sizes. Tubulin was used as loading control. (C) Representative images showing predominant localizations of Myc-hASUN fusions in transfected HeLa cells. Scale bars, 20 μm. (D) Quantification of localization patterns of Myc-hASUN fusion proteins in transfected HeLa cells.

hASUN^{mutNLS} (Figure 3.8A). When expressed in HeLa cells, Myc-hASUN was predominantly nuclear with some cytoplasmic or diffuse localization (Figure 3.5, A1-3; quantified in Table 3.2 and Figure 3.8D). In contrast, Myc-hASUN^{mutNLS} was predominantly cytoplasmic, thereby confirming that we had identified a functional NLS (Figure 3.8, C and D). For experiments presented in Figure 3.11, we also generated constructs for addition of a strong exogenous NLS (PKKKRKV; derived from SV40 large T antigen) to both hASUN and hASUN^{mutNLS} (C-terminal to the Myc tag) to produce Myc-NLS-hASUN and Myc-NLS-hASUN^{mutNLS}, respectively (Figure 3.8A) (Kalderon et al., 1984). As expected, both fusion proteins were predominantly nuclear when expressed in HeLa cells (Figure 3.8, C and D). We performed immunoblotting of lysates of transfected cells to confirm that all Myc-hASUN constructs used herein produced fusion proteins of the predicted sizes (Figure 3.8B).

Drosophila ASUN contains a functional NLS

We also identified a putative NLS in the C-terminal region of dASUN by using NLS prediction software (Figure 3.9A). We previously showed that GFP-tagged dASUN expressed in transfected HeLa cells localizes in the nucleus, cytoplasm, and between these two compartments, and we obtained similar results herein using Myc-tagged dASUN (Figure 3.9, A and B) (Anderson et al., 2009). By site-directed mutagenesis, we changed several charged residues to alanines within the candidate NLS of Myc-dASUN to generate Myc-dASUN^{mutNLS} (Figure 3.9A). Introduction of these mutations resulted in a significant shift of the fusion protein from the nucleus to the cytoplasm of transfected HeLa cells, thereby verifying functionality of the putative NLS in this system (Figure

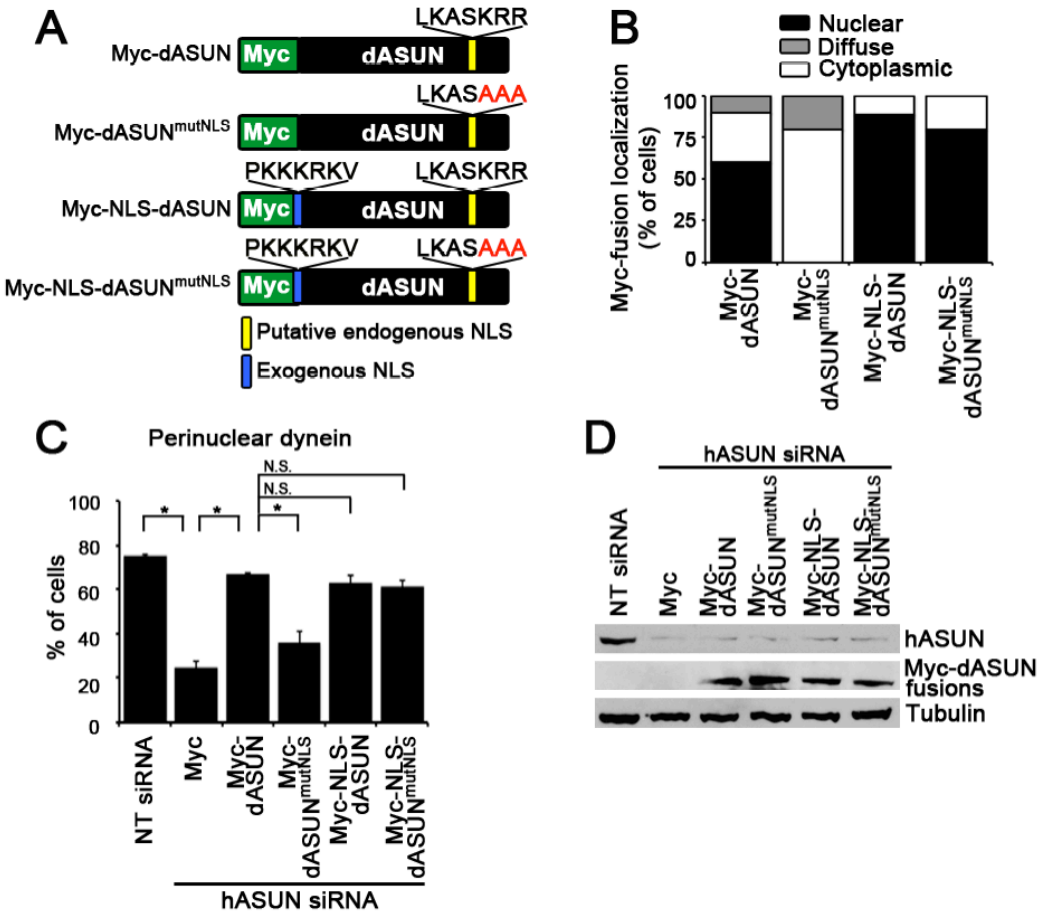

Figure 3.9. Nuclear-restricted dASUN restores dynein recruitment to the NE in HeLa cells lacking hASUN. (A) Schematic of Myc-tagged dASUN with predicted NLS (yellow box) in the C-terminal region of the protein. "A" (red text) indicates each residue of the NLS mutated to alanine in Myc-dASUNmutNLS. Exogenous NLS (blue box) is between Myc and either dASUN dASUNmutNLS to generate Myc-NLS-dASUN or Myc-NLS-dASUNmutNLS, respectively. (B) Quantification of dASUN fusion protein localization patterns in transfected HeLa cells. (C, D) HeLa cells were transfected with NT or hASUN siRNA plus dASUN expression constructs as indicated. (C) Quantification of cells with perinuclear dynein following the indicated siRNA and DNA transfections. Asterisks, $p<0.0001$ (compared to NT control). N.S. indicates non-significant statistical differences. (D) Anti-hASUN immunoblot confirmed depletion of hASUN in hASUN-siRNA cells, and anti-Myc immunoblot confirmed expression of Myc-dASUN fusion proteins of the expected size. Tubulin was used as loading control.

3.9B). For experiments presented later in this study, we also generated constructs encoding Myc-NLS-dASUN and Myc-NLS-dASUN^{mutNLS} (each containing a strong exogenous NLS placed C-terminal to the Myc tag) and confirmed that both of these fusion proteins were predominantly nuclear when expressed in HeLa cells (Figure 3.9, A and B).

We next tested whether the NLS that we identified in dASUN using transfected HeLa cells was also functional *in vivo*. We previously established transgenic *Drosophila* lines with testes-specific expression of CHY-tagged dASUN and introduced a copy of this transgene into the *asun* background (Figure 3.10A) (Anderson et al., 2009). In G2 spermatocytes, CHY-dASUN was predominantly nuclear with some diffuse localization (Figure 3.10, C and D). We used the same approach to express CHY-tagged dASUN^{mutNLS} (carrying mutations in the predicted NLS as described above) in *asun* testes (Figure 3.10A). CHY-dASUN^{mutNLS} was tightly localized to the cytoplasm of G2 spermatocytes, a pattern not observed for wild-type CHY-dASUN; thus, the NLS sequence we identified in dASUN using cultured human cells was also functional *in vivo* (Figure 3.10, C and D). For experiments presented in Figure 3.12, to enrich for dASUN in the nucleus, we used the same approach to express CHY-dASUN with a strong exogenous NLS (NLS-CHY-dASUN) in *asun* testes (Figure 3.10A). The NLS-CHY-dASUN fusion was even more tightly localized to the nucleus of G2 spermatocytes than CHY-dASUN (Figure 3.10, C and D). For all CHY-dASUN constructs described herein, fusion proteins of the predicted sizes were observed by immunoblotting of transgenic testes lysates (Figure 3.10B).

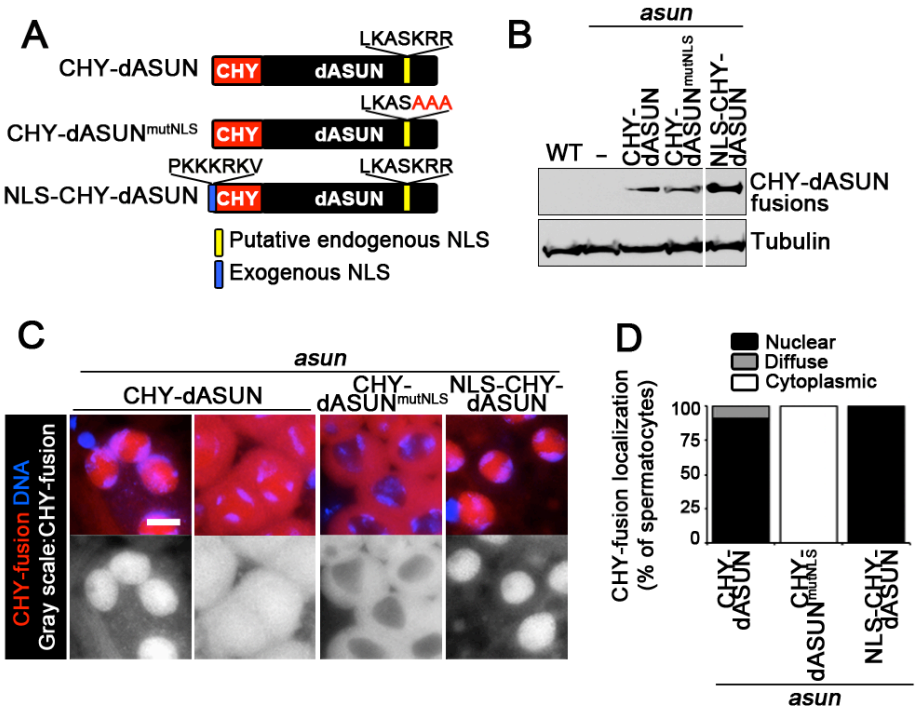

Figure 3.10. Functional NLS is conserved in *Drosophila* ASUN homologue. (A) Schematic of CHY-tagged dASUN with predicted NLS (yellow box) in the C-terminal region of the protein. "A" indicates each charged residue of the endogenous NLS mutated to alanine in CHY-dASUN^{mutNLS}. An exogenous NLS (blue box) was added to the N-terminal end of CHY-tagged dASUN to generate NLS-CHY-dASUN. (B) CHY immunoblot analysis of testes lysates from *asun* males with or without germline expression of CHY-dASUN fusions revealed proteins of the predicted sizes. An intervening lane just left of the last lane was removed. Wild-type (WT) males were used as negative control. Tubulin was used as loading control. (C) Representative images showing localizations of CHY-dASUN fusions in transgenic G2 spermatocytes. Scale bar, 50 μm. (D) Quantification of localization patterns of CHY-dASUN fusion proteins in transgenic G2 spermatocytes.

A nuclear pool of ASUN is required in HeLa cells for dynein localization

We used our hASUN expression constructs to address whether hASUN functions in the cytoplasm or nucleus of HeLa cells to promote dynein recruitment to the NE. We tested the capacity of cytoplasmic Myc-hASUN^{mutNLS} to restore perinuclear dynein to cells depleted of endogenous hASUN. Cells treated with NT or hASUN siRNA and transfected with Myc, Myc-hASUN, or Myc-hASUN^{mutNLS} constructs (refractory to hASUN siRNA) were analyzed using our dynein localization assay (Figure 3.11, A and B). As expected, we found that Myc-hASUN rescued the loss of perinuclear dynein caused by endogenous hASUN depletion (Figure 3.11A; quantified in Figure 3.11B). In contrast, dynein remained diffuse in the cytoplasm upon expression of Myc-hASUN^{mutNLS} in cells lacking endogenous hASUN, suggesting that hASUN may function in the nucleus to regulate dynein localization (Figure 3.11, A and B).

To further confirm that a nuclear pool of hASUN is required for dynein localization, and to rule out the trivial possibility that mutation of the NLS of hASUN might interfere with its activity in other ways (e.g. improper protein folding), we asked whether forced localization of Myc-hASUN^{mutNLS} to the nucleus via addition of an exogenous NLS would render it competent to restore perinuclear dynein in cells depleted of endogenous hASUN. Indeed, we found that dynein localized normally upon expression of Myc-NLS-hASUN or Myc-NLS-hASUN^{mutNLS} in hASUN-siRNA cells (Figure 3.11, A and B). These findings suggest that the mutations we introduced into the endogenous NLS of hASUN were not deleterious *per se* to the protein, but rather that nuclear residence is required for hASUN to exert its effect on dynein localization. Immunoblotting of cell lysates for endogenous hASUN and the Myc tag confirmed

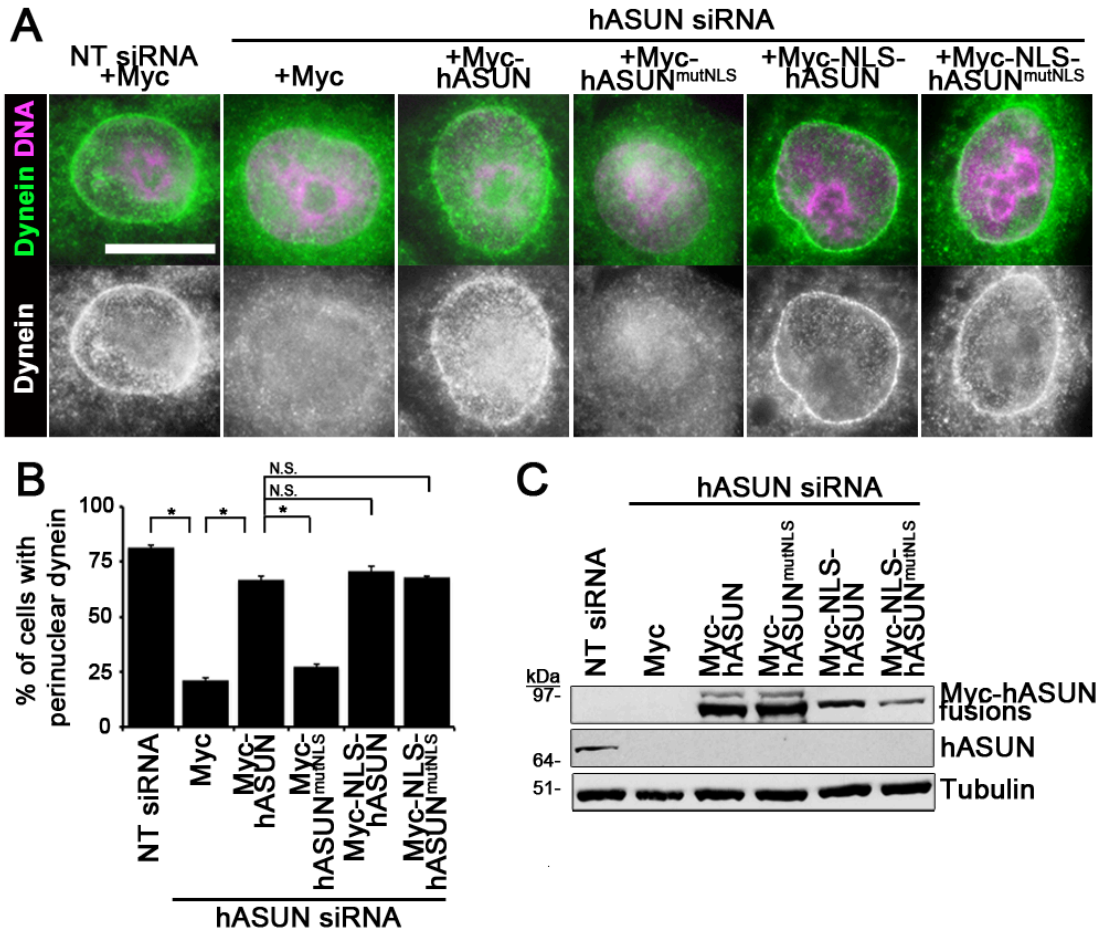

Figure 3.11. Nuclear pool of hASUN is required for dynein recruitment to the NE in HeLa cells. HeLa cells were transfected with NT or hASUN siRNA plus Myc (vector control) or Myc-hASUN expression constructs as indicated. (A) After nocodazole treatment, cells were fixed and stained for DIC and DNA. Representative images of cells are shown. Perinuclear dynein was restored only by expression of hASUN fusion proteins with nuclear localization. Scale bar, 20 μm. (B) Quantification of cells with perinuclear dynein following the indicated siRNA and DNA transfections. (C) hASUN immunoblot of lysates of transfected HeLa cells confirmed depletion of hASUN in hASUN-siRNA cells, and Myc immunoblot confirmed expression of Myc-hASUN fusion proteins of the predicted sizes. Tubulin was used as loading control. Asterisks, $p<0.0001$.

efficient depletion of hASUN by siRNA treatment and expression of all Myc-tagged hASUN fusions used herein (Figure 3.11C).

We next used our dASUN constructs to test whether dASUN acts within the cytoplasm or nucleus of transfected HeLa cells to promote dynein localization. We previously reported that loss of perinuclear dynein in hASUN-depleted HeLa cells was rescued by expression of Cherry-dASUN, and we report herein that similar results were obtained by expressing Myc-dASUN in hASUN-siRNA cells (Figure 3.9C) (Anderson et al., 2009). Consistent with our hASUN results, we found that expression of cytoplasmic-localized Myc-dASUN^{mutNLS} in hASUN-siRNA cells failed to restore perinuclear dynein, whereas nuclear-localized Myc-NLS-dASUN or Myc-NLS-dASUN^{mutNLS} were both competent to promote dynein localization (Figure 3.9C). Immunoblotting of cell lysates for endogenous hASUN and the Myc tag confirmed efficient depletion of hASUN by siRNA treatment and expression of all Myc-tagged dASUN fusions used herein (Figure 3.9D). Taken together, these data provide further support for a model in which a nuclear pool of ASUN is required for the recruitment of cytoplasmic dynein to the NE in cultured human cells and suggest that this mechanism might be conserved in *Drosophila*.

A nuclear pool of dASUN is required in *Drosophila* spermatocytes for dynein localization

We previously identified ASUN as a critical regulator of dynein localization during *Drosophila* spermatogenesis (Anderson et al., 2009). We used this system to determine whether the requirement for nuclear ASUN in regulating cytoplasmic dynein localization that we observed in HeLa cells is conserved *in vivo*. Using transgenic

Drosophila lines that we established (Figure 3.10A), we assessed the capacity of cytoplasmic CHY-dASUN^{mutNLS} or nuclear NLS-CHY-dASUN expressed in *asun* testes to promote dynein localization. As previously reported, we found that CHY-dASUN rescued loss of perinuclear dynein in *asun* spermatocytes (Figure 3.12, A and B) (Anderson et al., 2009). *asun* spermatocytes expressing CHY-dASUN^{mutNLS}, however, lacked perinuclear dynein; instead, dynein remained diffuse in the cytoplasm, similar to the phenotype of *asun* spermatocytes lacking a transgenic rescue construct (Figure 3.12, A and B). Expression of NLS-CHY-dASUN in *asun* spermatocytes restored perinuclear dynein to nearly wild-type levels, suggesting that a nuclear pool of dASUN is responsible for regulating the localization of cytoplasmic dynein motors in this system.

In addition to the failure of dynein localization, *asun* mutants display a range of defects: spermatocytes arrested at prophase I with unattached centrosomes, impaired sperm bundling, and male sterility (Anderson et al., 2009). This constellation of *asun* phenotypes is likely secondary to loss of perinuclear dynein in G2 spermatocytes, an event that occurred upstream of these defects. To determine if restoration of dynein on the NE of *asun* spermatocytes by NLS-CHY-dASUN expression was sufficient to rescue the most downstream defect, male sterility, we scored the number of live progeny per fertile male. We found that NLS-CHY-dASUN could restore fertility to *asun* males to the same degree as the CHY-dASUN control, whereas only partial rescue was achieved with CHY-dASUN^{mutNLS} (Figure 3.12C).

Taken together, these data suggest that a nuclear pool of ASUN plays a conserved role, from *Drosophila* to humans, in the recruitment of cytoplasmic dynein motors to the

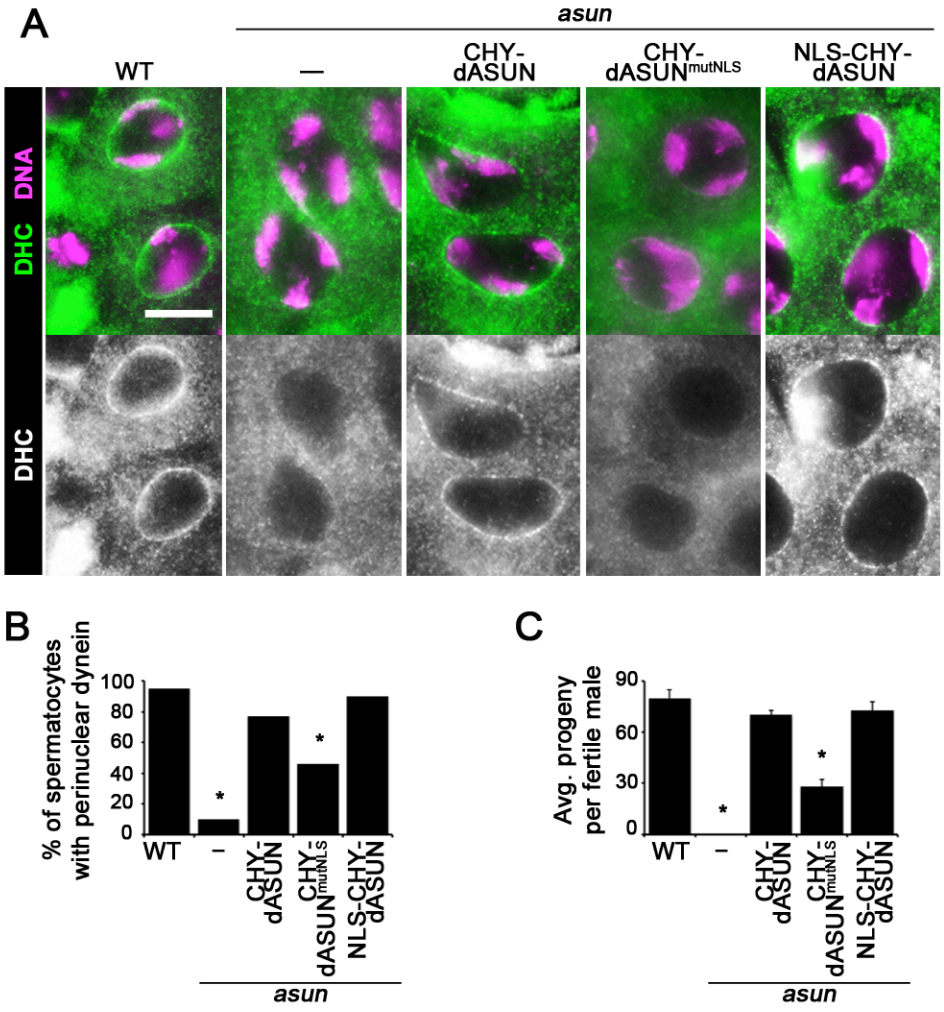

Figure 3.12. Nuclear pool of dASUN is required for dynein recruitment to the NE in *Drosophila* spermatocytes. (A, B) Testes dissected from wild-type (WT) or *asun* males with or without germline expression of CHY-tagged dASUN fusion proteins were stained for DHC and DNA. (A) Representative images of G2 spermatocytes. Perinuclear dynein was restored to *asun* G2 spermatocytes only by expression of dASUN fusion proteins with nuclear localization. Scale bar, 50 μm. (B) Quantification of G2 spermatocytes with perinuclear dynein. (C) Fertility assay shows the average number of progeny per fertile male. Asterisks, $p<0.0001$.

NE at G2/M. Combined with evidence presented herein that additional INT subunits likewise play an essential role in this recruitment step, we hypothesize that the Integrator complex mediates the processing of a critical RNA target(s) required for the production of a cytoplasmic protein that is directly involved in the regulation of dynein localization.

Discussion

A newly identified role for Integrator in promoting dynein recruitment to the NE

We previously described an essential role for ASUN in regulating dynein localization in *Drosophila* spermatogenesis and cultured human cells (Anderson et al., 2009; Jodoin et al., 2012). Recent studies have identified a second role for ASUN as an Integrator subunit required for snRNA-processing activity of the complex (Baillat et al., 2005; Chen et al., 2012; Malovannaya et al., 2010). Due to the seemingly divergent nature of these two roles, we initially speculated that ASUN might "moonlight" by performing cellular functions within the cytoplasm independently of INT. To disprove this model, we herein asked whether additional INT subunits, like ASUN, are required for dynein localization. Our finding that depletion of individual INT subunits recapitulates the loss of perinuclear dynein in hASUN-siRNA cells argues that ASUN functions within the Integrator complex to mediate this process as opposed to working independently. Given the established role of INT in snRNA processing, we considered that loss of perinuclear dynein in INT-depleted cells could be an indirect consequence of a failure to produce mature *ASUN* transcripts; our data, however, do not support this idea.

Conversely, we find that ASUN is required for stability of several INT subunits, further underscoring its importance for functioning of the complex.

A model for regulation of dynein localization by Integrator

We previously hypothesized that ASUN functions in the cytoplasm to promote redistribution of dynein from diffuse in the cytoplasm to NE-anchored at G2/M (Anderson et al., 2009; Jodoin et al., 2012). We considered that a pool of Integrator might exist in the cytoplasm that could mediate dynein recruitment to the NE via a mechanism independent of its snRNA-processing role in the nucleus. Our finding that INT subunits exhibit a range of localization patterns in HeLa cells (predominantly nuclear to predominantly cytoplasmic) neither strongly supports nor refutes this model.

Our identification of a functional NLS in *Drosophila* and mammalian ASUN homologues allowed us to manipulate the subcellular compartmentalization of ASUN and assess effects on dynein localization. We find that forced cytoplasmic localization of ASUN (via endogenous NLS mutation) hinders its capacity to promote dynein recruitment to the NE, whereas redirection of this mutant protein into the nucleus (via exogenous NLS addition) restores its function. These data indicate that Integrator likely acts from within the nucleus to control dynein localization in the cytoplasm. Furthermore, our observation that levels of several INT subunits are paradoxically decreased at G2/M, the stage at which dynein normally accumulates on the NE, suggests that Integrator may exert its effect on dynein by acting earlier in the cell cycle. We cannot exclude the possible existence of a sub-complex composed of a subset of INT subunits that are stable at G2/M; however, based on our finding that four subunits (IntS2, 5, 6, and 9) present at

reduced levels at G2/M are nonetheless required for dynein localization, it is unlikely that any such sub-complex alone would be sufficient to mediate dynein recruitment to the NE.

We propose a model in which nuclear-localized Integrator complex, including ASUN, mediates 3'-end processing of snRNA, which in turn is required for normal processing of mRNA encoding a key regulator(s) of cytoplasmic dynein localization. When Integrator activity is compromised (e.g. by knockdown of an essential subunit), production of critical transcript(s) during interphase is impaired, leading to reduction of perinuclear dynein at G2/M. To further elucidate mechanisms underlying the temporal and spatial control of dynein, it will be important to identify critical target(s) of INT involved in this process.

What are the critical targets of Integrator that mediate dynein localization?

Based on data presented herein, we hypothesize transcripts encoding a key regulator(s) of dynein localization would be misprocessed following down-regulation of INT. In a preliminary effort to identify such a target(s), we performed a high-throughput RNA-seq screen using both control-siRNA cells and IntS11-siRNA HeLa cells (T.R.A. and E.J.W., unpublished observations). We compared mRNA isolated from both populations with an emphasis on identifying transcripts that were aberrantly spliced in the absence of functional INT. While we observed several thousand alterations in splicing throughout the genome, we found no evidence for misprocessing of transcripts encoding 1) dynein-dynactin subunits or adaptor proteins or 2) components of the BICD2-RanBP2 or NudE/EL-CENP-F-Nup133 dynein-binding cassettes. We speculate that novel regulators of dynein localization could be the critical mRNA targets of INT involved in

this process. The identification of *Drosophila* ASUN (also known as Mat89Bb) as a positive regulator of siRNA, endo-siRNA, and microRNA pathways in three high-throughput screens, however, suggests that the Integrator complex may impinge on other classes of small RNAs and highlights the need for further studies of its activities (Zhou et al., 2008).

When comparing the list of individual INT subunits required for U7 snRNA processing and those required for dynein localization, only one discrepancy emerges (Table 3.1). IntS7 was previously shown to be essential for processing of U7 and spliceosomal snRNA using a cell-based reporter and through measurement of endogenous transcripts, but we find herein that it is dispensable for dynein recruitment to the NE (Chen et al., 2012; Ezzeddine et al., 2011). Given that we observed significant RNAi-mediated depletion (Figure 3.3), one possible explanation for this differential requirement is that the assays used to measure RNA processing might be more sensitive to perturbations of INT function than the dynein localization assay, perhaps because the latter is a more downstream event.

Additional cellular and developmental roles of Integrator

The Integrator complex mediates 3'-end processing of snRNAs that play essential roles in global gene expression. Given that Integrator is likely required for accurate production of a plethora of proteins, it is not surprising that loss of its activity has been associated with a wide range of cellular and developmental phenotypes. It was recently reported that siRNA-mediated down-regulation of IntS4 leads to defects in formation of nuclear structures known as Cajal bodies (Takata et al., 2012). Another group found that

IntS6 and IntS11 are required for proper differentiation of adipocytes in a cultured cell system; although the underlying mechanism remains unknown, the authors hypothesized that U1 and U2 snRNAs are involved (Otani et al., 2013a). In large-scale screens performed in zebrafish and *C. elegans*, *IntS7* homologues have been shown to be required for normal craniofacial development (Golling et al., 2002; Kamath et al., 2003). Mutation of *Drosophila IntS7* (*deflated*) results in abdominal phenotypes due to cell cycle and signaling defects (Rutkowski and Warren, 2009). Integrator is also essential for hematopoeisis in zebrafish: down-regulation of IntS5, IntS9, or IntS11 caused aberrant splicing of *smad1* and *smad5* transcripts, thereby generating a dominant-negative form of Smad that disrupts erythrocyte differentiation (Tao et al., 2009).

What remains to be elucidated is how perturbations in snRNA 3'-end formation generate phenotypes so specific yet so diverse. While the favored hypothesis is that global reduction in snRNA biosynthesis will negatively impact splicing of a subset of transcripts, the criteria for defining this set is unclear. It is likely that these sensitive transcripts will be enriched for either suboptimal splice sites, alternative splice sites, or minor spliceosome-dependent introns. Regardless of the root cause, our discovery of a new role for the Integrator complex in regulating dynein localization adds to the growing list of INT-dependent processes.

CHAPTER IV

THE snRNA-PROCESSING COMPLEX, INTEGRATOR, IS REQUIRED FOR CILIOGENESIS AND DYNEIN RECRUITMENT TO THE NUCLEAR ENVELOPE VIA DISTINCT MECHANISMS

This chapter has been accepted by *Biology Open*. (Jodoin JN, et al. 2013).

Introduction

Cytoplasmic dynein is a large, multimeric, minus-end-directed motor complex that associates with the dynein-activating complex, dynactin. (Holzbaur and Vallee, 1994; Kardon and Vale, 2009; Schroer, 2004). Two forms of cytoplasmic dynein exist within cells: dynein-1 and dynein-2. Dynein-1 is required for a variety of essential functions such as cargo transport along microtubules, centrosome assembly, organelle positioning, mitotic spindle positioning, and ciliogenesis, whereas dynein-2 is required for retrograde transport of cargo along primary cilia (PC) and maintenance of PC length (Palmer et al., 2011; Rajagopalan et al., 2009). Dynein complexes are subject to multiple layers of regulation, including binding of accessory proteins, phosphorylation, variations in subunit composition, and subcellular localization (Kardon and Vale, 2009).

During G2/M of cell division in multiple species, a pool of dynein anchored to the nuclear envelope (NE) facilitates nucleus-centrosome coupling, an essential step for proper mitotic spindle formation (Anderson et al., 2009; Bolhy et al., 2011; Gonczy et al., 1999; Jodoin et al., 2012; Malone et al., 2003; Robinson et al., 1999; Sitaram et al., 2012;

Splinter et al., 2010; Vaisberg et al., 1993). Three components are known to be required for dynein accumulation on the NE and subsequent nucleus-centrosome coupling in human cells. The first two components, Bicaudal D2 (BICD2) and Centromere protein F (CENP-F), independently bind dynein subunits/adaptor proteins and nucleoporins to stably tether dynein complexes to the NE (Bolhy et al., 2011; Splinter et al., 2010). The third recently identified component, the small nuclear RNA (snRNA) complex, Integrator (INT), likely regulates dynein recruitment to the NE in an indirect manner distinct from that of BICD2 and CENP-F (Jodoin et al., 2013a).

INT, a highly conserved nuclear complex consisting of 14 subunits, interacts with the C-terminal tail of the largest subunit of RNA-polymerase II to promote 3'-snRNA processing (Baillat et al., 2005; Chen and Wagner, 2010). These processed snRNAs play critical roles in gene expression via intron removal and further pre-mRNA processing (Matera et al., 2007). Analysis of INT has revealed that the complex must be intact to perform its RNA processing function: loss of individual INT subunits, with the exception of IntS10, leads to a nonfunctional complex (Chen et al., 2012). Various cellular functions have been ascribed to INT in cultured mammalian cells. IntS4 is required for formation of Cajal bodies (Takata et al., 2012) and IntS6 and IntS11 ensure proper differentiation of adipocytes (Otani et al., 2013b). INT has additionally been reported to be required for developmental functions *in vivo* (Golling et al., 2002; Kamath et al., 2003; Rutkowski and Warren, 2009). In zebrafish, IntS5, IntS9, and IntS11 are required for *smad1* and *smad5* mRNA processing (Tao et al., 2009). We recently reported an essential role for INT in recruitment of dynein to the NE at G2/M (Jodoin et al., 2013a).

PC are non-motile appendages that form in the majority of vertebrate cells. These structures act as sensory organelles and play essential roles in sensing and processing signals from the extracellular environment (Basten and Giles, 2013; Ko, 2012; Salisbury, 2004). To initiate primary ciliogenesis during G1, one of the two centrioles migrates to the plasma membrane, where it will dock and mature into a basal body (BB) that nucleates the PC (Kim and Dynlacht, 2013b). Prior to mitotic entry, the PC is resorbed to allow for the formation of the bipolar spindle (Wang et al., 2013). Across phyla, dynein has been shown to be required for ciliogenesis (Kim and Dynlacht, 2013b; Kim et al., 2011; Kong et al., 2013). Loss of dynein heavy chain, which results in decay of the complex, hinders PC formation (Draviam et al., 2006; Rajagopalan et al., 2009). Additionally, dynein is required for retrograde movement of proteins along the PC and regulation of PC length (Rajagopalan et al., 2009). While many centrosomal and interflagellar trafficking proteins are known to be critical for PC formation, more are hypothesized to exist (Graser et al., 2007; Kim and Dynlacht, 2013b).

In this work, we sought to determine if INT is required for additional dynein-dependent events within cultured human cells. We herein report a role for INT in promoting ciliogenesis.

Materials and methods

Cell culture, immunostaining, and microscopy

Cell lines were maintained at 37˚C and 5% CO_2 in DMEM (Life Technologies, Carlsbad, CA) containing 10% FBS, 1% L-glutamine, 100 μg/ml streptomycin, and 100

U/ml penicillin. siGENOME NT siRNA#5 (Dharmacon, Lafayette, CO) was used as negative control. siRNA oligonucleotides used herein for specific knockdowns have been previously described as follows: INT subunits (Jodoin et al., 2012), CETN2 and PCTN (Graser et al., 2007), BICD2 and RanBP2 (Splinter et al., 2010), CENP-F (Bolhy et al., 2011), and DHC (Rajagopalan et al., 2009). siRNA oligonucleotides were obtained from Dharmacon or Sigma-Aldrich (St. Louis, MO). Independent siRNA oligonucleotides used to silence IntS3 (IntS3 #2; SASI_Hs01_00063141), IntS4 (IntS4 #2; 5'-CAG CAU UGU UCU CAG AUC A-3'), IntS9 (IntS9 #2; 5'-GUG AAC UCU GCC CUU AGU A-3'), and IntS11 (IntS11 #2; SASI_Hs02_00350804) were obtained from Sigma-Aldrich. Immunoblot signals for INT subunit protein levels following siRNA treatment were quantified relative to tubulin using ImageJ.

Cells were transfected with siRNA oligonucleotides using DharmaFECT 1 transfection reagent (Dharmacon) and analyzed at 72 h post-siRNA treatment in all cases. To stimulate PC formation under conditions of serum starvation, cells at 100% confluence and at 48 h post-siRNA treatment were incubated in DMEM plus 0.5% FBS for 24 h prior to fixation. Where indicated, siRNA-treated cells in normal growth media were incubated in 5 μg/ml (16.6 μM) nocodazole (Sigma-Aldrich) for 3 h (HeLa cells) or 10 μg/ml (33.2 μM) nocodazole for 1 h (RPE cells) prior to fixation at 72 h post-siRNA treatment to enhance perinuclear localization of dynein. Primary antibodies were used as follows: acetylated tubulin (6-11B-1, 1:500, Sigma-Aldrich), γ-Tubulin (ab16504, 1:500, Abcam, Cambridge, MA), CEP164 (NBP-77006, 1:100, Novus Biologicals, Littleton, CO), CEP89 (HPA040056, 1:100, Sigma), FBF-1 (HPA023677; 1:100, Sigma), CETN2 (N-17-R, 1:200, Santa Cruz Biotechnology, Dallas, TX), PCTN (ab4448, 1:2000,

Abcam), Ninein (ab4447, 1:500, Abcam), dynein intermediate chain (74.1, 1:500, Abcam), and PH3 (Mitosis Marker, 1:1000, Millipore, Billerica, MA). Wide-field and confocal fluorescence microscopy methods were previously described (Efimov et al., 2007; Jodoin et al., 2013a).

PC length (visualized by acetylated tubulin staining) was measured from base to tip using ImageJ (National Institutes of Health, Bethesda, MD); at least 100 cells were scored per condition. For determination of the percentage of cells with PC or perinuclear dynein, experiments were performed ≥3 times with ≥200 cells scored per condition. For quantification of perinuclear dynein intensity, 10 representative cells were measured per condition; for each cell, 12 line scans distributed equally around the nuclear circumference were obtained. Line scan analyses were performed using ImageJ. Line scans presented within figures are 50 pixels in length and are oriented with the cytoplasmic end of each line to the left and the intranuclear end of each line to the right. Statistical analyses of data were performed using Student's unpaired *t*-test. For bar graphs, error bars indicate s.e.m.

Immunoblotting

Immunoblotting of cell lysates was performed as previously described (Jodoin et al., 2013a). The following primary antibodies were used: c-Myc (9E10, 1:1000), β-tubulin (E7, 1:1000, Developmental Studies Hybridoma Bank, University of Iowa, Iowa City, IA), CENP-F (14C10 1D8, 1:500, Abcam), BICD2 (1:2500; gift from A. Akhmanova) (Hoogenraad et al., 2001), dynein intermediate chain (74.1, 1:500, Santa Cruz Biotechnology), PCTN (ab4448, 1:2000, Abcam), CETN2 (N-17-R, 1:200, Santa

Cruz Biotechnology), RanBP2 (ab64276, 1:1000, Abcam), IntS1, IntS4, IntS7, IntS9, IntS10, IntS11, IntS12, and CPSF30 (1:1000, Bethyl Labs, Montgomery, TX).

Results and discussion

Individual INT subunits are required for PC formation

Given the role of INT in dynein recruitment to the NE at G2/M, we asked whether INT plays a broader role in regulating dynein-related functions. Specifically, we sought to determine if INT is required for PC formation, another dynein-dependent process. We performed siRNA-mediated down-regulation of individual INT subunits in human retinal pigment epithelial (RPE) cells and assessed PC formation. Prior to fixation and immunostaining for acetylated tubulin and γ-tubulin (to mark cilia and centrioles, respectively), the confluent monolayer of cells was subjected to serum starvation for 24 hours to stimulate PC formation.

Under these conditions, the frequency of non-targeting (NT)-siRNA cells with PC ranged from ~60-80% (data not shown). Primary ciliogenesis data are presented as the percentage of NT-siRNA cells. As a positive control, cells were depleted of Centrin-2 (CETN2), a centriolar component required for ciliogenesis (Graser et al., 2007; Salisbury, 2004). Following individual knockdown of most INT subunits tested (IntS1, 3, 4, 9, 11, or 12), we observed loss of PC to a degree comparable to that of CETN2-siRNA cells, suggesting that INT plays a critical role in PC formation (Figure 4.1). We observed

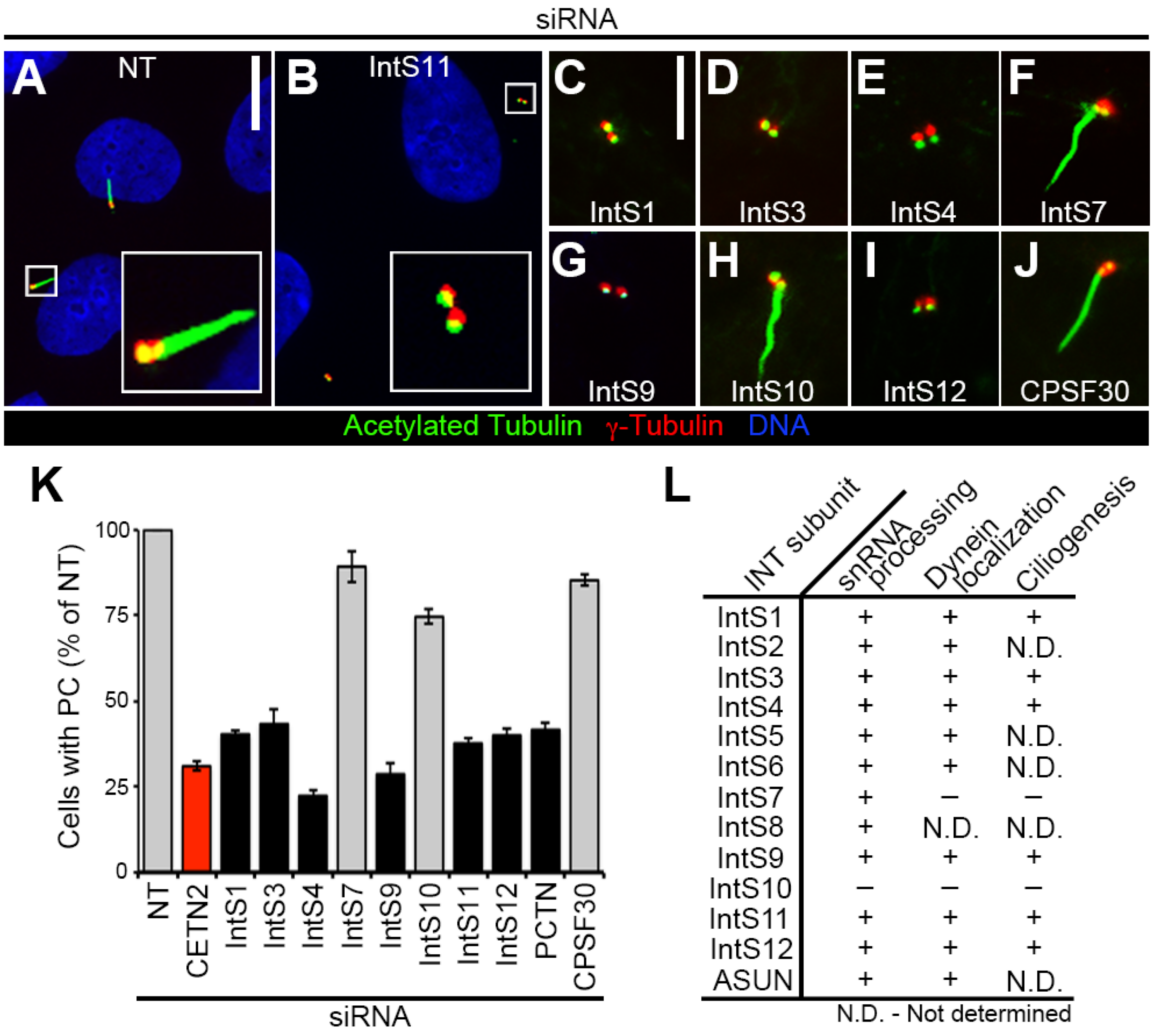

Figure 4.1. Loss of PC following INT depletion. RPE cells were transfected with siRNA, serum-starved, fixed, and stained for acetylated tubulin, γ-tubulin, and DNA. (A-J) Representative images show decreased PC formation after knockdown of most INT subunits tested. Scale bars, 10 (A,B) or 5 (C-J) μm. (K) Quantification of PC formation (normalized to NT-siRNA) in INT-depleted cells. Gray, $p<0.0001$; black, not significant (both relative to CETN2-siRNA, red). (L) Comparison of INT subunit requirements in snRNA processing (Chen et al., 2012), dynein localization , and ciliogenesis (presented herein). (+), required; (-), not required; (N.D.), not determined.

essentially identical results using a second independent siRNA for a subset of INT subunits, confirming that the loss of PC is not due to an off-target effect (Figure 4.2). Knockdown of IntS10, which is dispensable for both snRNA processing and dynein localization, similarly had no effect on PC formation, further confirming that this subunit is not a critical component of the INT complex. Data are conflicting for only one INT subunit, IntS7, which was previously reported to be required for snRNA processing, but not for dynein localization; we found that depletion of IntS7 had no effect on PC formation (Chen et al., 2012; Ezzeddine et al., 2011; Jodoin et al., 2013a) (Figure 4.1). A possible explanation for this discrepancy is that the snRNA-processing assay might be more sensitive than the assays designed to assess cytoplasmic events (perinuclear dynein accumulation and PC formation) that are presumably downstream of RNA processing. Efficient knockdown of all siRNA-targeted endogenous proteins in experiments presented herein was confirmed by immunoblotting (Figure 4.3).

To test whether the loss of PC in INT-depleted cells is specific to disruption of INT-mediated snRNA processing, and not secondary to a general disruption of RNA processing, we down-regulated Cleavage Polyadenylation Specificity Factor 30 (CPSF30) in cells and assessed PC formation. CPSF30 is a component of a complex required for the recruitment of machinery that mediates 3'-mRNA cleavage and poly(A) tail synthesis; depletion of CPSF30 leads to a deficiency, but not a complete loss, of poly(A) 3'-end formation in cells (Barabino et al., 1997). We found no significant effect on PC formation, however, in CPSF30-siRNA cells, suggesting a specific role for INT-mediated snRNA processing in PC formation (Figure 4.1).

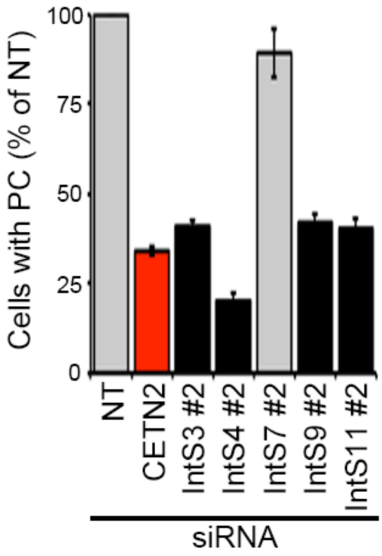

Figure 4.2. Loss of PC following INT down-regulation by independent siRNA sequences. RPE cells were transfected with indicated siRNAs, serum-starved, fixed, and stained for acetylated tubulin, γ-tubulin, and DNA. Quantification of PC formation (normalized to NT-siRNA) in siRNA-depleted cells. Gray, $p<0.001$; black, not significant (relative to CETN2-siRNA, red).

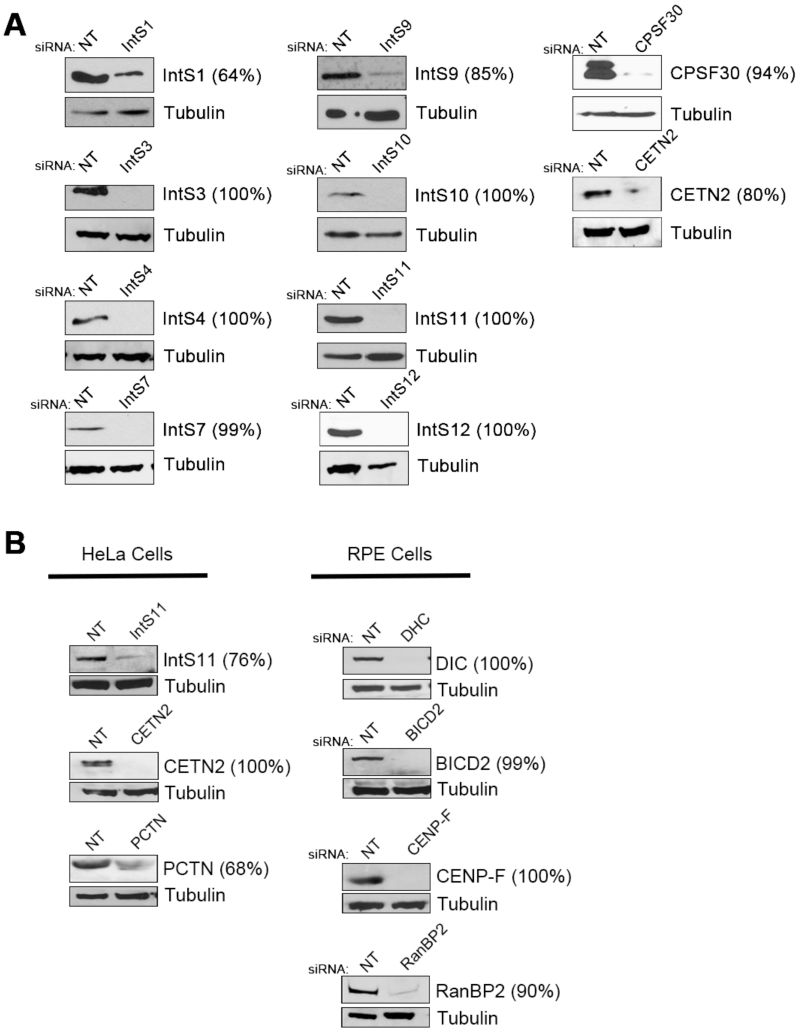

Figure 4.3- Confirmation of efficient knockdown of proteins by siRNA. RPE or Hela cells were transfected with siRNA as indicated. Immunoblots of cell lysates were probed with antibodies against INT subunits, perinuclear dynein regulators, ciliogenesis regulators, or related controls corresponding to data presented in Figs 1 and 3 (A) or Figs 3 and 4 (B). Depletion of each protein targeted by siRNA was confirmed. Tubulin was used as loading control. Percent of protein depletion following targeted knock down indicated next to each antibody.

In addition to loss of PC, we observed increased centriole separation following individual knockdown of most INT subunits tested (IntS1, 3, 4, 9, 11, or 12) (results for IntS4 and IntS11 shown in Figure 4.4; data not shown for other listed subunits). This phenotype has been reported in cells depleted of a subset of ciliogenesis regulators, although a strict correlation between the separation of centrioles and loss of PC has not been observed; hence, the functional significance of this phenotype is unclear (Graser et al., 2007; Salisbury, 2004). As for PC formation, we did not observe defects in centriole coupling following IntS7 or IntS10 depletion (results for IntS10 shown in Figure 4.4; data not shown for IntS7).

We considered the possibility that the lack of PC in INT-depleted cells could be secondary to a failure of these cells to arrest in G1 upon serum starvation. We previously showed that down-regulation of individual INT subunits does not lead to any gross defects in cell-cycle phasing under normal growth conditions (Jodoin et al., 2013a). To confirm that INT-depleted cells respond normally to serum starvation by arresting in G1, we performed fluorescence-activated cell sorting analysis. In contrast to INT-depleted cells growing asynchronously in 10% fetal bovine serum, INT-depleted cells arrested in G1 following serum starvation in the same manner as control cells (Figure 4.5). Taken together, these data reveal that INT is required for PC formation and centriole coupling, thereby adding to the growing list of INT-dependent cellular processes. We propose a model in which INT mediates processing of snRNA required for normal production of mRNA encoding a critical regulator of ciliogenesis.

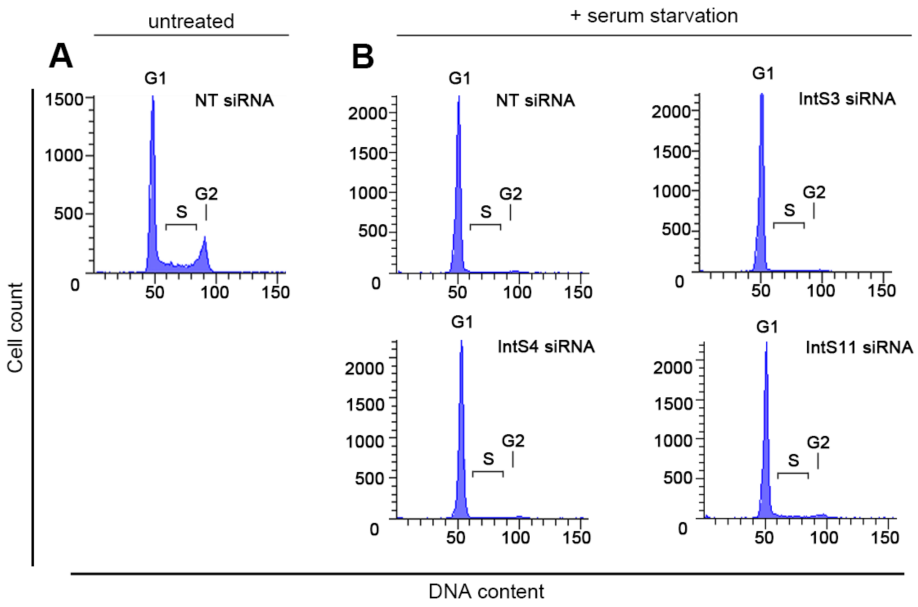

Figure 4.4. Confirmation of G1 arrest in serum-starved RPE cells following INT subunit knockdown. RPE cells were transfected with siRNA as indicated, serum-starved, fixed, and stained with propidium iodide. DNA content was analyzed by FACS as previously described (Jodoin et al., 2013). (A) Cell-cycle profile of NT-siRNA cells grown under normal media conditions (plus 10% FBS). (B) Cell-cycle profiles of NT-siRNA and INT-depleted cells following serum starvation revealed a similar degree of G1 arrest.

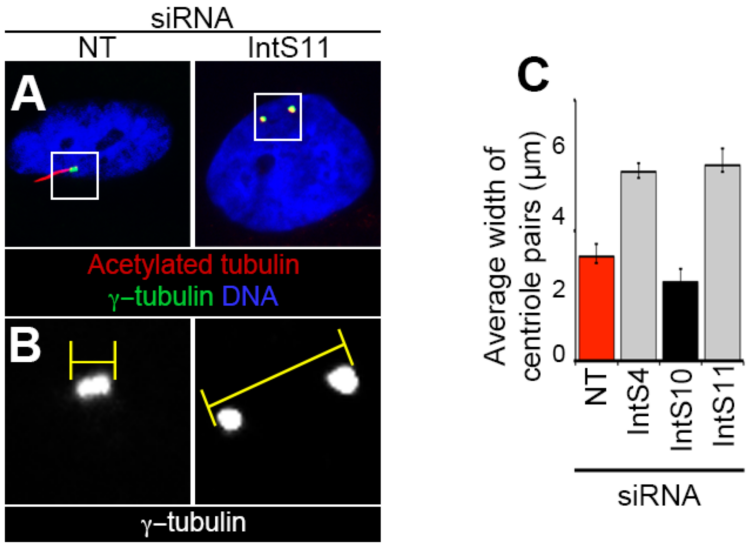

Figure 4.5. Increased frequency and degree of centriole pair separation following loss of INT activity. RPE cells were transfected with siRNA as indicated. Following siRNA treatment, PC formation was stimulated by serum starvation. After fixation, cells were stained for acetylated tubulin, g-tubulin, and DNA. (A) Separation of centriole pairs was observed following INT subunit-siRNA treatment. (B) Higher magnification of region enclosed within white box shows scoring system used to measure distance between centriole pairs (yellow bars). (C) Quantification of the average distance between centriole pairs following indicated siRNA treatment. Gray bars, $p<0.0001$; black, not significant (both relative to NT-siRNA, red). Distance between the outer borders of basal body pairs (marked by g-tubulin staining) was measured using ImageJ. Basal body pairs in at least 100 cells were scored per condition.

INT depletion does not affect a subset of proteins required for BB maturation and assembly

We considered the possibility that loss of PC following INT depletion could result from failure of BB maturation and/or abnormal BB composition. The process of BB maturation includes assembly of the distal appendage, which projects radially from the distal end of the cilium, serving to anchor the BB and cilium to the plasma membrane. Centrosomal protein 164 (Cep164), Centrosomal protein 89 (Cep89), and Fas-binding factor 1 (FBF-1) are distal appendage components required for PC production (Sillibourne et al., 2011; Tanos et al., 2013). We observed normal localization of these proteins to the base of the PC in INT-depleted cells (Figure 4.6A-C, quantified in Figure 4.7A-C). We also found that γ-tubulin localized normally to BB in INT-siRNA cells (Figure 4.1A-I). We next evaluated several core BB proteins essential for PC formation: CETN2, Pericentrin (PCTN), and Ninein (Graser et al., 2007; Salisbury, 2004). We found their localizations and intensities to be comparable in INT-depleted and control cells (Figure 4.6D-F; quantified in Figure 4.7D-F). Taken together, these data suggest that loss of PC in INT-depleted cells is unlikely to be secondary to defective processing of transcripts encoding the studied proteins.

PC formation is not required for dynein recruitment to the NE

We have identified two dynein-mediated processes that require INT: PC formation during G1 and dynein recruitment to the NE at G2/M (Figure 4.1) (Jodoin et al., 2013a). We reasoned that INT might ensure production of a single transcript encoding a common regulator of these processes or distinct transcripts that independently regulate

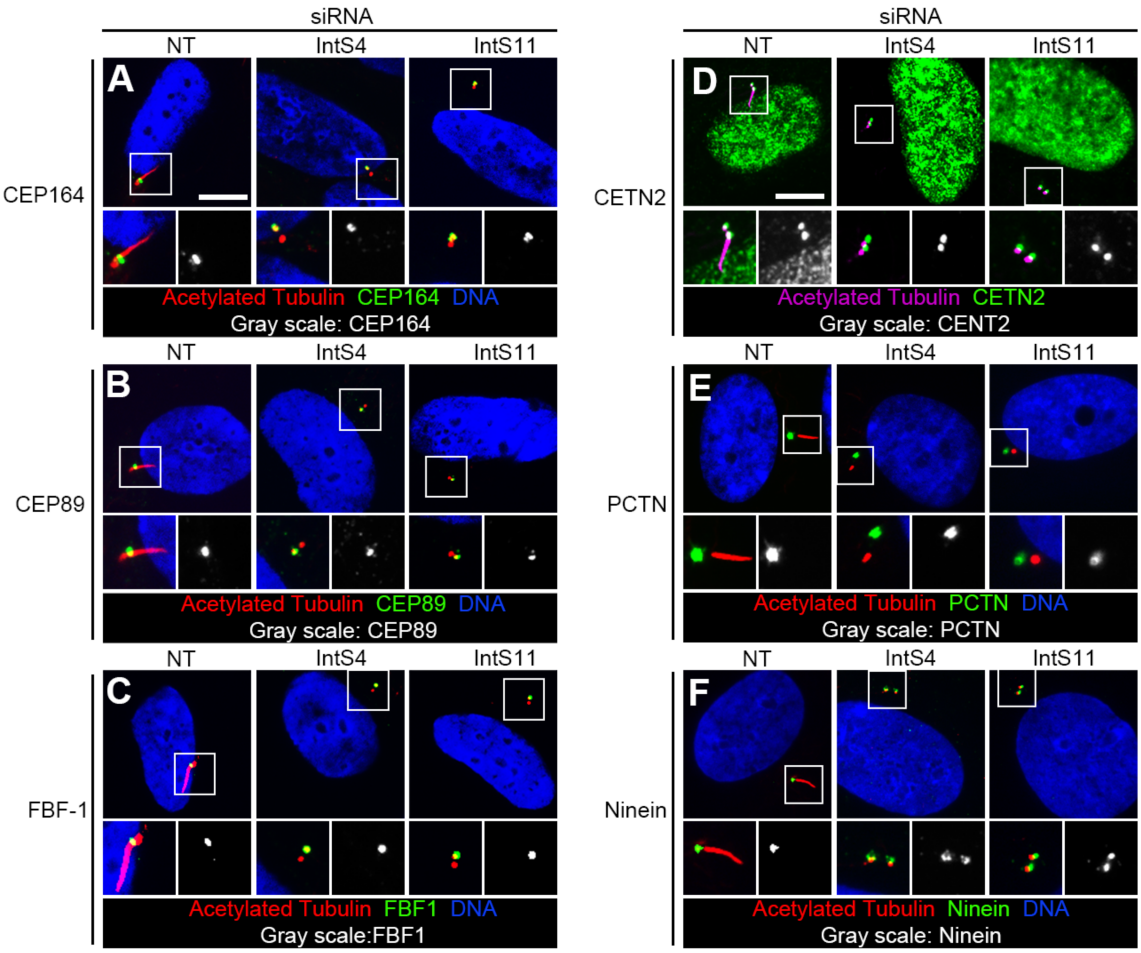

Figure 4.6. Normal BB composition following INT depletion. RPE cells were transfected with siRNA, serum-starved, fixed, and stained for acetylated tubulin, BB markers, and DNA. Representative images show normal localization of BB markers in INT-depleted cells. Higher-magnification views (bottom micrographs) of BB correspond with regions enclosed by white boxes. Scale bars, 10 μm.

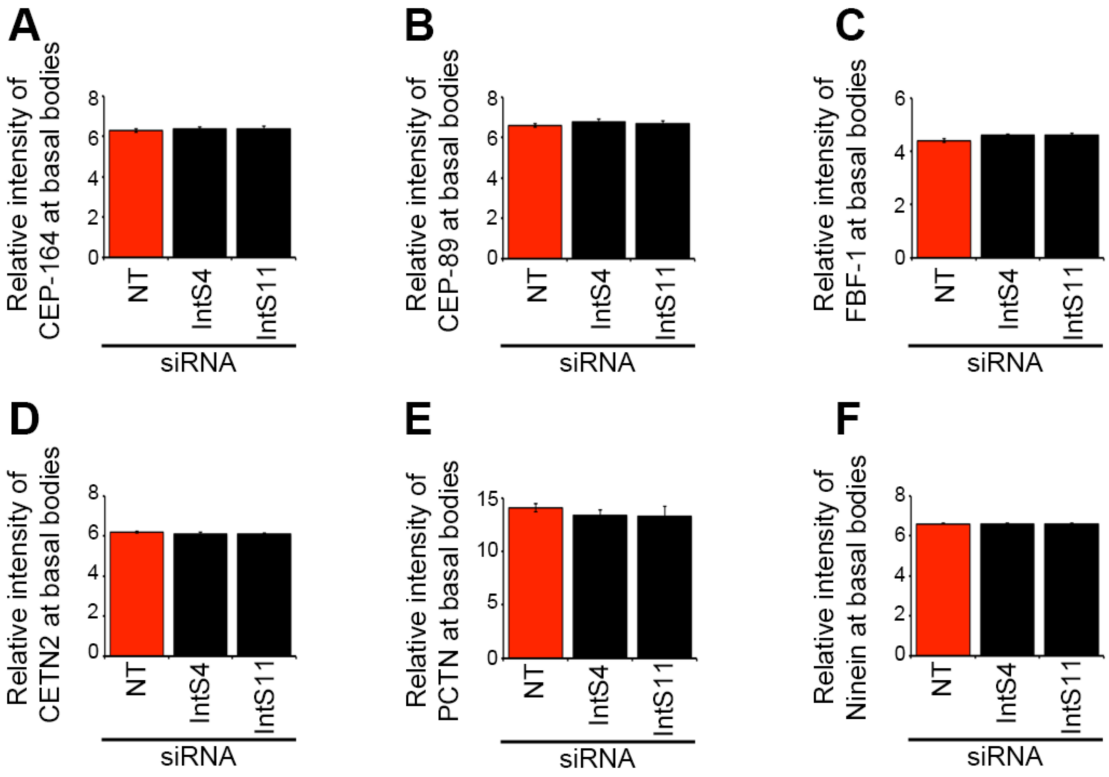

Figure 4.7. Characterization of basal body markers. Quantification of distal appendage (A-C) and basal body (D-F) signals for indicated markers (normalized to signals for acetylated tubulin). No significant changes in intensity were observed following depletion of individual INT subunits. Intensity of antibody signals on basal bodies was determined using ImageJ. Basal bodies in at least 100 cells were scored per condition. Black bar, not significant (relative to NT-siRNA, red).

each process. To help distinguish between these two possibilities, we sought to determine whether dynein enrichment on the NE and PC formation are interdependent or uncoupled events.

We first asked whether proteins essential for PC formation are also generally required for dynein recruitment to the NE. We performed siRNA-mediated knockdown of CETN2 and PCTN in HeLa cells and assessed dynein localization during prophase. We used the following criteria to identify prophase cells: positively immunostained for phosphorylated histone H3 (PH3) with an intact NE. HeLa cells have commonly been used to study the regulation of perinuclear dynein due to their highly enriched pool of dynein on the NE at G2/M (Bolhy et al., 2011; Jodoin et al., 2012; Jodoin et al., 2013a; Splinter et al., 2010). Prior to fixation and immunostaining for dynein intermediate chain (DIC) and PH3, siRNA-treated cells were incubated with 5 μM nocodazole to stimulate recruitment of dynein-dynactin complexes and their accessory proteins to the nuclear surface. This brief nocodazole treatment has been documented to enrich for functional dynein complexes on the NE in non-G1 cells (Beswick et al., 2006; Bolhy et al., 2011; Hebbar et al., 2008; Jodoin et al., 2012; Jodoin et al., 2013a; Splinter et al., 2010).

Consistent with our previous report, we observed drastic reduction of the fraction of cells with dynein accumulation on the NE following INT depletion: only 24% of IntS11-siRNA prophase cells exhibited perinuclear dynein compared to 92% of NT-siRNA prophase cells (Figure 4.8A,C) (Jodoin et al., 2012). We chose to focus on IntS11 for this experiment based on its role as the catalytic subunit of the INT complex (Chen and Wagner, 2010). In contrast, the fraction of prophase cells with perinuclear dynein following depletion of other ciliogenesis regulators, CETN2 or PCTN, was comparable to

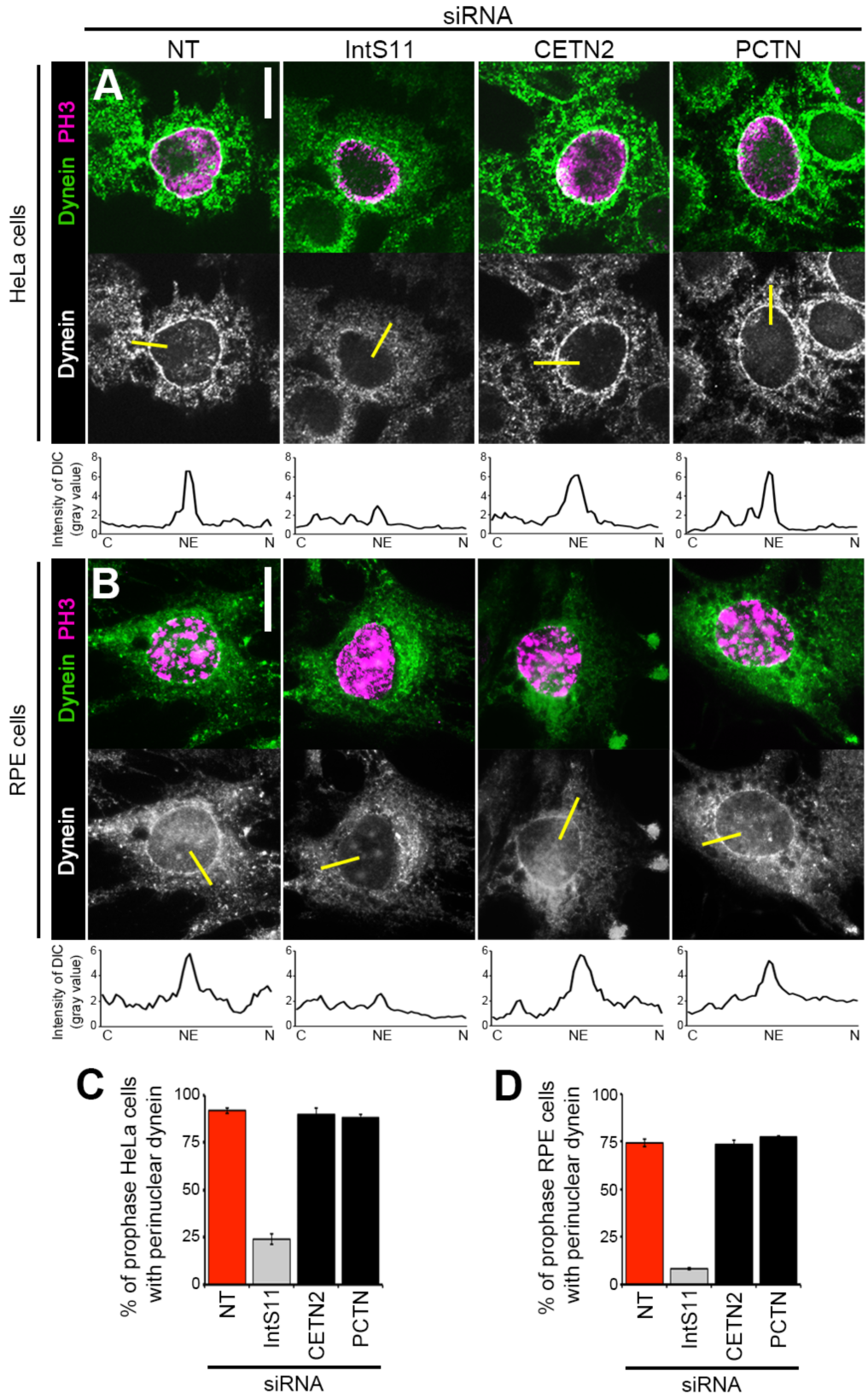
siRNA
NT
IntS11
CETN2
PCTN
A
HeLa cells
Dynein PH3
Dynein
Intensity of DIC (gray value)
C
NE
N
B
RPE cells
C
% of prophase HeLa cells with perinuclear dynein
D
% of prophase RPE cells with perinuclear dynein

Figure 4.8. Ciliogenesis regulators are not required for perinuclear dynein recrutiment. HeLa cells (A,C) or RPE cells (B,D) were transfected with siRNA, nocodazole-treated, fixed, and stained for dynein (DIC) and PH3. (A,B) Representative images show perinuclear dynein in prophase HeLa (A) or RPE cells (B) after indicated knockdowns. Yellow bars represent line scans that span the cytoplasm (C), nuclear envelope (NE), and nucleus (N) to measure peak DIC intensity on the NE; corresponding plots are shown below each micrograph. (C,D) Quantification of perinuclear dynein in HeLa (C) or RPE (D) prophase cells (PH3-positive with intact NE). Scale bars, 10 μm. Gray, $p<0.0001$; black bar, not significant (both relative to NT-siRNA, red).

that of NT-siRNA cells (90% and 88%, respectively; Figure 4.8A,C). We have previously reported that this NE-anchored pool of dynein is found in RPE cells (Jodoin et al., 2012). To determine if INT is required for dynein recruitment (in addition to primary ciliogenesis) in RPE cells, we assessed perinuclear dynein following down-regulation of IntS11. Dynein accumulation on the NE was found in 77% of NT-siRNA RPE prophase cells following treatment with 10 μM nocodazole (Figure 4.8B,D). Similar to our results with HeLa cells, we observed a severe reduction in the percentage of RPE prophase cells with NE-anchored dynein (down to 7%) following depletion of IntS11 (Figure 4.8B,D). This finding suggests that the role for INT in promoting perinuclear dynein is conserved and is not a consequence of the transformed nature of HeLa cells. As for HeLa cells, we found that the primary ciliogenesis regulators tested were not required for perinuclear dynein in RPE cells: loss of CETN2 or PCTN recapitulated what was observed in NT-siRNA cells (with PC formation in 76% and 78%, respectively, of siRNA-treated cells; Figure 4.8B,D).

As further confirmation of these findings, we quantified DIC immunofluorescence signals on the NE versus the cytoplasm and the average peak DIC intensity on the NE in both cell lines and found them greatly reduced in IntS11 cells as previously described, but unchanged in cells depleted of CETN2 or PCTN compared to NT-siRNA cells (Figure 4.9) (Jodoin et al., 2012; Jodoin et al., 2013a). These data reveal that INT differs from CETN2 and PCTN, two other proteins essential for ciliogenesis, in that it has a dual function in promoting perinuclear accumulation of dynein.

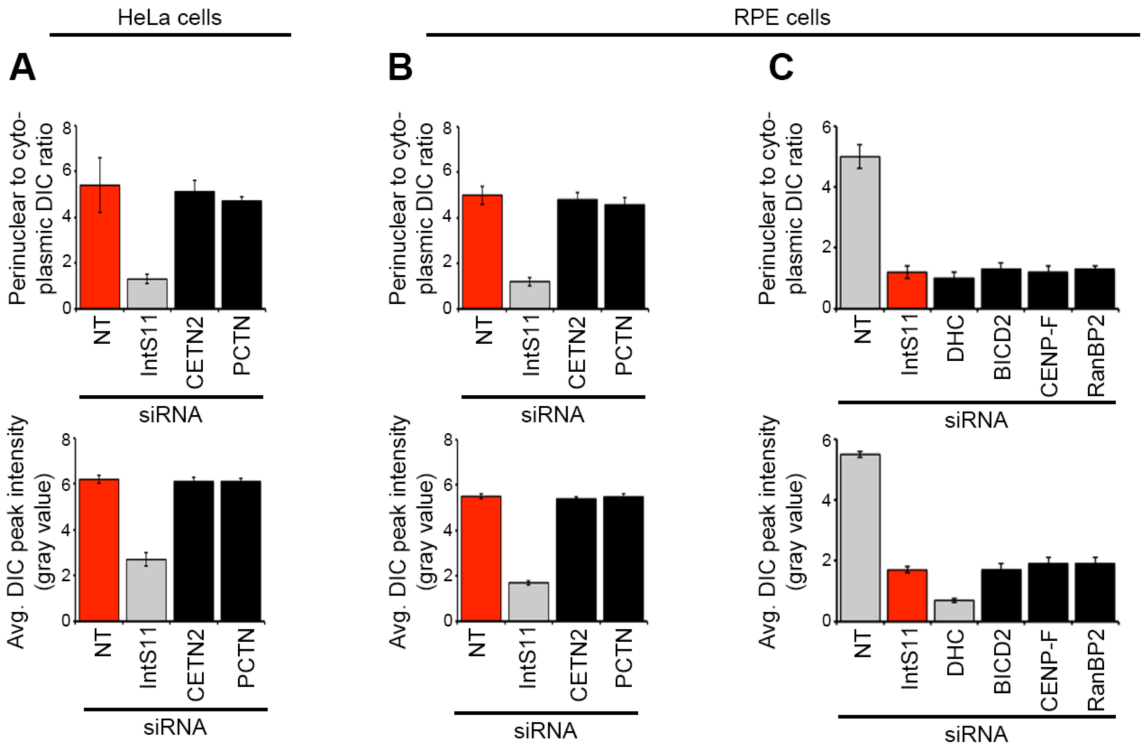

Figure 4.9. Quantification of perinuclear dynein following knockdown of ciliogenesis regulators. Bar graphs correspond to representative images of immunostained HeLa (A) or RPE (B,C) cells presented in Figures 3A,B and 4A. Line scans were drawn from the cytoplasm to inside the nucleus. Ratios of the intensity of the dynein signal on the NE to the cytoplasm (top) and average peak intensities of perinuclear dynein (bottom) are shown. Samples with $p<0.0001$ are shown in gray; black, not significant (relative to NT-siRNA (A,B) or IntS11-siRNA (C), red).

Perinuclear dynein is not required for PC formation

We next asked whether other proteins essential for perinuclear dynein accumulation are, like the INT complex, also required for primary ciliogenesis. BICD2 and CENP-F directly anchor dynein motors to the NE, whereas RanBP2 serves as the binding site for BICD2 within the nuclear pore complex; depletion of any of these proteins results in loss of perinuclear dynein in HeLa cells (Bolhy et al., 2011; Splinter et al., 2010). We confirmed that these known regulators of perinuclear dynein in HeLa cells are similarly required for NE-anchoring of dynein in cells capable of forming PC: depletion of BICD2, CENP-F, or RanBP2 in RPE cells resulted in a marked loss of perinuclear dynein compared to NT-siRNA cells (Figure 4.10A,C).

We disrupted the pool of dynein anchored on the NE in RPE cells by depleting proteins required for this process and assessed PC formation. Following siRNA treatment, cells were serum-starved and evaluated for the presence of PC. Loss of BICD2, CENP-F, or RanBP2 resulted in only a slight reduction in the fraction of cells with PC (80%, 91%, and 81% of NT-siRNA cells, respectively) compared to loss of INT subunits (e.g. 38% of NT-siRNA cells for IntS11; Figures 4.1K, 4.10B,D). Additionally we confirmed the previously reported requirement for dynein in PC formation: down-regulation of DHC resulted in the absence of PC in a majority of cells (Figure 4.10B,D) (Rajagopalan et al., 2009). These data suggest that, in contrast to the INT complex, other known regulators of perinuclear dynein accumulation are not strictly required for generation of PC.

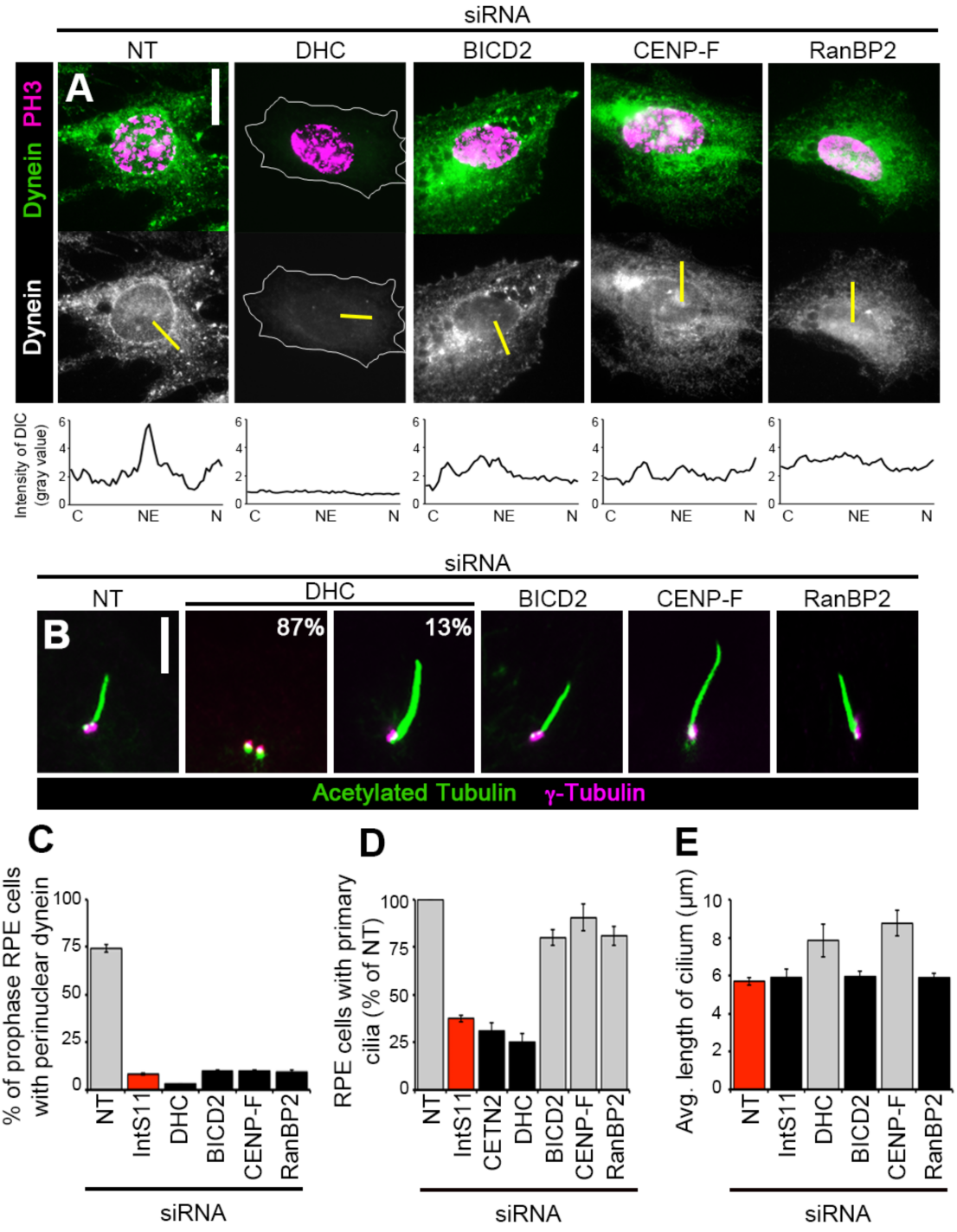
siRNA
NT
DHC
BICD2
CENP-F
RanBP2
A
Dynein PH3
Dynein
Intensity of DIC (gray value)
C
NE
N
siRNA
NT
DHC
BICD2
CENP-F
RanBP2
B
87%
13%
Acetylated Tubulin
γ-Tubulin
C
% of prophase RPE cells with perinuclear dynein
NT
IntS11
DHC
BICD2
CENP-F
RanBP2
siRNA
D
RPE cells with primary cilia (% of NT)
NT
IntS11
CETN2
DHC
BICD2
CENP-F
RanBP2
siRNA
E
Avg. length of cilium (μm)
NT
IntS11
DHC
BICD2
CENP-F
RanBP2
siRNA

Figure 4.10. Perinuclear dynein regulators are not required for primary ciliogenesis. RPE cells were transfected with siRNA and either nocodazole-treated, fixed, and stained for dynein (DIC) and PH3 (A,C) or serum-starved, fixed, and immunostained for acetylated tubulin and γ-tubulin (B,D,E). (A) Representative images show perinuclear dynein in prophase cells (PH3-positive and intact NE) after indicated knockdowns. Yellow bars represent line scans that span the cytoplasm (C), nuclear envelope (NE), and nucleus (N) to measure peak DIC intensity on the NE; corresponding plots are shown below each micrograph. (B) Representative images show PC after indicated knockdowns. Percentages in the DHC-siRNA micrographs indicate frequency at which each phenotype (no cilium, left; elongated cilium, right) was observed. (C-E) Quantification of prophase cells with perinuclear dynein (C), PC presence (D), or average PC length (E) after indicated knockdowns. Gray, $p<0.0001$; black bar, not significant (relative to IntS11-siRNA (C,D) or NT (E), red). Scale bars, 10 μm (A) or 5 μm (B).

For the subset of cells with PC, we also assessed PC length in these experiments. As previously reported, we observed increased PC length following depletion of dynein when the PC was present (Figure 4.10B,E) (Palmer et al., 2011). Similarly, CENP-F-siRNA cells exhibited longer PC compared to NT-siRNA cells, although BICD2 or RanBP2 depletion had no effect (Figure 4.10B,E). These data suggest that CENP-F, while not required for PC formation, has a role in regulating PC length; a role for CENP-F in this process has not been previously reported to our knowledge. We speculate that CENP-F may influence PC length through its regulation of cytoplasmic dynein-2, which is essential for maintaining normal PC length (Palmer et al., 2011; Rajagopalan et al., 2009). No change in PC length, however, was observed in cells depleted of IntS11 (Figures 4.1B, 4.10E). This finding suggests that INT promotes PC formation via a dynein-independent mechanism.

Taken together, the data presented herein showing that the pool of dynein anchored on the NE at the G2/M transition is not required for promoting primary ciliogenesis in G1, and vice versa, supports our hypothesis that dynein recruitment to the NE and PC formation are regulated by distinct INT-dependent mechanisms (Figures 4.8, 4.10, and 4.11A). We propose the following model to explain how INT may regulate these two cytoplasmic events that occur at different cell-cycle stages. INT is required for proper processing of snRNAs, which in turn are required for efficient processing of mRNAs encoding at least two critical proteins that independently promote ciliogenesis in G1 and dynein recruitment to the NE at G2/M (Figure 4.11B1). We cannot, however, exclude an alternative model in which INT functions through a common critical target required to mediate both of these events. In this case, INT would ensure efficient

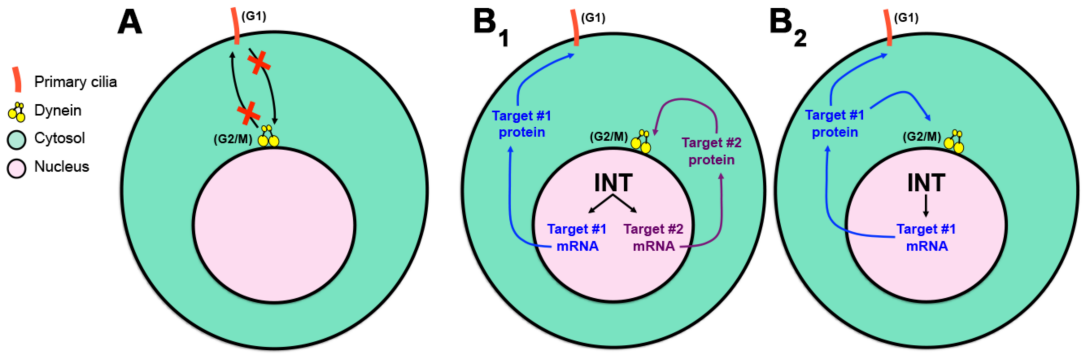

Figure 4.11. Model for independent regulation of dynein recruitment and ciliogenesis by INT. See text for details.

processing of transcripts encoding a single (as yet unidentified) protein that plays essential roles in promoting both ciliogenesis during G1 and perinuclear dynein accumulation at G2/M (Figure 4.11B2). Further studies will be required to identify the critical target(s) of the INT complex that mediate these and other important cellular processes.

CHAPTER V

CONCLUSIONS AND FUTURE DIRECTIONS

ASUN regulates perinuclear dynein in an INT-dependent manner

I have now presented two roles for ASUN in cultured human cells: 1) in the recruitment of dynein to the NE at G2/M that subsequently mediates nucleus-centrosome coupling (Jodoin et al., 2012), and 2) as an essential subunit of the RNA-processing complex, INT (Chen et al., 2012). My work provides strong evidence that the role for hASUN in dynein recruitment is directly linked to its role as a subunit of INT (Jodoin et al. 2013a), I reported that the down-regulation of hASUN in cultured human cells results in a defect in recruitment and anchoring of dynein motors at G2/M. Additionally I observed defects in nucleus-centrosome coupling, bipolar spindle formation, and progression through mitosis; the loss of perinuclear dynein is likely the cause for these downstream defects. I reported that the down-regulation of individual INT subunits by siRNA recapitulates the phenotype observed in hASUN-siRNA cells, with few exceptions. More importantly, I showed that hASUN functions from within the nucleus, the site of RNA-processing by INT, in regulating dynein recruitment. The finding that hASUN and other INT subunits are essential for regulating dynein recruitment to the NE advances what is currently known in both the dynein and INT fields. Only two pathways have previously been identified to be required for dynein anchoring at the G2/M transition. Additionally, only a few cellular defects have been reported following the loss

of INT (Akhmanova and Hammer, 2010; Golling et al., 2002; Kamath et al., 2003; Otani et al., 2013a; Rutkowski and Warren, 2009; Takata et al., 2012).

Prior to my work, two proteins were reported to directly anchor dynein on the NE of cultured human cells: BICD2 and CENP-F (Bolhy et al., 2011; Splinter et al., 2010). I have expanded this field by showing that hASUN and individual INT subunits are additionally required for this process, albeit its mechanism for regulation of perinuclear dynein appears to vary greatly from these two proteins. While BICD2 and CENP-F interact directly with the motor and NPCs to anchor dynein on the NE (Bolhy et al., 2011), I found no evidence to suggest that hASUN or INT strongly interact with the motor or NPCs. I reported that hASUN and other INT subunits do not localize on the NE at G2/M: instead, their localization patterns range from diffuse in the cytoplasm, throughout the cell, to predominantly nuclear, and several INT subunits are present at low levels at this stage of the cell cycle (Jodoin et al., 2013a). I also found that the NE localization of BICD2 and CENP-F are not dependent on hASUN. Moreover, I reported that in the absence of hASUN, BICD2, or CENP-F, dynein lacks the capacity to be recruited and/or anchored to the NE (Jodoin et al., 2012). Based on these data, I proposed a model in which hASUN and the INT complex work in a manner distinct from that of BICD2 and CENP-F to mediate dynein recruitment, likely at the RNA-processing level.

While it may appear to be a straightforward process to directly anchor the motor to the NE at the correct cell cycle stage, the fact that it requires so many components would argue that it is not. Due to the massive size of the motor complexes and the density of the cytosol that the motor must migrate through to reach the nuclear surface, perhaps it is not surprising that a network of proteins are required for this process. To fully

understand this process, it will be essential to identify all factors required for dynein recruitment and NE-anchoring at G2/M. The identification that an RNA-processing complex plays a vital role in dynein anchoring further supports my hypothesis that additional players remain unknown.

Based on my work, I propose that INT functions indirectly to promote dynein accumulation on the nuclear surface prior to mitotic entry. I found that a subset of INT subunits is present at low levels at the G2/M transition, suggesting that the INT complex does not function at this cell cycle stage (Jodoin et al., 2013a). This finding is not surprising because others have previously shown that the activity of RNApolII is repressed in mitosis, and INT requires an active RNApolII for snRNA processing (Baillat et al., 2005; Parsons and Spencer, 1997). We considered the possibility that INT sub-complexes may form amongst the subunits present at normal levels at G2/M; many of the subunits present at low levels at this stage, however, are required for the recruitment of dynein to the NE, arguing that any sub-complex present would not be sufficient to mediate this process. I proposed that INT functions at the RNA-processing level to regulate perinuclear dynein, although its mechanism remains unclear. I hypothesize that INT is required for the proper pre-mRNA processing of an unknown critical target that is required to regulate dynein recruitment to the NE at G2/M.

INT is a regulator of ciliogenesis

To determine if INT plays a broader role in dynein regulation in the cell or if its role in regulating the motor is limited to the G2/M transition, we assessed an additional dynein-dependent process in the cell. Similar to the coupling of centrosomes to the NE at

G2/M, ciliogenesis is another function dependent on the molecular motor dynein (Jodoin et al., 2013b). For the proper formation of PC in cells, the mother centriole must migrate to and dock within the plasma membrane, where it will undergo the BB maturation process (Kim and Dynlacht, 2013a). These steps are essential for ciliogenesis, as the cilium will arise from the mature BB. Dynein is an essential regulator of ciliogenesis and is required for the establishment of the PC as well as for maintaining cilia length. In addition to dynein, numerous centrosomal and interflagellar trafficking proteins have been shown to be essential for this process, with more components being added to the list over time. My work has now enhanced what is known about primary ciliogenesis by showing that individual INT subunits are essential for this process.

The down-regulation of individual INT subunits in RPE cells results in a severe decrease in the formation of PC in cells arrested in G1 via serum starvation (Jodoin et al., 2013b). Further characterization of this phenotype in INT-siRNA cells revealed no obvious defects in either the maturation of the BB, as evidenced by the proper formation of distal appendages, or the composition of the BB, as evidenced by the presence of known [core?] components. With no obvious structural defects observed, how INT could be regulating this cytoplasmic event remains a question. The majority of proteins required for primary ciliogenesis localize to the centrosome, mature BB, and/or along the length of the cilium. I have not observed these localization patterns for any of the INT subunits, and many subunits reside exclusively within the nucleus; these findings suggest that INT does not regulate ciliogenesis via a direct interaction with the BB and/or PC. Instead, my work is consistent with a model in which INT regulates ciliogenesis through RNA processing. I have found that, like other INT subunits, hASUN is essential for PC

formation (my unpublished data). Additionally, I found that nuclear-localized hASUN is required for PC formation (as I previously showed for dynein recruitment), further supporting the model that INT regulates primary ciliogenesis at the RNA-processing level (my unpublished data).

It will be necessary to further characterize the underlying defect that leads to the loss of PC formation in INT-siRNA cells to determine how INT regulates primary ciliogenesis. To confirm, or exclude, that INT is regulating PC at the RNA-processing level, identifying the critical target(s) through which INT mediates PC formation will be essential. I speculate that INT is required for the proper production of an unknown protein(s) that interacts directly with the BB and/or PC to mediate this process.

Mechanism for INT-dependent regulation of dynein recruitment and ciliogenesis

I next sought to determine if these two cellular events were independent or if they stemmed from a single process (Jodoin et al., 2013b). I found that disrupting the pool of dynein anchored on the NE did not lead to a loss of PC. Conversely, inhibiting PC formation did not lead to a loss of dynein recruitment to the NE. These data support the model that perinuclear dynein is not upstream of primary ciliogenesis, and vice versa. Based on my findings, I proposed a model in which INT is functioning through distinct mechanisms to perform these two functions at different cell cycle stages. I hypothesized that INT is required for the proper processing of at least two mRNA targets encoding different proteins that function to promote primary ciliogenesis in G1 and dynein recruitment to the NE at G2/M (Figure 4.11B1) (Jodoin et al., 2013b). As an alternative model, it is possible that INT is functioning through one common critical mRNA target,

which will perform both functions during different stages of the cell cycle (Figure. 4.11B2). To provide further validation for either model, the critical targets would need to be identified.

Identification of critical targets of INT

To answer the question as to how INT is regulating both dynein recruitment and primary ciliogenesis, it will be essential to identify the critical targets of INT required for these functions. Taking an open-ended approach to identify the RNA transcripts misprocessed following loss of functional INT, our collaborator performed a high-throughput RNA-sequence screen using two populations of treated cells: control-siRNA and IntS11-siRNA HeLa cells (T.R.A. and E.J.W., unpublished observations). When comparing mRNAs isolated under these two conditions, with an emphasis on identifying transcripts that were aberrantly spliced in the absence of functional INT, we are able to assess both the type of splicing defects and the degree of misprocessing for individual RNA transcripts. Though this screen yielded thousands of candidates, its quantitative nature allowed us to prioritize those sequences that are most highly sensitive to disruption of INT-dependent RNA processing. In an effort to identify the INT targets required for dynein recruitment and/or PC formation, I evaluated the list of the most sensitive candidates for known regulators of each process, but this approach was not fruitful. The findings from this preliminary screen lead me to speculate that novel regulators of both dynein localization and primary ciliogenesis could be the critical mRNA targets of INT.

To elucidate these novel targets, I would propose to perform a secondary screen involving siRNA-mediated knockdown of the misprocessed transcripts in INT-depleted

cells that were identified in the preliminary screen described above, looking specifically for the loss of dynein on the NE of G2/M HeLa cells or the loss of ciliogenesis in G1-arrested RPE cells. To identify proteins needed for dynein recruitment, siRNA-treated cells would be exposed to a 3-hour incubation with 5 μM nocodazole to enhance the presence of functional dynein motors on the NE. Cells would be stained for dynein intermediate chain and PH3 to readily identify prophase cells. A reduction of perinuclear dynein residing on the NE at G2/M would signify that we have depleted a critical regulator of perinuclear dynein. To identify proteins essential for primary ciliogenesis, siRNA-treated cells would be subjected to serum starvation for 24 hours, which arrests the cells in G1 to allow PC formation. Cells would be stained for acetylated tubulin to mark PC; lack of PC following siRNA treatment would signify that we have targeted a regulator of primary ciliogenesis. Identification of new players in either process would represent a significant advance, as a complete understanding of the mechanisms underlying these processes is lacking.

The requirement of INT for dynein function

My work has shown that dynein recruitment to the NE at the G2/M transition is not required to promote the formation of primary cilia in G1 cells, and vice versa. Though we have determined that INT is independently promoting these events, it does not necessarily mean that INT is functioning through independent mechanisms. Based on the phenotypes we observed in RPE cells, loss of dynein recruitment and ciliogenesis, I examined the common factors required for these events. A functional dynein motor is essential for both events; loss of function in the motor leads to both phenotypes observed

in INT-depleted cells. Additional evidence to suggest that INT is required for proper function of dynein is the unpublished observation that ASUN is required for proper Golgi formation (Irina Kaverina, Vanderbilt). Dynein on the Golgi surface is required to maintain the "ribbon-like" formation of the Golgi. Loss of ASUN results in the scattering of Golgi fragments, a phenotype observed following loss of dynein function.

Following depletion of INT subunits, I observed no obvious defects in formation of the dynein motor complex. When the integrity of the dynein complex is compromised, decay of its subunits is observed, as many of the subunits are not stable outside of the complex. To assess if INT is required for the integrity of the dynein complex, I assessed the levels of dynein and dynactin components in control and INT-depleted cells by immunoblotting. Additionally, I performed sedimentation gradient analysis to assess whether the complex remained intact following the loss of INT. I found no change in the levels of dynein-dynactin subunits or in the sucrose density gradient profile of the motor in INT subunit-siRNA cells.

Additional work will need to be done to determine if there is a role for INT in promoting formation/stability of dynein motor complexes. I propose that performing direct analysis of the dynein motor complex may provide a clear answer. To do this, dynein motor complexes could be isolated from cells following a control knockdown or INT subunit knockdown and analyzed by mass spectrometry to identify the subunit composition of the dynein motor complex in each sample. I would specifically look for components present in the control cells that are missing in the INT subunit knockdown cells. To follow up on any hits from this screen, I would determine if INT is required for the processing of the dynein component in question by assessing its mRNA levels and

proper splicing following the loss of INT. To further confirm that aberrant RNA processing by INT leads to defects in this component, I would perform a rescue experiment in which I would express cDNA encoding the component lacking in the knockdown cells; this cDNA should not require any additional processing by INT to be functional. If expression of this cDNA rescued the lack of perinuclear dynein observed in INT-depleted cells, I would conclude that we have identified a critical target of INT that functions within the dynein complex.

Established cellular roles for INT

These newly identified roles for INT add to a growing list of INT-dependent cellular processes downstream of its 3'-end processing role (Jodoin et al., 2013b). In cultured mammalian cells, IntS4 was found to be essential for the formation of Cajal bodies, nuclear structures required for mRNA biogenesis and recycling (Takata et al., 2012), while IntS6 and IntS11 are required for proper differentiation in adipocytes (Otani et al., 2013a). *In vivo*, INT has been shown to be required for developmental functions in zebrafish, *C. elegans,* and *Drosophila* (Kamath et al., 2003; Otani et al., 2013a; Rutkowski and Warren, 2009; Tao et al., 2009). In zebrafish, IntS5, IntS9, and IntS11 have been shown to be required for the splicing of *smad1* and *smad5* transcripts, which are essential for erythrocyte differentiation (Tao et al., 2009). IntS7 is required for proper craniofacial development in the worm, as well as proper craniofacial and abdominal development in the fly (Golling et al., 2002; Kamath et al., 2003; Rutkowski and Warren, 2009).

My work has significantly expanded the relatively new field of the Integrator snRNA processing complex as well as the RNA maturation field. The machinery required for RNA processing and maturation has long thought to involve "housekeeping" genes essential for cellular homeostasis. Thus, the very specific phenotypes that have recently been associated with the loss of INT are quite striking. The loss of INT function does not lead to cell death, indicating that some sort of compensation is occurring within cells. The specific phenotypes associated with INT down regulation could suggest that certain subsets of transcripts are more sensitive to the loss of INT and/or that the compensation mechanism is not capable of properly processing these transcripts. Further investigation and identification of these unknown targets of INT will shed more light on how INT is functioning within cells to promote dynein localization, ciliogenesis, and other processes.

INT-independent roles for ASUN

Considering the different "pools" of ASUN observed in the cell, it will be important to determine if hASUN has additional roles in the cytoplasm. hASUN localization shifts between predominantly nuclear, predominantly cytoplasmic, or evenly distributed throughout the cell. While I have shown that the nuclear pool of ASUN is required for the recruitment of dynein (Jodoin et al., 2013a) and for primary ciliogenesis (my unpublished data), we have no insight into the function of the cytoplasmic pool. Additionally, a subset of INT subunits localize to the cytoplasm as opposed to being exclusively nuclear. I found that IntS11 is localized throughout the cytoplasm and nucleus, whereas IntS9, which together with IntS11 forms a heterodimer required for proper RNA processing, is localized to the nucleus. If IntS11 were solely required to

form a heterodimer with IntS9 for INT function, why would these two subunits display different localization patterns? This discrepancy in patterns suggests that IntS11 and possibly other INT subunits that localize to the cytoplasm have alternative functions beyond snRNA processing. Moreover, it will be interesting to determine if the subunits found in the cytoplasm are forming sub-complexes of INT.

To determine if INT sub-complexes exist in the cytoplasm, I would propose to isolate the cytoplasmic fraction of cells by using a nuclear-cytoplasmic fractionation technique. Using the cytoplasmic fraction, co-immunoprecipitation experiments could be performed to determine whether or not the cytoplasmic INT subunits interact. If sub-complexes were formed in the cytoplasm, further work would be needed to identify their functions.

To determine whether the cytoplasmic localization of certain INT subunits is required for specific cellular functions, I would propose to perform studies similar to those I used to characterize the nuclear pool of ASUN. If the cytoplasmic subunits are forced to remain in the nucleus, I hypothesize that they would no longer have the capacity to perform their cytoplasmic functions. To force a nuclear localization, I would add exogenous NLS tags to the proteins, thereby shifting them to be predominantly nuclear. If this method proved to be insufficient for sequestering the cytoplasmic INT subunits to the nucleus, I would inhibit their export out of the nucleus by the use of the Exportin inhibitor, Leptomyocin, or by mutating any predicted nuclear export signals. In the case of adding an exogenous NLS or mutating the nuclear export signal, I would knock down the INT subunit and perform a rescue experiment in which I would express the

corresponding nuclear-localized construct. Following sequestration of the normally cytoplasmic INT subunits within the nucleus, I would assess the cells for ensuing defects.

INT-independent roles for ASUN

To further address this prospect of INT-independent roles of ASUN, I considered the interaction between hASUN and the dynein adaptor protein, LIS1, previously reported in publications from our lab (Jodoin et al., 2012; Sitaram et al., 2012). In cultured human cells, co-immunoprecipitation experiments revealed a weak (albeit reproducible) interaction between ASUN and LIS1 that is conserved for both the mammalian *Drosophila* homologes. This interaction appears to be highly conserved amongst species: the *Drosophila* homologue of ASUN interacted with the human homologue of LIS1 when expressed in cultured cells. I originally hypothesized that hASUN regulates the recruitment of dynein motors at G2/M through this interaction with a dynein-bound adapter protein. This type of mechanism would be similar to that of CENP-F, which interacts with the dynein-bound adaptor proteins, NudE/L, to anchor dynein. More striking was the observation that these two components interact genetically *in vivo*: the *Drosophila* homologues of *asun* and *Lis1* cooperate to properly position the centrosome and promote perinuclear dynein in the testes, and the double mutants display a severe decrease in testes size (Sitaram et al., 2012). My finding that nuclear-localized hASUN is functioning via the INT complex to regulate the recruitment of dynein, however, argues against this model. Nonetheless, given the strong interaction between these genes in fly spermatogenesis, it would be interesting to perform experiments to further characterize the interaction between ASUN and LIS1 in higher organisms. There

is currently no evidence that LIS1 interacts with or is regulated by the INT complex, leading me to speculate that this interaction could represent an INT-independent function of hASUN.

To test whether hASUN regulates LIS1 in an INT-dependent manner, I would first propose to determine if ASUN and LIS1 directly interact or exist within a complex. My results from previous co-immunoprecipitations of cell lysates have suggested that these two proteins form a complex with each other. One caveat to these previous experiments is that I was working with the overexpression of tagged proteins. To test for a direct interaction, I would perform binding assays using purified, recombinant proteins. Next, I would determine whether or not additional INT subunits interact with LIS1. I would purify individual INT subunits and, using the same binding assay, would determine if they interact with purified LIS1. Once all interactions have been confirmed, I would propose to identify the interaction sites between the interacting proteins. Mutation of these sites could be performed to block these interaction, and the consequences to the cell, or fly, could be assessed. Additionally, it would be interesting to determine if hASUN and LIS1 work in concert to promote dynein localization and positioning of the centrosomes in cultured human cells as they do in *Drosophila* spermatogenesis. These studies would allow us to more definitely determine whether hASUN and LIS1 interact and would reveal the functional relevance of this interaction in the regulation of dynein localization.

REFERENCES

Akhmanova, A. and Hammer, J. A., 3rd. (2010). Linking molecular motors to membrane cargo. *Curr Opin Cell Biol* 22, 479-87.

Albrecht, T. R. and Wagner, E. J. (2012). snRNA 3' end formation requires heterodimeric association of integrator subunits. *Mol Cell Biol* 32, 1112-23.

Allan, V. J. (2011). Cytoplasmic dynein. *Biochem Soc Trans* 39, 1169-78.

Anderson, M. A., Jodoin, J. N., Lee, E., Hales, K. G., Hays, T. S. and Lee, L. A. (2009). Asunder is a critical regulator of dynein-dynactin localization during Drosophila spermatogenesis. *Mol Biol Cell* 20, 2709-21.

Asthana, J., Kuchibhatla, A., Jana, S. C., Ray, K. and Panda, D. (2012). Dynein light chain 1 (LC8) association enhances microtubule stability and promotes microtubule bundling. *J Biol Chem* 287, 40793-805.

Bader, J. R. and Vaughan, K. T. (2010). Dynein at the kinetochore: Timing, Interactions and Functions. *Semin Cell Dev Biol* 21, 269-75.

Baillat, D., Hakimi, M. A., Naar, A. M., Shilatifard, A., Cooch, N. and Shiekhattar, R. (2005). Integrator, a multiprotein mediator of small nuclear RNA processing, associates with the C-terminal repeat of RNA polymerase II. *Cell* 123, 265-76.

Barabino, S. M., Hubner, W., Jenny, A., Minvielle-Sebastia, L. and Keller, W. (1997). The 30-kD subunit of mammalian cleavage and polyadenylation specificity factor and its yeast homolog are RNA-binding zinc finger proteins. *Genes Dev* 11, 1703-16.

Basten, S. G. and Giles, R. H. (2013). Functional aspects of primary cilia in signaling, cell cycle and tumorigenesis. *Cilia* 2, 6.

Basto, R., Lau, J., Vinogradova, T., Gardiol, A., Woods, C. G., Khodjakov, A. and Raff, J. W. (2006). Flies without centrioles. *Cell* 125, 1375-86.

Beaudouin, J., Gerlich, D., Daigle, N., Eils, R. and Ellenberg, J. (2002). Nuclear envelope breakdown proceeds by microtubule-induced tearing of the lamina. *Cell* 108, 83-96.

Beswick, R. W., Ambrose, H. E. and Wagner, S. D. (2006). Nocodazole, a microtubule de-polymerising agent, induces apoptosis of chronic lymphocytic leukaemia cells associated with changes in Bcl-2 phosphorylation and expression. *Leuk Res* 30, 427-36.

Bettencourt-Dias, M., Rodrigues-Martins, A., Carpenter, L., Riparbelli, M., Lehmann, L., Gatt, M. K., Carmo, N., Balloux, F., Callaini, G. and Glover, D. M. (2005). SAK/PLK4 is required for centriole duplication and flagella development. *Curr Biol* 15, 2199-207.

Boettcher, B. and Barral, Y. (2013). The cell biology of open and closed mitosis. *Nucleus* 4, 160-5.

Bolhy, S., Bouhlel, I., Dultz, E., Nayak, T., Zuccolo, M., Gatti, X., Vallee, R., Ellenberg, J. and Doye, V. (2011). A Nup133-dependent NPC-anchored network tethers centrosomes to the nuclear envelope in prophase. *J Cell Biol* 192, 855-71.

Bourdon, V., Naef, F., Rao, P. H., Reuter, V., Mok, S. C., Bosl, G. J., Koul, S., Murty, V. V., Kucherlapati, R. S. and Chaganti, R. S. (2002). Genomic and expression analysis of the 12p11-p12 amplicon using EST arrays identifies two novel amplified and overexpressed genes. *Cancer Res* 62, 6218-23.

Branzei, D. and Foiani, M. (2008). Regulation of DNA repair throughout the cell cycle. *Nat Rev Mol Cell Biol* 9, 297-308.

Burgess, S. A. and Knight, P. J. (2004). Is the dynein motor a winch? *Curr Opin Struct Biol* 14, 138-46.

Chen, J., Ezzeddine, N., Waltenspiel, B., Albrecht, T. R., Warren, W. D., Marzluff, W. F. and Wagner, E. J. (2012). An RNAi screen identifies additional members of the Drosophila Integrator complex and a requirement for cyclin C/Cdk8 in snRNA 3'-end formation. *RNA* 18, 2148-56.

Chen, J. and Wagner, E. J. (2010). snRNA 3' end formation: the dawn of the Integrator complex. *Biochem Soc Trans* 38, 1082-7.

Chen, J., Waltenspiel, B., Warren, W. D. and Wagner, E. J. (2013). Functional analysis of the integrator subunit 12 identifies a microdomain that mediates activation of the Drosophila integrator complex. *J Biol Chem* 288, 4867-77.

Draviam, V. M., Shapiro, I., Aldridge, B. and Sorger, P. K. (2006). Misorientation and reduced stretching of aligned sister kinetochores promote chromosome missegregation in EB1- or APC-depleted cells. *EMBO J* 25, 2814-27.

Dujardin, D. L., Barnhart, L. E., Stehman, S. A., Gomes, E. R., Gundersen, G. G. and Vallee, R. B. (2003). A role for cytoplasmic dynein and LIS1 in directed cell movement. *J Cell Biol* 163, 1205-11.

Efimov, A., Kharitonov, A., Efimova, N., Loncarek, J., Miller, P. M., Andreyeva, N., Gleeson, P., Galjart, N., Maia, A. R., McLeod, I. X. et al. (2007). Asymmetric CLASP-dependent nucleation of noncentrosomal microtubules at the trans-Golgi network. *Dev Cell* 12, 917-30.

Ezzeddine, N., Chen, J., Waltenspiel, B., Burch, B., Albrecht, T., Zhuo, M., Warren, W. D., Marzluff, W. F. and Wagner, E. J. (2011). A subset of Drosophila integrator proteins is essential for efficient U7 snRNA and spliceosomal snRNA 3'-end formation. *Mol Cell Biol* 31, 328-41.

Fuller, M. T. (1993). Spermatogenesis. In *The Development of Drosophila melanogaster*, (ed. e. M. Bate and A. Martinez-Arias), pp. 71-147. Cold Spring Harbor, NY.: Cold Spring Harbor Laboratory Press.

Godin, J. D. and Humbert, S. (2011). Mitotic spindle: focus on the function of huntingtin. *Int J Biochem Cell Biol* 43, 852-6.

Golling, G., Amsterdam, A., Sun, Z., Antonelli, M., Maldonado, E., Chen, W., Burgess, S., Haldi, M., Artzt, K., Farrington, S. et al. (2002). Insertional mutagenesis in zebrafish rapidly identifies genes essential for early vertebrate development. *Nat Genet* 31, 135-40.

Gonczy, P., Pichler, S., Kirkham, M. and Hyman, A. A. (1999). Cytoplasmic dynein is required for distinct aspects of MTOC positioning, including centrosome separation, in the one cell stage Caenorhabditis elegans embryo. *J Cell Biol* 147, 135-50.

Graser, S., Stierhof, Y. D., Lavoie, S. B., Gassner, O. S., Lamla, S., Le Clech, M. and Nigg, E. A. (2007). Cep164, a novel centriole appendage protein required for primary cilium formation. *J Cell Biol* 179, 321-30.

Greenspan, R. J. (2004). Fly pushing: The Theory and Practice of Drosophila Genetics. Cold Spring Harbor, NY: Cold Spring Harbor Laboratory Press.

Gunsalus, K. C., Bonaccorsi, S., Williams, E., Verni, F., Gatti, M. and Goldberg, M. L. (1995). Mutations in twinstar, a Drosophila gene encoding a cofilin/ADF homologue, result in defects in centrosome migration and cytokinesis. *J Cell Biol* 131, 1243-59.

Hagiwara, H., Ohwada, N. and Takata, K. (2004). Cell biology of normal and abnormal ciliogenesis in the ciliated epithelium. *Int Rev Cytol* 234, 101-41.

Hebbar, S., Mesngon, M. T., Guillotte, A. M., Desai, B., Ayala, R. and Smith, D. S. (2008). Lis1 and Ndel1 influence the timing of nuclear envelope breakdown in neural stem cells. *J Cell Biol* 182, 1063-71.

Hirokawa, N., Noda, Y., Tanaka, Y. and Niwa, S. (2009). Kinesin superfamily motor proteins and intracellular transport. *Nat Rev Mol Cell Biol* 10, 682-96.

Holzbaur, E. L. and Vallee, R. B. (1994). DYNEINS: molecular structure and cellular function. *Annu Rev Cell Biol* 10, 339-72.

Hoogenraad, C. C., Akhmanova, A., Howell, S. A., Dortland, B. R., De Zeeuw, C. I., Willemsen, R., Visser, P., Grosveld, F. and Galjart, N. (2001). Mammalian Golgi-

associated Bicaudal-D2 functions in the dynein-dynactin pathway by interacting with these complexes. *EMBO J* 20, 4041-54.

Hu, D. J., Baffet, A. D., Nayak, T., Akhmanova, A., Doye, V. and Vallee, R. B. (2013). Dynein recruitment to nuclear pores activates apical nuclear migration and mitotic entry in brain progenitor cells. *Cell* 154, 1300-13.

Ishikawa, H. and Marshall, W. F. (2011). Ciliogenesis: building the cell's antenna. *Nat Rev Mol Cell Biol* 12, 222-34.

Jaspersen, S. L. and Winey, M. (2004). The budding yeast spindle pole body: structure, duplication, and function. *Annu Rev Cell Dev Biol* 20, 1-28.

Jodoin, J. N., Shboul, M., Sitaram, P., Zein-Sabatto, H., Reversade, B., Lee, E. and Lee, L. A. (2012). Human Asunder promotes dynein recruitment and centrosomal tethering to the nucleus at mitotic entry. *Mol Biol Cell* 23, 4713-24.

Jodoin, J. N., Sitaram, P., Albrecht, T. R., May, S. B., Shboul, M., Lee, E., Reversade, B., Wagner, E. J. and Lee, L. A. (2013a). Nuclear-localized Asunder regulates cytoplasmic dynein localization via its role in the Integrator complex. *Mol Biol Cell* 24, 2954-65.

Jodoin, J. N., Shboul, M., Albrecht, T. R., Lee, E., Wagner, E. J., Reversade, B. and Lee, L. A. (2013b). The snRNA-processing complex, Integrator, is required for ciliogenesis and dynein recrutiment to the nuclear envelope via distinct mechanisms. *Biology Open* (In press)

Kalderon, D., Roberts, B. L., Richardson, W. D. and Smith, A. E. (1984). A short amino acid sequence able to specify nuclear location. *Cell* 39, 499-509.

Kamath, R. S., Fraser, A. G., Dong, Y., Poulin, G., Durbin, R., Gotta, M., Kanapin, A., Le Bot, N., Moreno, S., Sohrmann, M. et al. (2003). Systematic functional analysis of the Caenorhabditis elegans genome using RNAi. *Nature* 421, 231-7.

Kardon, J. R. and Vale, R. D. (2009). Regulators of the cytoplasmic dynein motor. *Nat Rev Mol Cell Biol* 10, 854-65.

Kemphues, K. J., Raff, E. C., Raff, R. A. and Kaufman, T. C. (1980). Mutation in a testis-specific beta-tubulin in Drosophila: analysis of its effects on meiosis and map location of the gene. *Cell* 21, 445-51.

Kim, S. and Dynlacht, B. D. (2013a). Assembling a primary cilium. *Curr Opin Cell Biol*.

Kim, S. and Dynlacht, B. D. (2013b). Assembling a primary cilium. *Curr Opin Cell Biol* 25, 506-11.

Kim, S., Zaghloul, N. A., Bubenshchikova, E., Oh, E. C., Rankin, S., Katsanis, N., Obara, T. and Tsiokas, L. (2011). Nde1-mediated inhibition of ciliogenesis affects cell cycle re-entry. *Nat Cell Biol* 13, 351-60.

Ko, H. W. (2012). The primary cilium as a multiple cellular signaling scaffold in development and disease. *BMB Rep* 45, 427-32.

Kolomeisky, A. B. and Fisher, M. E. (2007). Molecular motors: a theorist's perspective. *Annu Rev Phys Chem* 58, 675-95.

Kong, S., Du, X., Peng, C., Wu, Y., Li, H., Jin, X., Hou, L., Deng, K., Xu, T. and Tao, W. (2013). Dlic1 deficiency impairs ciliogenesis of photoreceptors by destabilizing dynein. *Cell Res* 23, 972.

Kops, G. J. and Shah, J. V. (2012). Connecting up and clearing out: how kinetochore attachment silences the spindle assembly checkpoint. *Chromosoma* 121, 509-25.

Lara-Gonzalez, P., Westhorpe, F. G. and Taylor, S. S. (2012). The spindle assembly checkpoint. *Curr Biol* 22, R966-80.

Lee, L. A., Lee, E., Anderson, M. A., Vardy, L., Tahinci, E., Ali, S. M., Kashevsky, H., Benasutti, M., Kirschner, M. W. and Orr-Weaver, T. L. (2005). Drosophila genome-scale screen for PAN GU kinase substrates identifies Mat89Bb as a cell cycle regulator. *Dev Cell* 8, 435-42.

Li, M. G., Serr, M., Newman, E. A. and Hays, T. S. (2004). The Drosophila tctex-1 light chain is dispensable for essential cytoplasmic dynein functions but is required during spermatid differentiation. *Mol Biol Cell* 15, 3005-14.

Lim, H. H., Zhang, T. and Surana, U. (2009). Regulation of centrosome separation in yeast and vertebrates: common threads. *Trends Cell Biol* 19, 325-33.

Lippincott-Schwartz, J. (2002). Cell biology: ripping up the nuclear envelope. *Nature* 416, 31-2.

Malone, C. J., Misner, L., Le Bot, N., Tsai, M. C., Campbell, J. M., Ahringer, J. and White, J. G. (2003). The C. elegans hook protein, ZYG-12, mediates the essential attachment between the centrosome and nucleus. *Cell* 115, 825-36.

Malovannaya, A., Li, Y., Bulynko, Y., Jung, S. Y., Wang, Y., Lanz, R. B., O'Malley, B. W. and Qin, J. (2010). Streamlined analysis schema for high-throughput identification of endogenous protein complexes. *Proc Natl Acad Sci U S A* 107, 2431-6.

Mason, F. M. and Martin, A. C. (2011). Tuning cell shape change with contractile ratchets. *Curr Opin Genet Dev* 21, 671-9.

Matera, A. G. and Shpargel, K. B. (2006). Pumping RNA: nuclear bodybuilding along the RNP pipeline. *Curr Opin Cell Biol* 18, 317-24.

Matera, A. G., Terns, R. M. and Terns, M. P. (2007). Non-coding RNAs: lessons from the small nuclear and small nucleolar RNAs. *Nat Rev Mol Cell Biol* 8, 209-20.

McGrail, M. and Hays, T. S. (1997). The microtubule motor cytoplasmic dynein is required for spindle orientation during germline cell divisions and oocyte differentiation in Drosophila. *Development* 124, 2409-19.

Mische, S., He, Y., Ma, L., Li, M., Serr, M. and Hays, T. S. (2008). Dynein light intermediate chain: an essential subunit that contributes to spindle checkpoint inactivation. *Mol Biol Cell* 19, 4918-29.

Newby, M. I. and Greenbaum, N. L. (2002). Sculpting of the spliceosomal branch site recognition motif by a conserved pseudouridine. *Nat Struct Biol* 9, 958-65.

Nguyen Ba, A. N., Pogoutse, A., Provart, N. and Moses, A. M. (2009). NLStradamus: a simple Hidden Markov Model for nuclear localization signal prediction. *BMC Bioinformatics* 10, 202.

Nilsen, T. W. (2003). The spliceosome: the most complex macromolecular machine in the cell? *Bioessays* 25, 1147-9.

Otani, Y., Nakatsu, Y., Sakoda, H., Fukushima, T., Fujishiro, M., Kushiyama, A., Okubo, H., Ohno, H., Nishimura, F., Kamata, H. et al. (2013a). Integrator complex plays an essential role in adipose differentiation. *Biochem Biophys Res Commun*.

Otani, Y., Nakatsu, Y., Sakoda, H., Fukushima, T., Fujishiro, M., Kushiyama, A., Okubo, H., Tsuchiya, Y., Ohno, H., Takahashi, S. et al. (2013b). Integrator complex plays an essential role in adipose differentiation. *Biochem Biophys Res Commun* 434, 197-202.

Palmer, K. J., MacCarthy-Morrogh, L., Smyllie, N. and Stephens, D. J. (2011). A role for Tctex-1 (DYNLT1) in controlling primary cilium length. *Eur J Cell Biol* 90, 865-71.

Parsons, G. G. and Spencer, C. A. (1997). Mitotic repression of RNA polymerase II transcription is accompanied by release of transcription elongation complexes. *Mol Cell Biol* 17, 5791-802.

Payne, C., Rawe, V., Ramalho-Santos, J., Simerly, C. and Schatten, G. (2003). Preferentially localized dynein and perinuclear dynactin associate with nuclear pore complex proteins to mediate genomic union during mammalian fertilization. *J Cell Sci* 116, 4727-38.

Rajagopalan, V., Subramanian, A., Wilkes, D. E., Pennock, D. G. and Asai, D. J. (2009). Dynein-2 affects the regulation of ciliary length but is not required for ciliogenesis in Tetrahymena thermophila. *Mol Biol Cell* 20, 708-20.

Redwine, W. B., Hernandez-Lopez, R., Zou, S., Huang, J., Reck-Peterson, S. L. and Leschziner, A. E. (2012). Structural basis for microtubule binding and release by dynein. *Science* 337, 1532-6.

Robinson, J. T., Wojcik, E. J., Sanders, M. A., McGrail, M. and Hays, T. S. (1999). Cytoplasmic dynein is required for the nuclear attachment and migration of centrosomes during mitosis in Drosophila. *J Cell Biol* 146, 597-608.

Rubin, G. M. and Spradling, A. C. (1982). Genetic transformation of Drosophila with transposable element vectors. *Science* 218, 348-53.

Rutkowski, R. J. and Warren, W. D. (2009). Phenotypic analysis of deflated/Ints7 function in Drosophila development. *Dev Dyn* 238, 1131-9.

Sachdev, P., Menon, S., Kastner, D. B., Chuang, J. Z., Yeh, T. Y., Conde, C., Caceres, A., Sung, C. H. and Sakmar, T. P. (2007). G protein beta gamma subunit interaction with the dynein light-chain component Tctex-1 regulates neurite outgrowth. *EMBO J* 26, 2621-32.

Salina, D., Bodoor, K., Eckley, D. M., Schroer, T. A., Rattner, J. B. and Burke, B. (2002). Cytoplasmic dynein as a facilitator of nuclear envelope breakdown. *Cell* 108, 97-107.

Salisbury, J. L. (2004). Primary cilia: putting sensors together. *Curr Biol* 14, R765-7.

Schafer, K. A. (1998). The cell cycle: a review. *Vet Pathol* 35, 461-78.

Schroer, T. A. (2004). Dynactin. *Annu Rev Cell Dev Biol* 20, 759-79.

Sillibourne, J. E., Specht, C. G., Izeddin, I., Hurbain, I., Tran, P., Triller, A., Darzacq, X., Dahan, M. and Bornens, M. (2011). Assessing the localization of centrosomal proteins by PALM/STORM nanoscopy. *Cytoskeleton (Hoboken)* 68, 619-27.

Sitaram, P., Anderson, M. A., Jodoin, J. N., Lee, E. and Lee, L. A. (2012). Regulation of dynein localization and centrosome positioning by Lis-1 and asunder during Drosophila spermatogenesis. *Development* 139, 2945-54.

Sivaram, M. V., Wadzinski, T. L., Redick, S. D., Manna, T. and Doxsey, S. J. (2009). Dynein light intermediate chain 1 is required for progress through the spindle assembly checkpoint. *EMBO J* 28, 902-14.

Splinter, D., Tanenbaum, M. E., Lindqvist, A., Jaarsma, D., Flotho, A., Yu, K. L., Grigoriev, I., Engelsma, D., Haasdijk, E. D., Keijzer, N. et al. (2010). Bicaudal D2,

dynein, and kinesin-1 associate with nuclear pore complexes and regulate centrosome and nuclear positioning during mitotic entry. *PLoS Biol* 8, e1000350.

Stebbings, L., Grimes, B. R. and Bownes, M. (1998). A testis-specifically expressed gene is embedded within a cluster of maternally expressed genes at 89B in Drosophila melanogaster. *Dev Genes Evol* 208, 523-30.

Stevens, N. R., Raposo, A. A., Basto, R., St Johnston, D. and Raff, J. W. (2007). From stem cell to embryo without centrioles. *Curr Biol* 17, 1498-503.

Stuchell-Brereton, M. D., Siglin, A., Li, J., Moore, J. K., Ahmed, S., Williams, J. C. and Cooper, J. A. (2011). Functional interaction between dynein light chain and intermediate chain is required for mitotic spindle positioning. *Mol Biol Cell* 22, 2690-701.

Takata, H., Nishijima, H., Maeshima, K. and Shibahara, K. (2012). The integrator complex is required for integrity of Cajal bodies. *J Cell Sci* 125, 166-75.

Tanaka, T., Serneo, F. F., Higgins, C., Gambello, M. J., Wynshaw-Boris, A. and Gleeson, J. G. (2004). Lis1 and doublecortin function with dynein to mediate coupling of the nucleus to the centrosome in neuronal migration. *J Cell Biol* 165, 709-21.

Tanenbaum, M. E., Akhmanova, A. and Medema, R. H. (2010). Dynein at the nuclear envelope. *EMBO Rep* 11, 649.

Tanenbaum, M. E., Vale, R. D. and McKenney, R. J. (2013). Cytoplasmic dynein crosslinks and slides anti-parallel microtubules using its two motor domains. *Elife* 2, e00943.

Tanos, B. E., Yang, H. J., Soni, R., Wang, W. J., Macaluso, F. P., Asara, J. M. and Tsou, M. F. (2013). Centriole distal appendages promote membrane docking, leading to cilia initiation. *Genes Dev* 27, 163-8.

Tao, S., Cai, Y. and Sampath, K. (2009). The Integrator subunits function in hematopoiesis by modulating Smad/BMP signaling. *Development* 136, 2757-65.

Vaisberg, E. A., Koonce, M. P. and McIntosh, J. R. (1993). Cytoplasmic dynein plays a role in mammalian mitotic spindle formation. *J Cell Biol* 123, 849-58.

Vallee, R. (1993). Molecular analysis of the microtubule motor dynein. *Proc Natl Acad Sci U S A* 90, 8769-72.

Vassilev, L. T. (2006). Cell cycle synchronization at the G2/M phase border by reversible inhibition of CDK1. *Cell Cycle* 5, 2555-6.

Wahl, M. C., Will, C. L. and Luhrmann, R. (2009). The spliceosome: design principles of a dynamic RNP machine. *Cell* 136, 701-18.

Wang, G., Chen, Q., Zhang, X., Zhang, B., Zhuo, X., Liu, J., Jiang, Q. and Zhang, C. (2013). PCM1 recruits Plk1 to the pericentriolar matrix to promote primary cilia disassembly before mitotic entry. *J Cell Sci* 126, 1355-65.

Wong, R., Hadjiyanni, I., Wei, H. C., Polevoy, G., McBride, R., Sem, K. P. and Brill, J. A. (2005). PIP2 hydrolysis and calcium release are required for cytokinesis in Drosophila spermatocytes. *Curr Biol* 15, 1401-6.

Yasutis, K. M. and Kozminski, K. G. (2013). Cell cycle checkpoint regulators reach a zillion. *Cell Cycle* 12, 1501-9.

Zhang, X., Lei, K., Yuan, X., Wu, X., Zhuang, Y., Xu, T., Xu, R. and Han, M. (2009). SUN1/2 and Syne/Nesprin-1/2 complexes connect centrosome to the nucleus during neurogenesis and neuronal migration in mice. *Neuron* 64, 173-87.

Zhou, K., Rolls, M. M., Hall, D. H., Malone, C. J. and Hanna-Rose, W. (2009). A ZYG-12-dynein interaction at the nuclear envelope defines cytoskeletal architecture in the C. elegans gonad. *J Cell Biol* 186, 229-41.

Zhou, R., Hotta, I., Denli, A. M., Hong, P., Perrimon, N. and Hannon, G. J. (2008). Comparative analysis of argonaute-dependent small RNA pathways in Drosophila. *Mol Cell* 32, 592-9.